Design of a Laboratory System for the Prediction of Wireline Tool Sticking

by

Cecilia Mariana Prieto

B.S., Mechanical Engineering (1998)
Massachusetts Institute of Technology

Submitted to the Department of Mechanical Engineering in partial fulfillment of the requirements for the degree of

Master of Science

at the

MASSACHUSETTS INSTITUTE OF TECHNOLOGY

June 1999

Author . . . .
Department of Mechanical Engineering
May 24, 1999

Certified by . . . .
Ernesto Blanco
Adjunct Professor of Mechanical Engineering
Thesis Supervisor

Accepted by . . . .
Ain A. Sonin
Chairman, Department Committee on Graduate Students

Design of a Laboratory System for the Prediction of Wireline Tool Sticking

by

Cecilia Mariana Prieto

Submitted to the Department of Mechanical Engineering
on May 24, 1999, in partial fulfillment of the
requirements for the degree of
Master of Science

Abstract

This thesis is the design of an apparatus that simulates differential pressure sticking downhole in an oil well. This equipment is to be used to further understand differential pressure sticking and to observe how Schlumberger measurement tool designs can be changed to reduce this effect. The apparatus builds a mudcake, embeds a test piece in the mudcake and measures the force required to pull the test piece free. This apparatus was designed, built and tested.

Thesis Supervisor: Ernesto Blanco
Title: Adjunct Professor of Mechanical Engineering

Contents

List of Figures

List of Tables

Chapter 1

Overview

1.1 Introduction

In the oil industry, tools are lowered downhole in an oil well to perform a series of tasks ranging from drilling to taking measurements of the formation to determine the location of oil. These tools repeatedly get stuck and cannot be raised, lowered or rotated. This is even more frequent for tools that have to remain stationary for a long period of time. Once a tool gets stuck, special procedures have to be taken to pull the tool free. These procedures can take a long time and in the oil industry, time is extremely expensive.

This is the case for Schlumberger, the leading supplier of services and technology to the international petroleum industry. Its tools, in particular its measurement tools provided by the division Wireline & Testing, get stuck due to a phenomenon called differential pressure sticking. This occurs when a tool or cable is pinned against the borehole wall due to a differential pressure between the borehole and the rock formation. Because of this differential pressure, mud filters through the rock and starts building a mudcake around the wall. The tool gets stuck when it becomes embedded in the mudcake. A theoretical model of this type of tool sticking has been developed [10]. However, the phenomenon is still not completely understood nor is it known how these incidents can be reduced. Thus, this thesis develops the design of a laboratory test equipment to simulate the conditions downhole where differential pressure sticking occurs. This apparatus, referred to as the Wireline Stickance Tester, is to be used to further understand differential pressure sticking and to observe how tool designs can be changed to reduce this effect.

This chapter provides a background and an explanation of differential pressure sticking. It also states, in further detail, the motivation for the design of the laboratory equipment and the functional requirements for the equipment.

Chapter 2 describes the development of the equipment, certain design issues which had to be considered and a small prototype of the final design.

Chapter 3 presents the final design and Chapter 4 shows the performance of the tester and a discussion of possible improvements.

1.2 Motivation

When a tool gets stuck, special procedures are taken to pull the tool out, which requires all pending work to stop. These procedures can take up to 24 hours and it becomes extremely expensive since the daily rig costs around $100,000 per day. If for example, the customer needs to determine if there is oil at a particular rock formation, a measurement tool is lowered down into the oil well and the cost of the rig, the cost of the the measurement tool and the service provided is charged to the customer. Thus the longer a job takes to complete, the more expensive it becomes to the customer.

As described previously, the most common problem for Wireline tools is differential pressure sticking, especially for the tools that must remain stationary for long periods of time. This is the case for the RFT (Repeat Formation Tester) and the MDT (Modular Dynamics Formation Tester) tools, which stop to take samples from different formations in the well. Wireline & Testing, like the competition, has always considered differential sticking, a phenomenon that cannot be changed. Therefore, up until now, most of the attention has been focused on tool reliability in order to minimize the occurrence of failures while the job is running and thus, reducing the cost to the customer. However, as seen in Figure 1-1, sticking is far worse of a problem than tool failure. Therefore, Wireline & Testing is beginning to believe that if differential pressure sticking can be understood then, tool sticking frequency may be reduced.

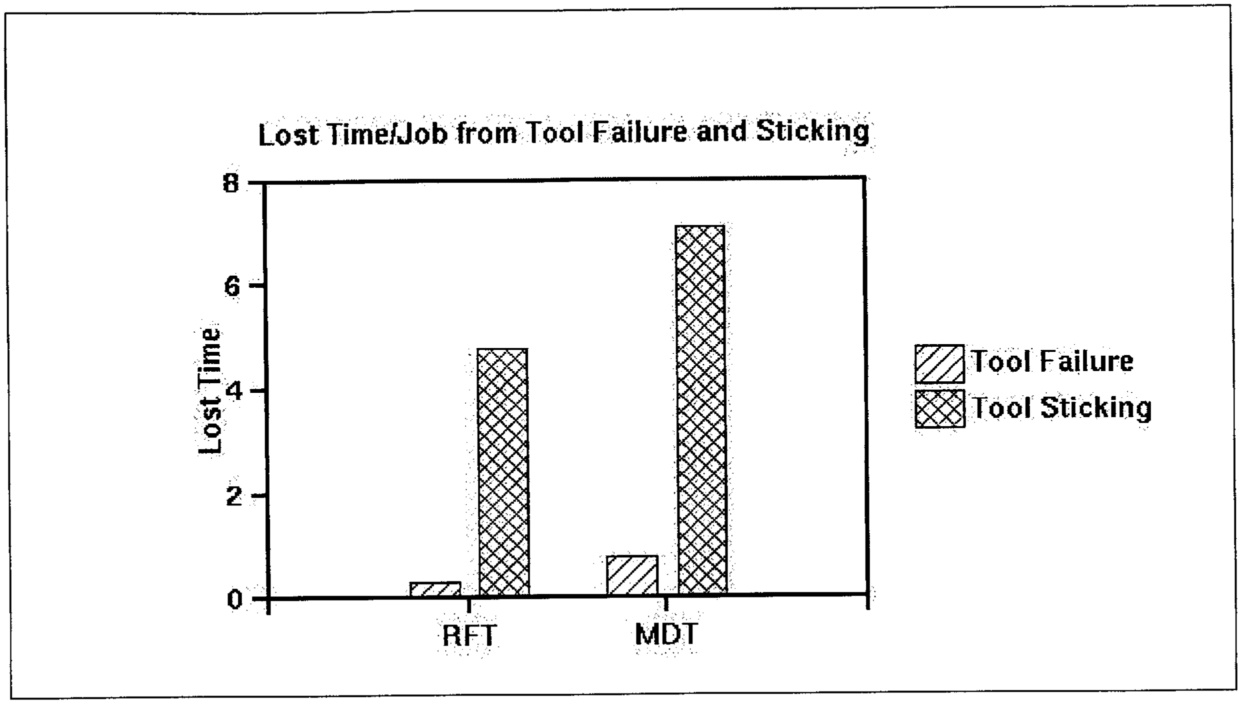

Figure 1-1: Frequency of Tool Sticking vs. Tool Failure

Several ideas to reduce sticking has been suggested. It is believed, for example, that the tool geometry can influence sticking. Changing the surface of the tool to a golf ball type of surface or making the cross-sectional area smaller could reduce the sticking frequency. A slimmer or a lower density tool might help. Designing micro-standoffs on the cable or tool, or drilling holes on the cable so that the differential pressure on the surface is reduced are some other ideas. Applying a voltage across the tool or cable has been suggested as well as applying a thinly lubricated surface or designing a cable that could inflate and deflate .

These ideas have raised more questions. It is undetermined, for example, if the spiral type of surface on the cable reduces the likelihood of differential sticking or if it actually embeds itself deeper into the mudcake and increases sticking probability. If the surface of the cable were to be made smoother, would this reduce sticking?

Such issues remain unanswered. Therefore, this thesis proposes the design of the Wireline Stickance Tester, which reproduces differential pressure sticking. This apparatus can be used to test the effectiveness of these ideas and to gain a better understanding of this phenomenon. The Tester simulates the conditions downhole by building a mudcake inside an annulus filter, embedding different test pieces in the mudcake and measuring the force required to pull the test piece free.

1.3 Schlumberger

Schlumberger is a company whose main activity is providing oilfield services. This involves exploration, production and completion services needed in the industry. Schlumberger is divided into smaller companies, specializing in different aspects of the oil industry. Two of these companies will be mentioned in this thesis: Dowell and Wireline & Testing.

Dowell provides services in well construction, well production and well intervention. This includes cementing of the well, providing and developing drilling fluids used at the well, and the control of sand and water. The drilling fluid, whose main purpose is lubrication for drilling, is what is commonly called mud. This mud is the main contributor to differential pressure sticking.

Wireline & Testing is the company that funded this thesis and is the interested party in the design of the Stickance Tester. This division provides tools and services to make measurements of physical properties of underground formation. The measurements taken using these tools are crucial to reveal where oil and gas are deposited and to indicate the producibility of the formation. After the well is drilled, Wireline & Testing brings a computerized mobile laboratory to the well and lowers its instruments on a cable called a wireline. These instruments are encased in a slim cylindrical tool known as a sonde. After they have been lowered to a desired depth, they are pulled slowly back to the surface, continuously measuring the properties of the rock formation that they pass through. The data is then transmitted on the wireline to the surface and is digitally recorded and plotted on a graph called a log. Depending on the type of tool that is used, the tool may also stop to take particular samples of the formation. Figure 1-2 shows a schematic of the system.

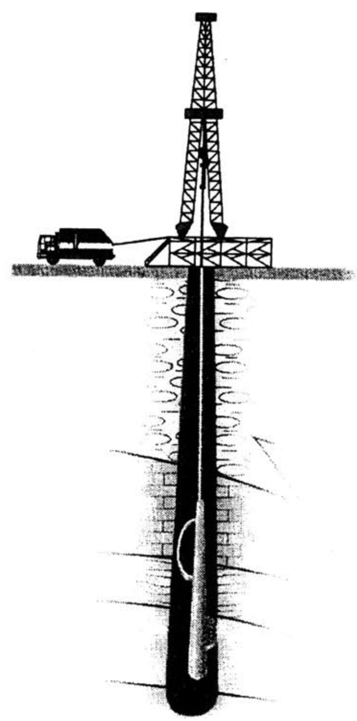

Figure 1-2: Wireline & Testing

1.4 Sticking

Sticking happens when a tool or the cable gets stuck in the well and cannot be raised, lowered or rotated and special procedures have to be taken into "fish" the tool out. The reasons for sticking are many but generally they are broken down to three categories: differential, mechanical and formation related, as illustrated in Figure 1-3 [13].

One form of mechanical sticking is key seating, where a tool or cable becomes wedged in a groove cut by the cable or the drillpipe. Another form of mechanical sticking is when the well passage is blocked by ledges or overhangs. The tool can

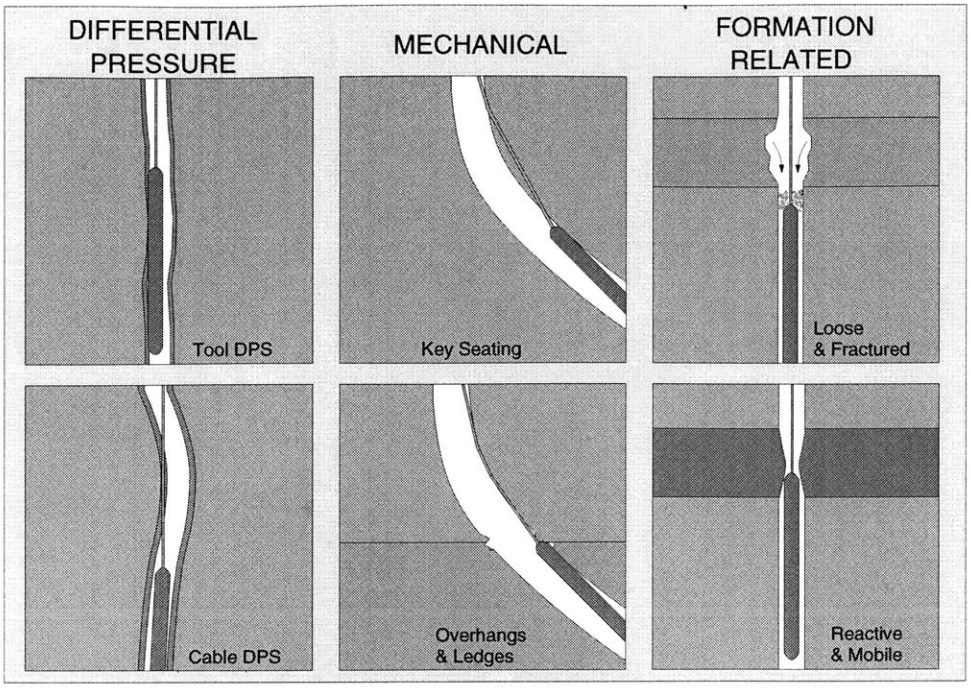

Figure 1-3: Modes of Sticking

easily slide past the overhang but when it is pulled upwards it is caught and trapped. Formation-related sticking is caused by the constriction of the borehole by mechanically or chemically unstable formations. Unconsolidated or reactive rock can block the borehole and constrain the tool from moving up. Differential pressure sticking, which is the most common form of sticking for Wireline tools, occurs when the tool or the cable becomes embedded in mudcake and is pinned to the borehole wall by the forces created by the pressure difference between the mud and the formation.

1.5 Differential Pressure Sticking

Differential pressure sticking occurs in permeable zones where gas and other pore fluids are found. In addition to acting as a lubricator for drilling, mud is also used to prevent the ingress of these fluids from pouring into the borehole. The mud density is adjusted so that the hydrostatic pressure is greater than the pressure within the pores of the surrounding rock. Because the pressure at the well is higher than the pressure at the formation, the mud starts filtering through the permeable rock. Over time, a low permeability layer called filter cake or mudcake is formed around the wall. This mudcake acts as a seal of the formation to the borehole.

Sticking occurs when the tool or cable becomes embedded in this mudcake. Because it is unlikely a well bore is drilled so straight that the wireline cable or tool does not come into contact with a borehole wall, the cable or tool starts to interact with the compacted layer of the mudcake. The cable acts almost as dental floss, as it is moved up and down, destroying the layer of mudcake and embedding itself in it. Once the mudcake has been destroyed, mud filtration begins again and a new mudcake is formed, sucking the cable or tool in. If the tool then stops, the new mudcake starts forming, bonding the tool or cable to the well. The combination of differential pressure, the new formation of a mudcake, and the stopping of the tool, causes the tool to get stuck. See Figure 1-4 [13].

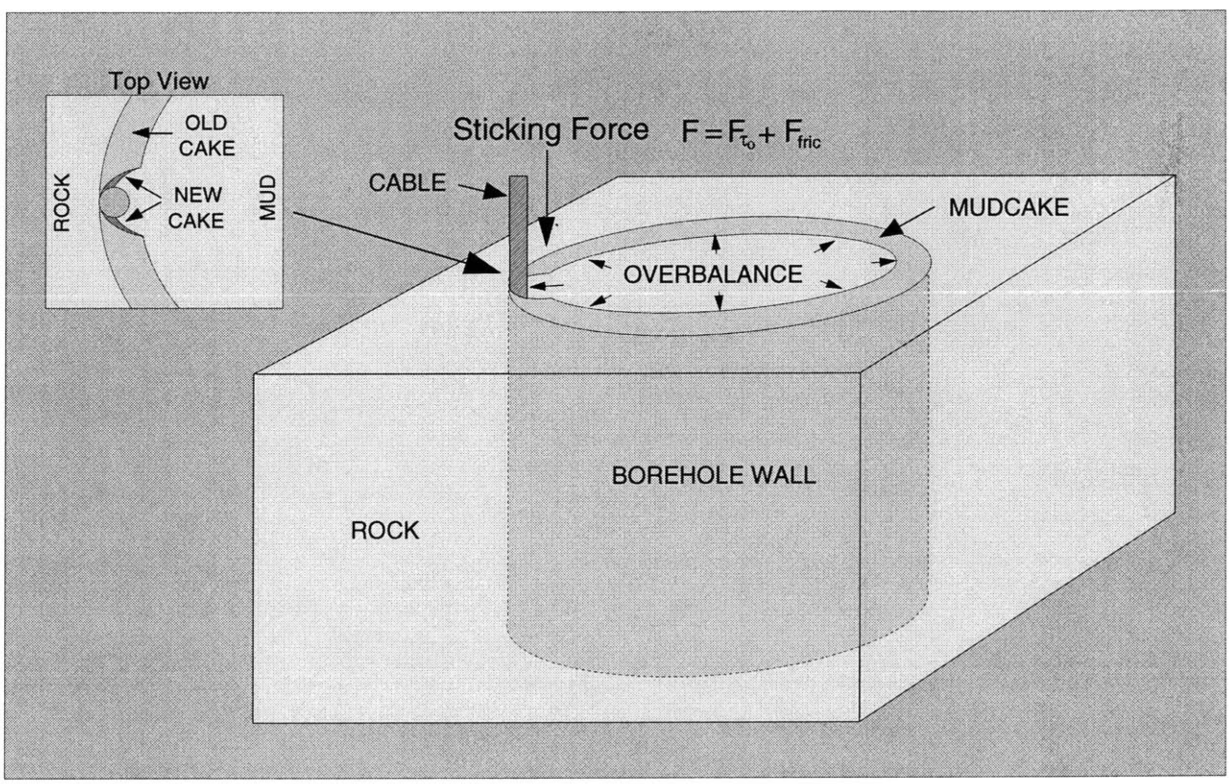

Figure 1-4: Differential Pressure Sticking

In summary, four simultaneous conditions have to exist for a tool or cable to get differentially stuck:

1. An overbalance or pressure difference between the formation and the well bore
2. A permeable zone for mud filtration to occur
3. Damage of mudcake by the tool or cable
4. Stopping of the tool

If these conditions do not occur simultaneously, differential pressure sticking will not occur. For example: an overbalance and permeable rock can exist and the tool can stop. But if the tool has not damaged the mudcake then a new filtration will not occur and the mudcake will not build around the tool. Therefore, the force required to pull out the tool would only be the frictional force acting on the tool. Any type of "suction" force on the tool would not be observed.

Once these four conditions occur, a sticking force begins acting on the tool. This sticking force has been quantified in a theoretical model developed by Gerry Meeten and John Sherwood [10]. The model is based on laboratory measurements and research on compressible mudcakes. It states that the sticking force or the force required to pull the tool free once it becomes differentially stuck is:

$$F_{free} = (2L_{cyl}D_e^{1/2})(\beta^{1/2}\tau_o)t^{1/4} \tag{1.1}$$

where,

L_{cyl} = contact length

$D_e = \frac{D}{1-\frac{D}{D_W}}$ = effective diameter

D = diameter of tool or cable

D_w = diameter of borehole wall

β = mudcake thickness parameter

τ_o = mudcake yield strength

t = time the tool has remained stationary

The magnitude of the sticking force is believed to be subject to mud properties $(\beta^{1/2}\tau_o)$, geometry of the tool $(2L_{cyl}D_e^{1/2})$, and the time the tool is stationary $(t^{1/4})$.

The contact length can vary depending on the straightness of the borehole wall. The well does not have to deviate much in order for the cable tension to force large cable length into the mudcake. Hole size and tool diameter are also important. The larger the ratio of well diameter to cable or tool diameter, the easier the tool can get stuck.

The mudcake properties that influence the probability of sticking are many. The mudcake thickness parameter, β, is a function of solids volume fraction of the mud, mud density and temperature. It is a parameter that determines the rate at which the mudcake is built, where the thickness of the mudcake δ is:

$$\delta = \beta t^{1/2} \tag{1.2}$$

The shear stress of the mud, τ_o, is a function of differential pressure, temperature (mud gels with increasing temperature) and mud type. The mud type can be water-based, oil-based or polymer water-based mud. In addition, lubricants can be added to the mud and these also influence the shear strength of the mudcake. Notice that the temperature and pressure influence the sticking force only implicitly by affecting the mud composition.

The significance of stationary time is important as well. The sticking forces grow rapidly immediately after the tool stops and slows down as time passes. This means that the first few minutes that the tool stops could be the most critical time with the highest probability of the tool getting stuck. A hypothetical pulling limit for the wireline cable or tool with the following values is shown in Figure 1-5:

$D_w = 8.5$ in

$D = 5$ in (diameter of tool)

$D = 0.5$ in (diameter of cable)

$L_{cyl} = 1$ ft (effective contact length for tool)

$L_{cyl} = 10$ ft (effective contact length for cable)

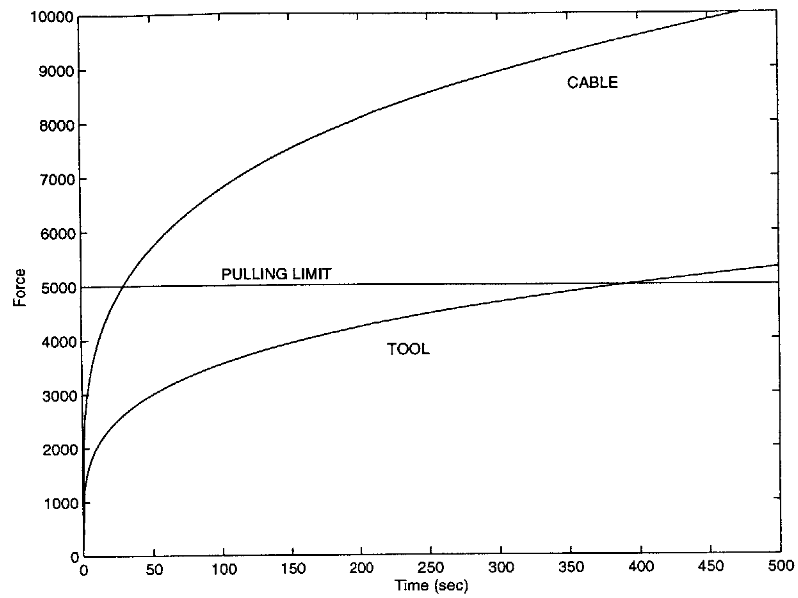

Figure 1-5: Sticking Forces

$\beta = 0.001\ in/s^{1/2}$ (moderately weighted water-based mud)

$\tau_o = 50$ psi (water-based mud with 500 psi overbalance)

The sticking force increases until the force becomes larger than the pulling limit at the rig and the tool or cable gets stuck. Whether the cable or tool will get stuck first depends on the contact length of the cable or tool. In this hypothetical case, the cable will exceed the pulling limit first. This is the general case because the contact length of the cable is normally much larger than that of the tool. However, because the area of the tool is larger than that of the cable, the effective diameter D_e is larger, and the tool could get stuck first if the contact length is not large enough.

1.6 Existing Designs and Other Published Testing Procedures

Dowell, the Schlumberger division that engineers the mud, has already tried reducing sticking by designing a mud that will form a less "sticky" mudcake. It has developed a laboratory test equipment called a Stickance Tester which is used to quantify the nature of the filter cake and the probability of tools getting stuck. The body of the device is a modified high temperature, high pressure (HTHP) mud filtration cell (see Figure 2-3). This HTHP cell is a standard piece of equipment used frequently in Dowell and Dowell field sites. For the Stickance Tester, the top end-cap of the cell has been modified to allow entry of a spring-steel wire through an o-ring seal set in the center of the cap. A new entry port is drilled to allow the cell to be pressurized via a gas line or a cylinder. The end of the steel wire in the cell is fixed to a 1.5 inch diameter polished steel ball which rests on the filter medium. The end of the wire protruding from the cell is connected to an electronic torque meter. Because the Tester has the same dimensions as the HTHP cell, it can be placed on a standard heater used for the HTHP cells to raise the temperature to $150°F$.

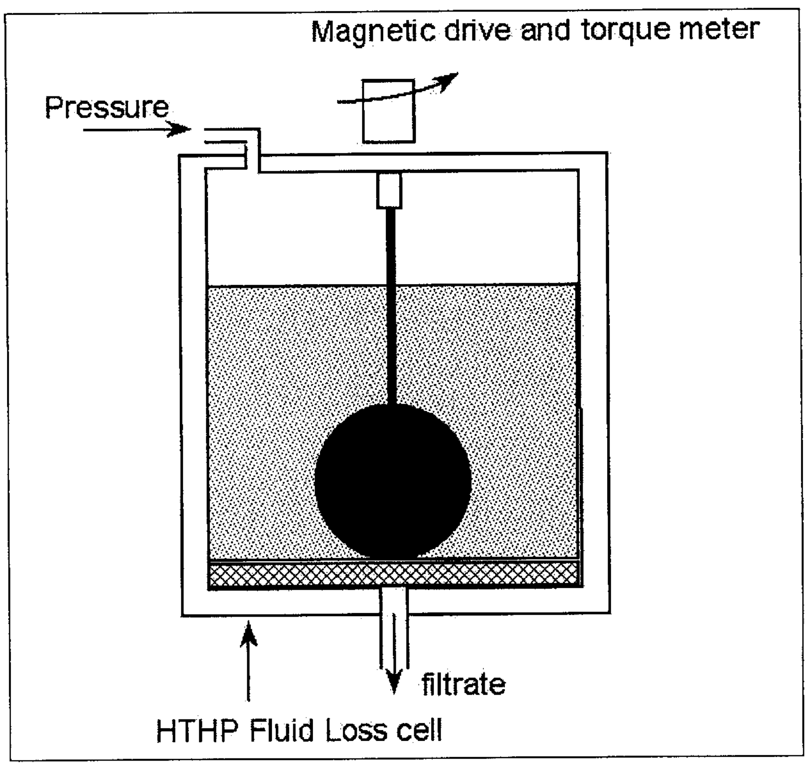

Figure 1-6: Dowell Stickance Tester

The Stickance Test is carried out by filling the cell with mud and heating it to a desired temperature. A differential pressure of 500 psi is applied and the mudcake begins to firm as the fluid flows through the filter paper. Approximately every five minutes, the torque meter is turned and the force required to move the sphere is measured. This is done for 30 min, applying a torque every 5 min. The torque data versus time to the power of 3/4 is plotted which normally gives a straight line. The slope of the line is calculated and it is called the "stickance" factor of the mud.

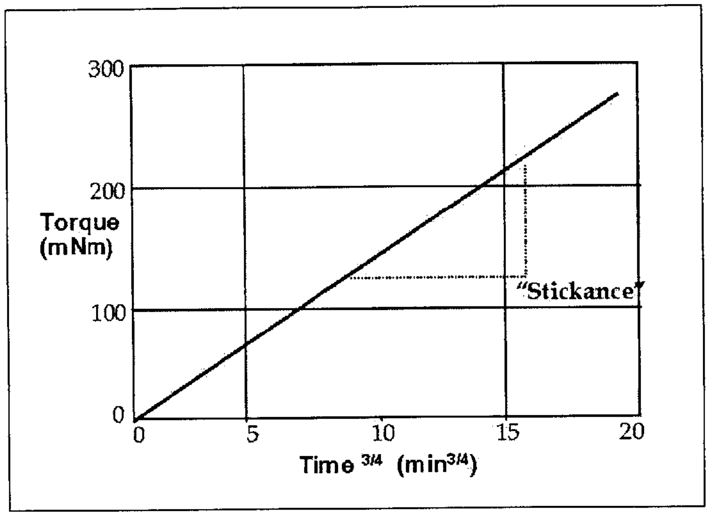

Figure 1-7: Torque vs. Time

From the theory in the previous section, the relationship between the stickance of the mudcake and the torque to free the ball can be derived to be [10]:

$$M_o = 2/3\pi {D_{ball}}^{3/2}\beta^{3/2}\tau_o t^{3/4} \tag{1.3}$$

where M_o is the torque required to free the stuck ball, D_{ball} is the diameter of the ball, τ_0 is the shear yield stress of the cake and t is the filtration time. Therefore, the stickance, S, becomes equal to :

$$S = 2/3\pi D_{ball}^{3/2}\beta^{3/2}\tau_o \tag{1.4}$$

so that,

$$M_o = S{\cdot}t^{3/4} \tag{1.5}$$

As the stickance increases the torque required to free the ball increases, as shown

Authors	Substrate Geometry	Pipe Geometry	Cake Formation	Direction of Force	Max Temp ($^{\circ}F$)	Max Diff. Pressure (psi)
Krol	Cylinder	Cylinder	Static or Dynamic	Axial	300	2000
Helmick and Longley	Cylinder or disc	Cylinder	Static or Dynamic	Axial or radial	Ambient	100
Annis and Monaghan	Disc	Disc	Static	Axial	Room	500
Bushnell-Watson	Cylinder	Cylinder	Static or Dynamic	Rotation	150	100
Reid (Dowell Stickance Tester)	Disc	Sphere	Static	Rotation	400	1200
Clark and Almquist	Cylinder	Cylinder	Static or Dynamic	Axial	300	2000
Park and Lummus	Disc	Sphere	Static	Axial	400	3000
Courteille and Zurdo	Cylinder	Cylinder	Dynamic	?	255	1000
Haden and Welch	Cylinder	Cylinder	Dynamic	Axial	Room	15

Table 1.1: Differential Pressure Apparatus

in Figure 1-7. Therefore the "stickance" is a measurable parameter to describe the likelihood of tools getting stuck.

For Dowell, this tester works well to design drilling muds that have a low stickance factor. However, for Wireline, this tester does not fully describe the conditions its tools are subject to. First, Wireline can only apply axial pull to its tools. Thus a torque measurement is not accurate. Secondly, Wireline wants to modify its tools to reduce sticking and the ball does not simulate the tool geometry correctly. Thus, Wireline wants a modified Stickance Tester where a modified stickance factor can be measured for different geometries and compare their tendencies of sticking.

Other methods of assessing the differential sticking tendencies have been developed previously. Some were designed to understand sticking for drilling tool; others were designed to take direct measurements on mud and mudcakes. A list of published differential pressure apparatus is summarized in Table 1.1. These apparatus vary in pressures, temperatures, geometries and simulated dynamic or static conditions in the well. (Unlike Wireline tools, drilling tools are subject to dynamic mud flow in the well.)

1.7 Functional Requirements for the Design of the Wireline Stickance Tester

It is desired to design a Stickance Tester that can measure the tendency of objects with different geometries to get stuck. Most of the above apparatus are large and complicated and do not have the desired requirements. The apparatus that measure axial pulling forces provide dynamic mud flow and filtration. This is not a critical factor since Wireline tools are used under static filtration. Therefore, a simpler mechanism without dynamic flow is desired. The Dowell Stickance Tester is the closest to what is needed but, for Wireline tools, torque measurements are irrelevant. In addition a cylindrical filter medium and a pipe geometry are desired since this simulates Wireline downhole conditions better.

The following are the design requirements for the Stickance Tester:

- Build mudcake inside an annulus to simulate a wellbore hole
- Measure axial force to pull free stuck object
- Allow changeable test objects so that different geometries or designs can be tested
- Apply differential pressure of 1000 psi
- Withstand temperature of 450°F
- Be able to test existing cable
- Scale tool and well diameters so the diameter ratio is the same as real conditions
- Provide safety

Chapter 2

Development

2.1 Initial Design Overview

The Stickance Tester has to perform the following steps:

1. Build a mudcake inside a cylinder simulating the mudcake formation around the well bore wall.

2. Embed a test piece in the mudcake.

3. Apply axial pull to the test piece and measure the force required to pull the test piece free from the mudcake.

4. Perform the test several times and plot force against time.

5. Test different test piece geometries.

Figure 2-1 is a sketch of what an initial design might look like. The filter is cylindrical and, unlike the Dowell Stickance Tester, the mudcake forms vertically inside the filter. The vessel is pressurized at 1000 psi and the filter, which is open to the atmosphere, will have a 1000 psi differential pressure across its walls. This will allow the mud to pass through the filter and build a mudcake. The rod penetrates the vessel and a sensor measures an axial force outside the vessel.

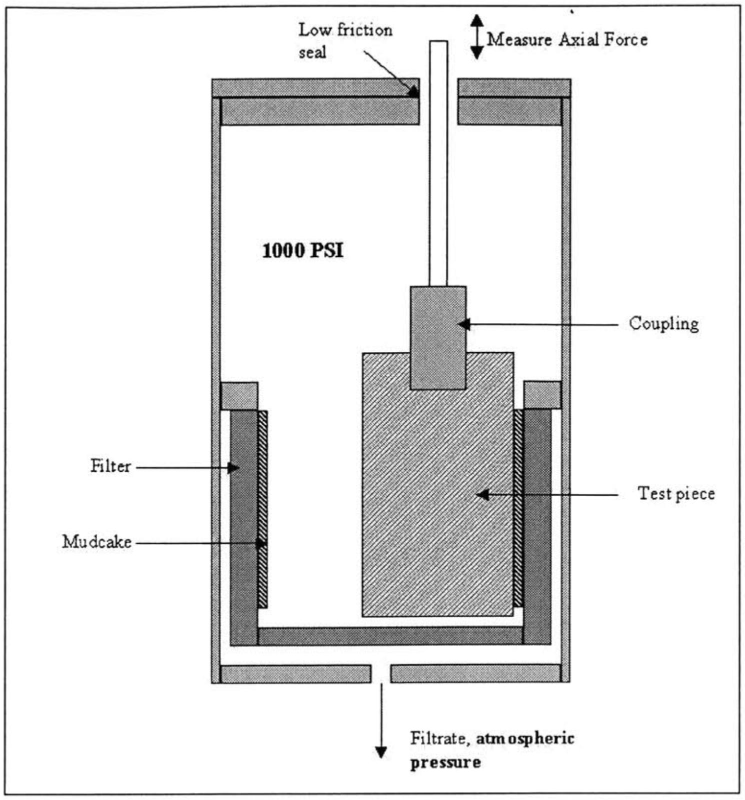

Figure 2-1: Schematic of an Initial Design

2.2 Identifying Issues

Proceeding with the design of the Stickance Tester, requires the resolution of several key issues. For example, the time it takes to build a mudcake thick enough to produce a measurable sticking force on a test piece must be determined. In real conditions, mud can be inside a well for weeks before a Wireline tool is lowered downhole, thus the sticking forces are very high. Equation 1.2 shows that the mudcake thickness builds by $t^{1/2}$. This means that after a long period of time, the mudcake will reach a maximum thickness. However, the time that it takes to build a mudcake thick enough to perform realistic measurements is unknown.

The Dowell Stickance Tester uses filter paper to build a mudcake. However, for this design, a cylindrical solid filter is needed. Ceramic filters have been thought to work but whether these will simulate a real permeable rock formation is not known. Also questionable is whether the mudcake will have uniform thickness along the length of the filter. The gravity could influence the solid contents of the mud and build a mudcake thicker at the bottom of the filter than at the top. Where the test piece is touching the mudcake along the length the filter could influence the force measurements.

To choose the type of force sensor in the design, the magnitude of the sticking forces must be determined for a particular filter diameter and a certain mudcake thickness. Whether the seals on the rod will influence greatly the force measurements if the force sensor is placed outside the pressurized vessel is also a concern. If this were to be the case, then it is uncertain whether the frictional force of the seals could be subtracted from the total measured force.

Finally, because several size test pieces have to be tested, the gap between the mudcake and the side of the test piece will vary depending on the size of each piece. This gap might be adjusted by making several parts of the tester non-concentric. However, this idea needs to be evaluated.

To resolve these issues a prototype of a Stickance Tester was designed.

2.3 Design of a Prototype of a Stickance Tester

This prototype uses the bottom assembly of a Dynamic Fluid Loss Cell which is used by Dowell to run mud experiments. This assembly, Figure[1] 2-2 has a cylindrical ceramic filter with an inside diameter of 1 in, outside diameter of 1.5 in and a length of 1.5 in. The filter is placed inside a housing that has a low pressure line connected to the atmosphere. The top and bottom of the filter are sealed so that the mud can only filter through its wall if it is pressurized from the inside.

A housing and a top cap assembly were designed to screw to the bottom piece of the Dynamic Fluid Loss Cell. The test piece penetrates through the top cap assembly[2]as shown in Figure 2-3.

[1]This drawing has been modified with Photoshop to show the part of the cell that was used in the prototype. However this is not an accurate picture. See Figure Appendix A.1 for the engineering drawing of the Dynamic Fluid Loss Cell

[2]See Appendix A.2 for engineering drawings of these machined parts

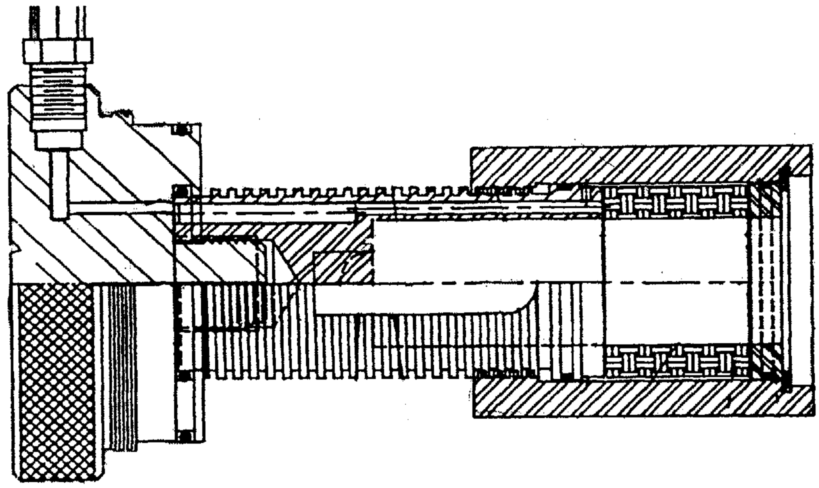

Figure 2-2: Bottom Part of the Dynamic Fluid Loss Cell

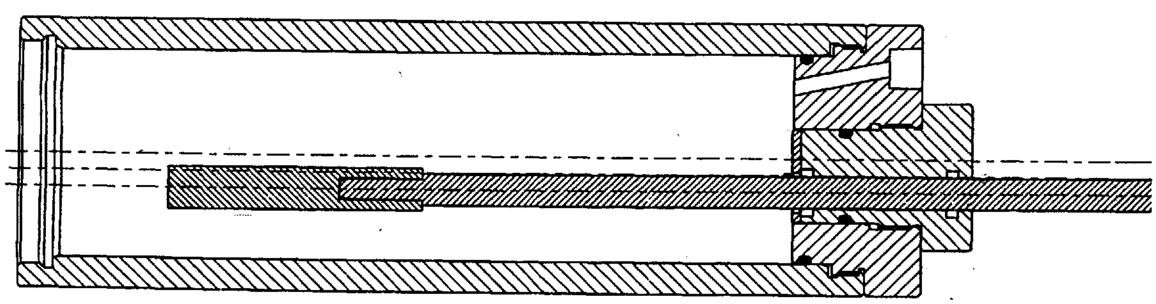

Figure 2-3: Prototype Assembly without the Fluid Loss Cell

The top assembly that screws to the housing is made of three parts: a top cap that screws to the housing, a middle cap that screws to the the top cap and the rod that penetrates the middle cap. These three pieces are non-concentric to each other. Thus, the gap between the rod and the housing can vary depending on how far each piece has been screwed in with respect to the others. Figure 2-4 illustrates this idea. This is the mechanism that was designed to vary the gap between the filter and the test piece.

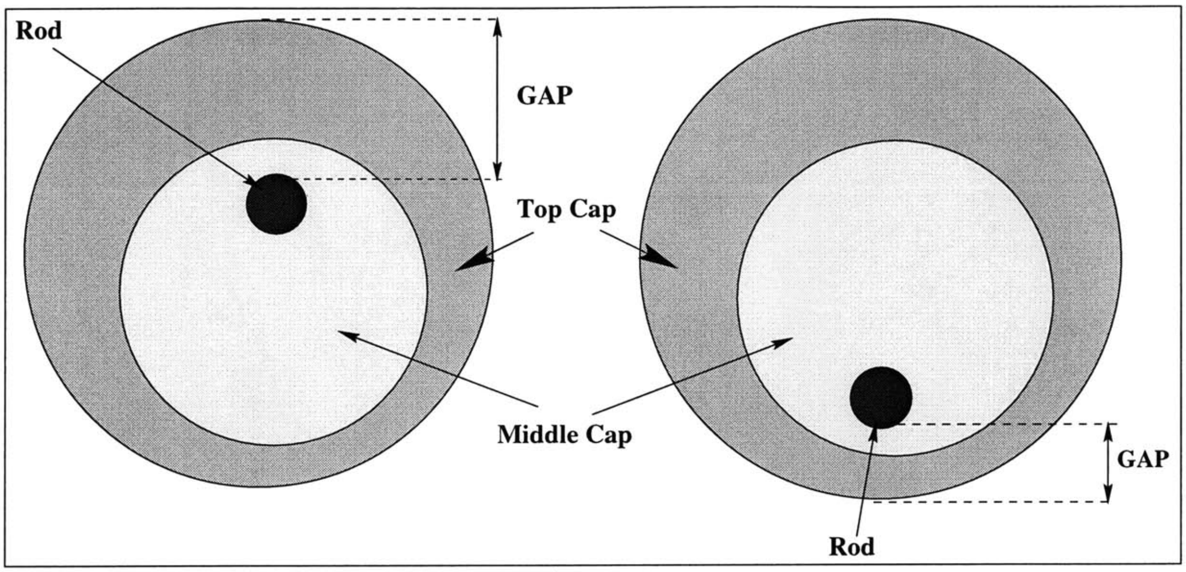

Figure 2-4: Top Views of Top Cap Assembly

The test piece for this prototype is a 2 inch long and 0.5 inch diameter steel rod (the ratio of this rod diameter to the inside diameter of the filter is the same as the ratio of the tool diameter to the diameter of the borehole) which is press-fitted to a 3/8 in steel rod. A seal which is composed of a nitrile o-ring and a graphite filled PTFE gland (see Appendix A.3 for further specifications) fits at the inside diameter of the middle cap. This seal has good low friction and wear properties. At the bottom of the inside diameter of the middle cap, an excluder is placed in order to maintain the seal free of mud and give the rod more stability if it were to slip out of plumb.

The top cap has a 1/4-18NPT thread opening to allow pressurization of the vessel.

2.4 Test Set-Up and Experimental Procedure

The assembled cell is filled with mud and it is placed on a stand. This stand has a bottom platform attached to a ball screw actuator which can be moved up or down to an accuracy of 0.002 inches. The steel rod connects to a load cell at the top of the stand and a nitrogen tank connects to the top cap to pressurize the cell (see Figure 2-5).

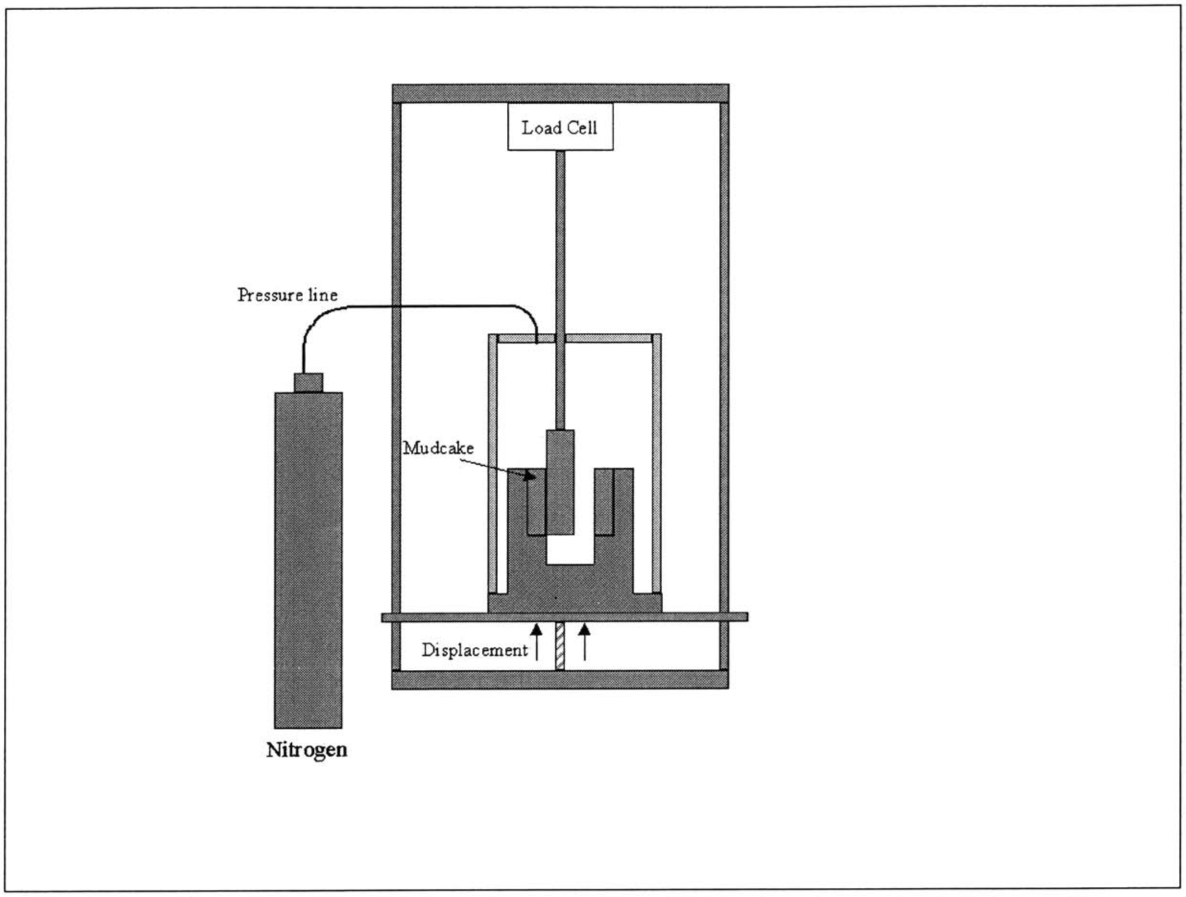

Figure 2-5: Test Set-Up of Prototype

Before the cell is placed on the stand, the non-concentric top caps are rotated relative to each other until the rod touches the side of the filter (this can be easily felt). Once the cell is placed on the stand, the stand is lowered until the top of the 0.5 in diameter test piece touches the top cap. (This allows the mudcake to form without the interference of the rod). The cell is pressurized to a 1000 psi and the mud starts filtering through the bottom part of the dynamic fluid loss cell. Once the mudcake is built, the rod is lowered relative to the vessel (the platform is displaced upwards) until it hits the dynamic fluid loss cell. The load cell force measurement increases drastically when this happens. During the displacement of the rod, the mudcake is destroyed and a new mudcake starts forming around the test piece. The rod is left for 5 min at that position. It is then displaced up very slowly (the platform moves down) measuring the force. The force increases as the rod is pulled upwards until it hits a peak force when it decreases drastically. The peak force indicates the rod has been pulled free. Once pulled free, the rod is moved 1/8 inch up and left there for 5 min. This procedure is repeated 5 times and the force is plotted against time. Note that the test piece always touches the whole surface of the filter because the dynamic cell has a 0.75 inch vertical length for the rod to move down to. However, this constrains the experiment to six measurements per test.

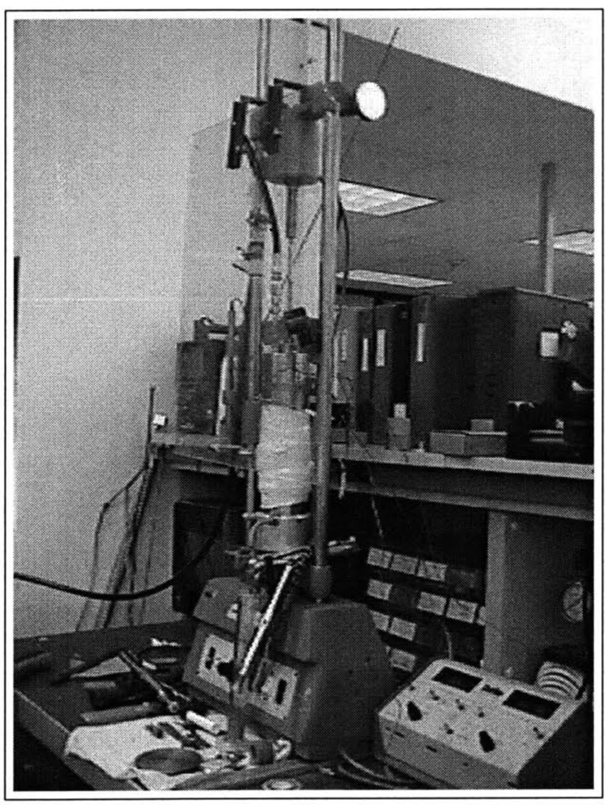

Figure 2-6: Picture of Temperature Test

2.5 Test Results and Conclusions

Six experiments were completed (see Figure 2-6 for picture of a test). All tests used 9 lb/gal water-based mud and were pressurized at 1000 psi. The first three were performed using filters that had a pore size of 10 micro-inches. The other three tests used 35 micro-inch filters. The final test was heated to 217°F using heating coils. To measure the force applied to the rod by the pressure and friction forces, a breakaway force was measured before the rod touched the mudcake. Appendix A.4 shows the force minus the initial breakaway force against time. All experiments showed that

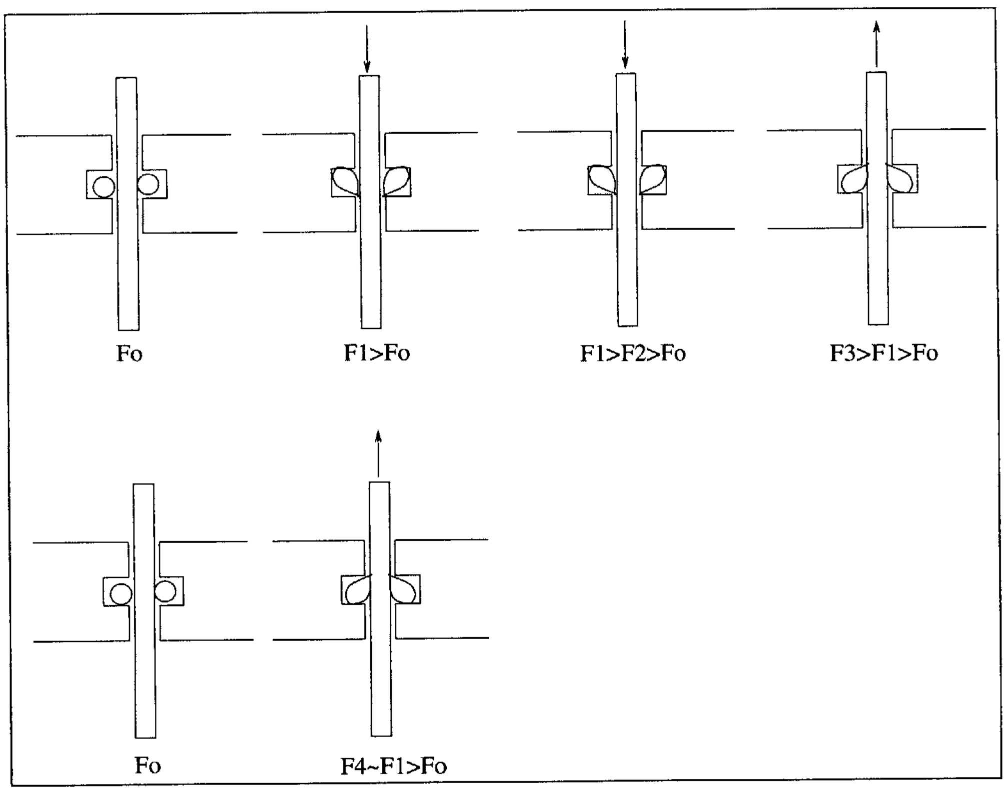

Figure 2-7: O-rings Dynamics

the friction due to the o-rings could not be considered negligible. When the system was pressurized and static, the load cell read a certain force, Fo, which would be considered to be force due to the rod's being pushed upwards by the pressure. If the rod was lowered, a force F_1, was measured which was higher than the initial force Fo. Thus, F_1 was considered to be the pressure force plus the friction force of the seals. However, if the rod was lowered again, another force, F_2, was measured which was lower than F_1 even though it was expected that the friction force plus the pressure force would remain the same. If then the rod was displaced upwards, the force measured, F_3, was higher than F_1, the force required to move the rod down initially. Finally, if the rod was initially moved upwards before moving it down at all, the force measured, F_4, was about the same as the force to move it down initially, F_1.

These force measurements were found to be affected by the o-rings energizing and grabbing the rod as shown in Figure 2-7. If the o-ring had already been deformed downwards, the force to move further down is less than if the o-ring had been deformed in the other direction. The combination of the o-ring's energizing and the constant pressure force made it hard to obtain an accurate force measurement.

Finally, for the last experiment, the temperature measured was considered inaccurate since a thermocouple was placed between the heating coils and the housing. Therefore, the temperature reading did not reflect the temperature inside the cell.

In summary, the following issues were established:

- For this specific filter size, a 1/4 inch thick mudcake was built in 30 to 40 minutes.
- The mudcake formed was uniform along the length of the filter.
- Force measurements were in the order of 50 lb force with the above conditions.
- 35 micro-inch pore size filters built a mudcake faster than a 10 micro-inch filter for a 9 lb/gal density mud.
- The non-concentric method to vary gap worked well.
- Seals should be eliminated in the force reading.
- Disassembling between experiments was messy; a drain valve to drain the mud should be designed.
- Temperature measurement was inaccurate.

Chapter 3

Wireline Stickance Tester Design

3.1 Overview

The Stickance Tester final design has maintained some features of the prototype. It uses the non-concentric method and a similar filtering mechanism. An actuator rod which penetrates the vessel is used to move the test piece axially. Finally, the system can be pressurized with a nitrogen tank and it is rated to withstand 1000 psi and $400°F$. See Figure 3-1 for a schematic of the design and Figure 3-2 for a cross section of the pressure vessel.

However, to eliminate the inaccurate force measurements due to the seals, a load cell is placed inside the pressure vessel in between the test piece and the actuator rod. The actuator rod is hollow so that the wires of the load cell can exit the vessel through the inside of the rod. An air cylinder is used as an actuator and it is placed on top of the stand and connected to the rod. In order to measure the temperature inside the vessel, this tester has a thermocouple housing which allows a thermocouple to penetrate inside the tester. In addition, a drain valve is located at the bottom of the tester to drain the mud before disassembly takes place.

The Stickance Tester has been scaled up. The filter is half the scale of a real oil-well diameter. A well diameter varies between 6.6 to 8.5 inches. The inside diameter of the filter measures 3.5 inches. For this particular size, the sticking forces are estimated

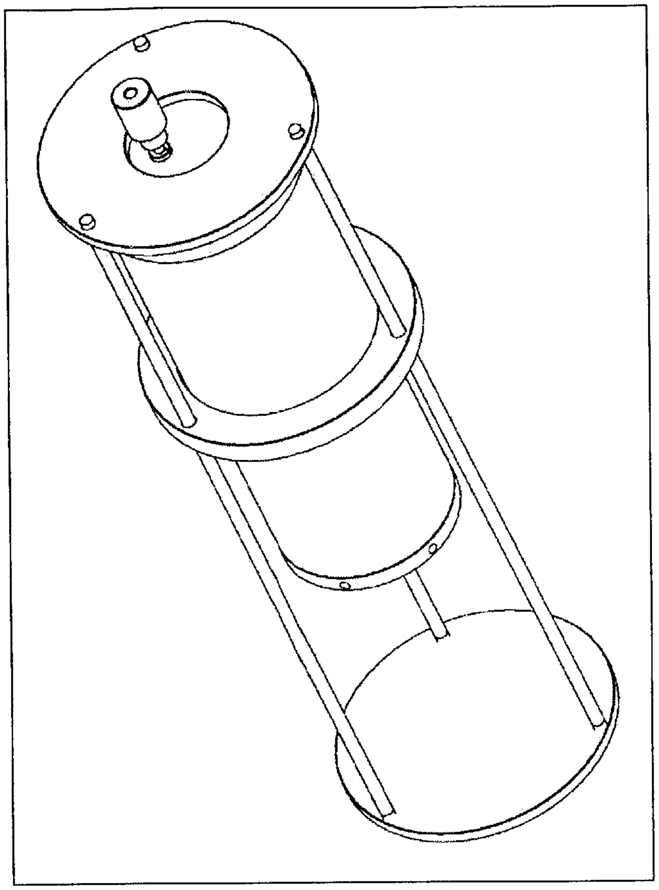

Figure 3-1: Stickance Tester on the Test Stand

to vary between 100 to 500 lbs force[1]. Thus, the load cell has been rated to measure forces up to 500 lbs.

Appendices B.1 and B.2 show all engineering drawings of machined parts and outsourced parts.

3.2 Filter Housing Assembly

The Filter Housing Assembly holds the filter and produces a differential pressure across its walls leading to the formation of a mudcake. The pressure difference is created by pressurizing the vessel and connecting the outside diameter of the filter

[1]This number was determined by applying equation 1.1 and approximating β and τ_o from experiments performed in the previous section

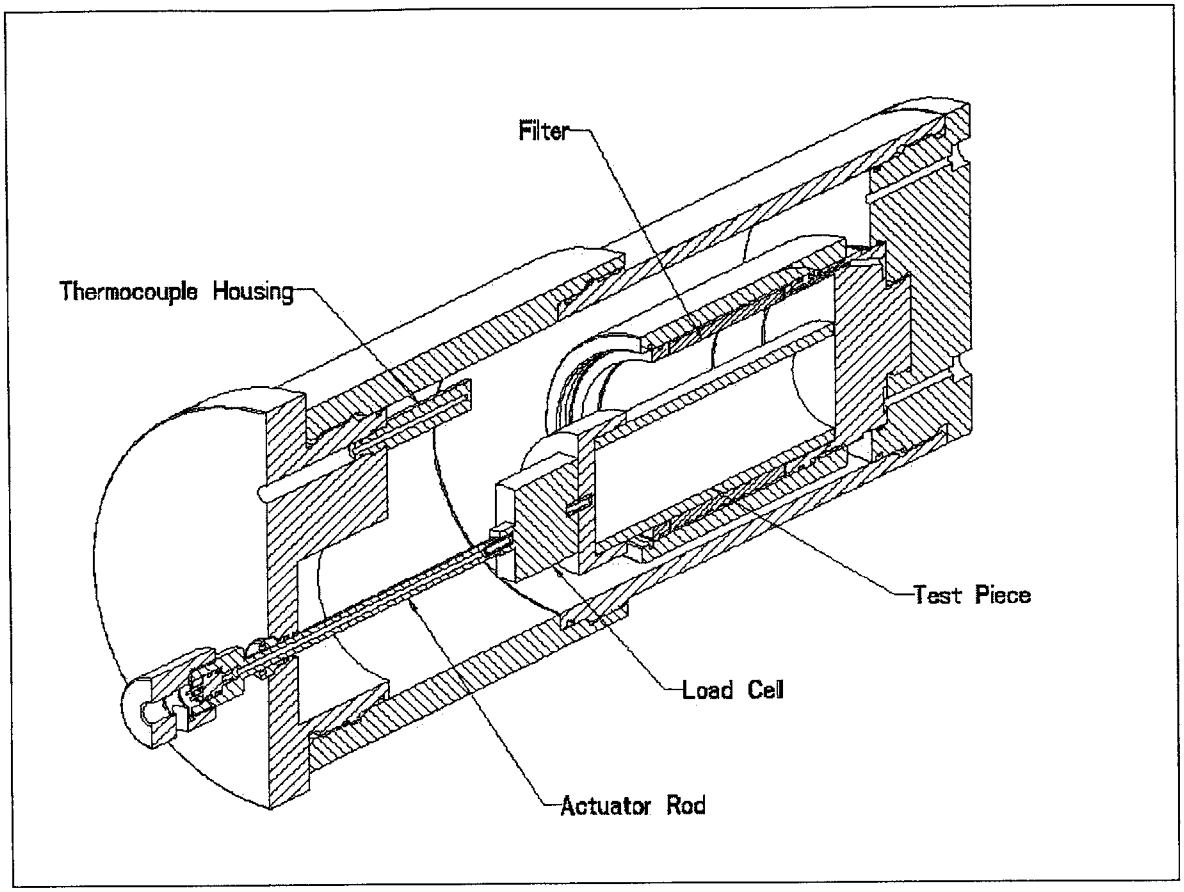

Figure 3-2: Cross-Section of the Pressure Vessel

to the atmosphere through a low pressure line. Because the filter is sealed at the top and at the bottom, the pressure gradient exists only across its wall.

Figure 3-3 shows the Filter Housing Assembly. The filter is placed inside the filter housing (mrcd308) and it is sealed at the top and bottom by putting it in between two gaskets (3). The filter and the gaskets are held in place by a a snap ring (2) and a filter ring (mrcd309) which has an o-ring (6) to prevent any ingress of mud through its side. The filter housing, which is already screwed to the pressure line screw (mrcd307), can be screwed in further. This compresses the filter between the snap ring and the line screw, sealing the top and bottom of the filter. The pressure line screw has a pressure line that connects to the atmosphere through the bottom cap (mrcd306). Thus the outside diameter of the filter is at atmospheric pressure and the inside diameter is at the pressure of the vessel. To replace the filter, the snap ring is taken out and the housing is screwed further into the pressure line screw so that it pushes the filter out.

See Figure 3-4 for a picture of the Filter Housing Assembly and Figure 3-5 for a picture of the ceramic filter, gaskets and filter ring.

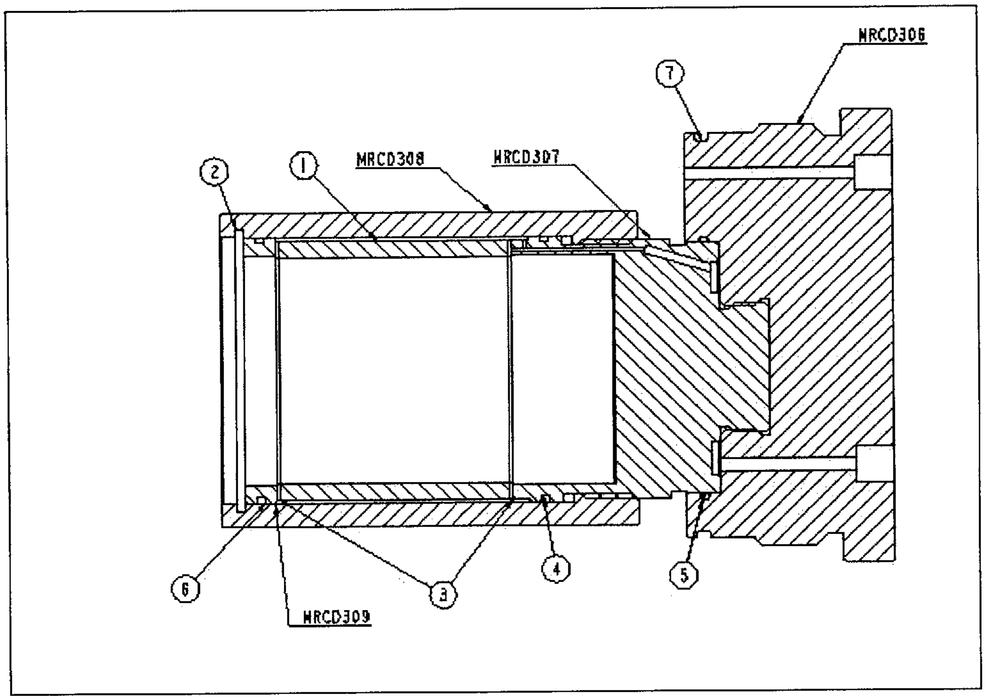

Figure 3-3: Cross-Section of the Filter Assembly

3.3 Load Cell Assembly

The load cell (1), is connected between the test piece (mrcd312) and the actuator rod (mrcd316); see Figure 3-6. The load cell is custom made, can measure compression and tension forces up to 500 lbs and is designed to withstand 1000 psi and 400°F. It requires an excitation voltage of 10Vdc and its output is measured in microvolts (see Figure B-30 in Appendix B.3 for calibration data). The actuator rod is hollow and the signal and excitation wires of the load cell pass through the inside of the rod and are connected to a pressure bulk head (DH549219). The pressure bulk head, which is

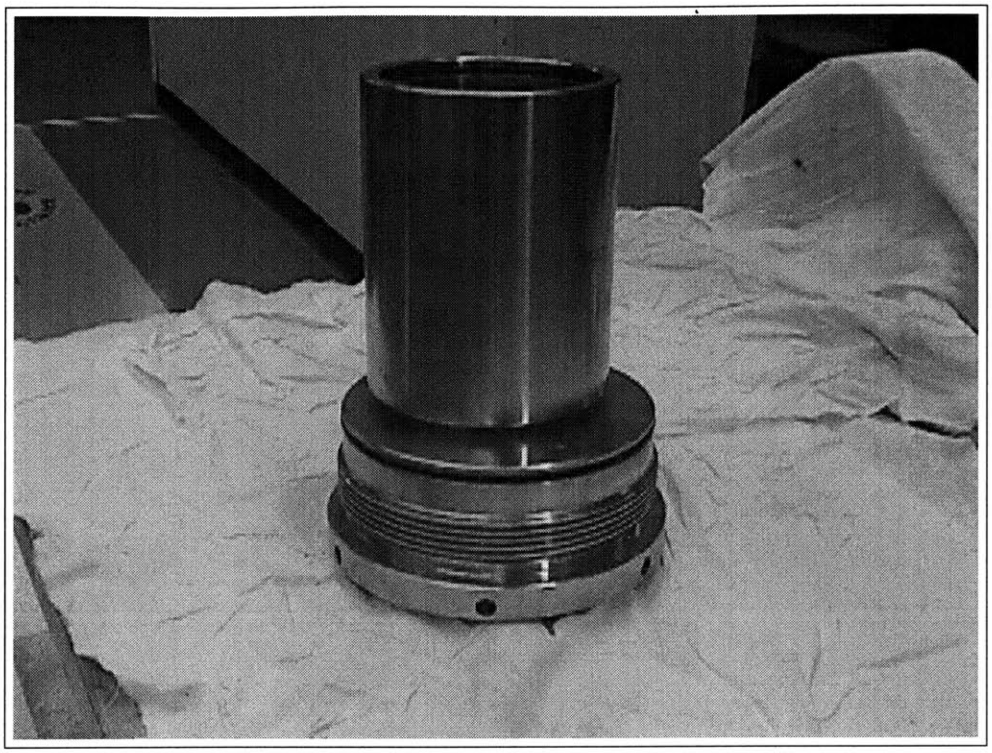

Figure 3-4: Picture of the Filter Housing Assembly

held in place by a snap ring (2), allows the signal to be read at the atmosphere but still maintains a full seal. Finally, the shaft connector (mrcd317) is screwed to the actuator rod.

However, before the load cell is assembled, the actuator rod needs to penetrate the top cap first, then the rod can be connected to the load cell and the wires to the pressure bulk head. See Figure 3-7 for a picture of the completed assembly and Figure 3-8 for a picture of load cell components. Before the pressure bulk head can be secured in place, the load cell has to be filled with silicon grease in order to protect all the electronics inside. The load cell has a grease fitting installed so that it can be filled with grease using grease gun. The grease is forced into all internal recesses within the cell and into the internal diameter of the actuator rod. Once the grease excrudes out to the other end of the rod, the pressure bulk head can be snapped in place. The load cell is now protected from the mud environment that it will be submerged in. The grease will act as a displacement barrier to moisture and other

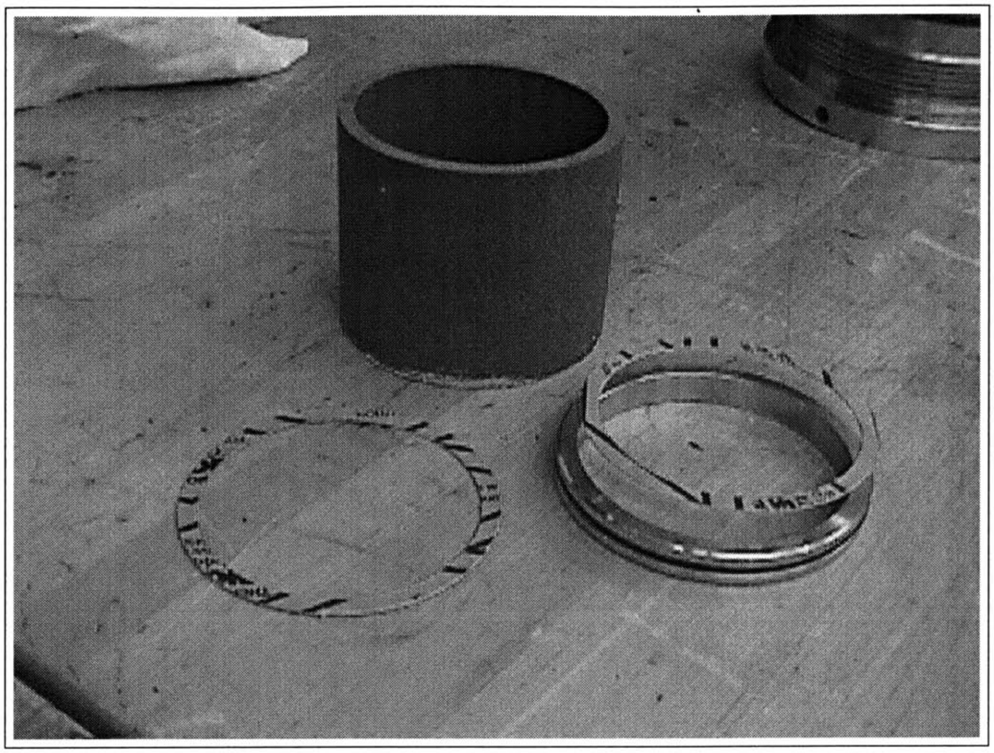

Figure 3-5: Picture of the Filter, Gaskets and Filter Ring

contaminants.

This assembly is designed for different test pieces. However, a coupling, such as the mrcd311, needs to be machined for each test piece. The coupling requires a 1/4-28UNF-2B thread at one end and the pressfitting of the test piece at the other end. For example, for the experiments performed, a real wireline cable was also used as a test piece. In this case, a different coupling was machined for the cable and the cable was pressfitted and welded to the coupling; see Figure B-19 in Appendix B.1.

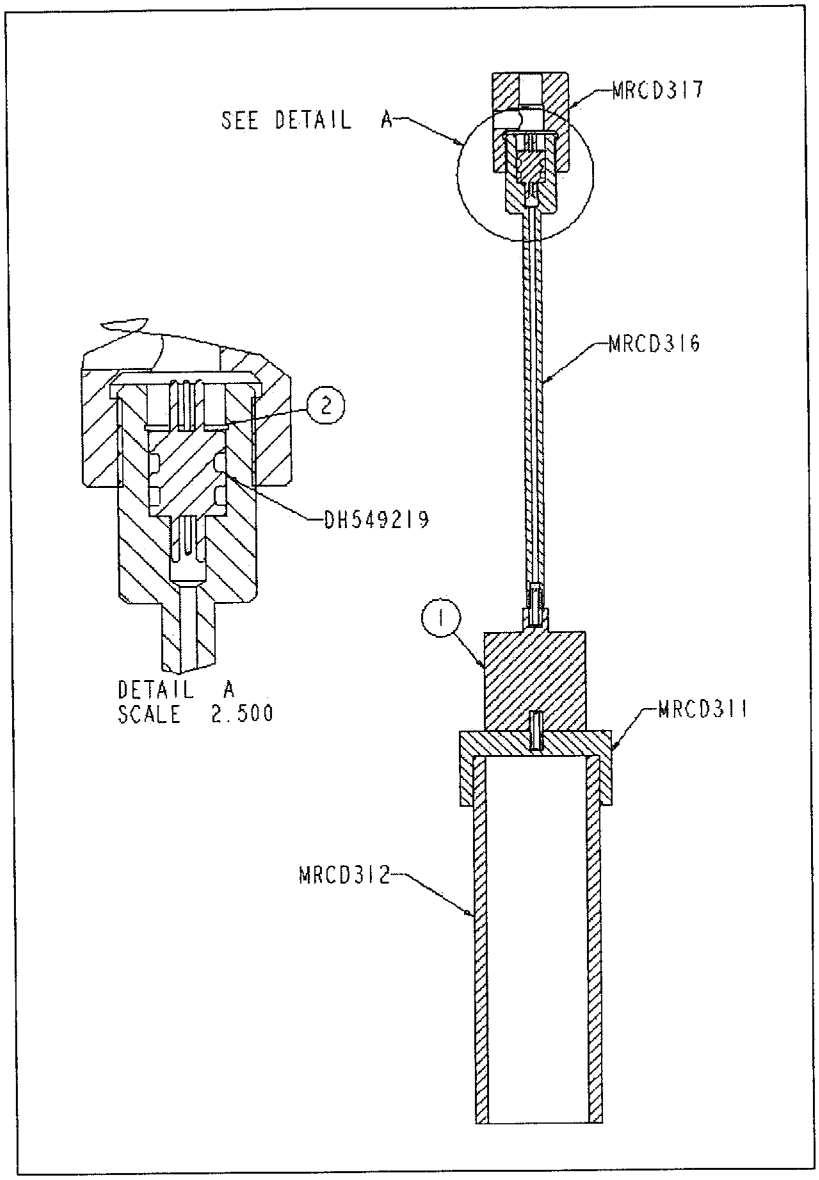

Figure 3-6: Cross-Section of the Load Cell Assembly

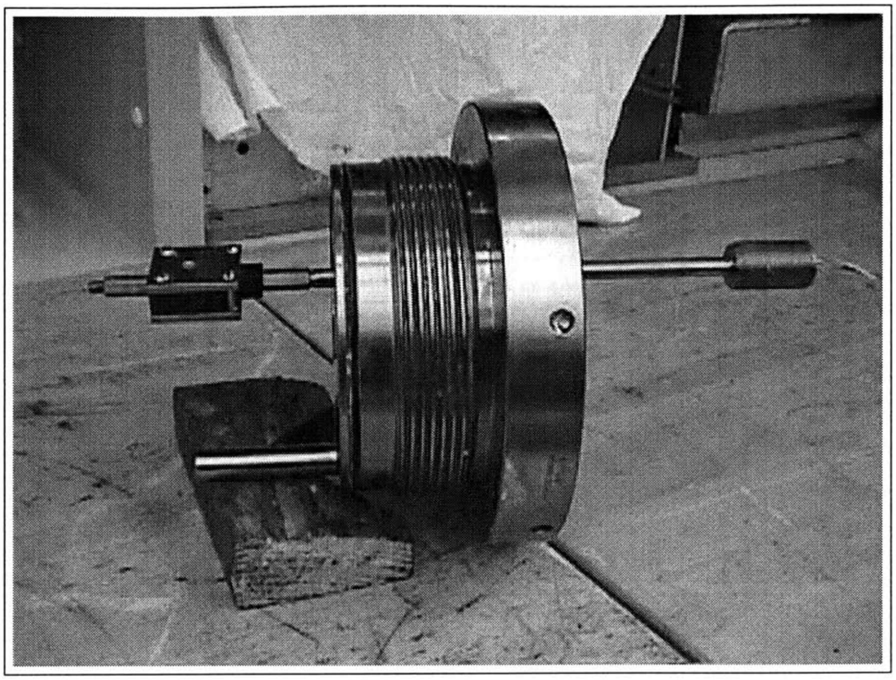

Figure 3-7: Picture of Load Cell Assembly

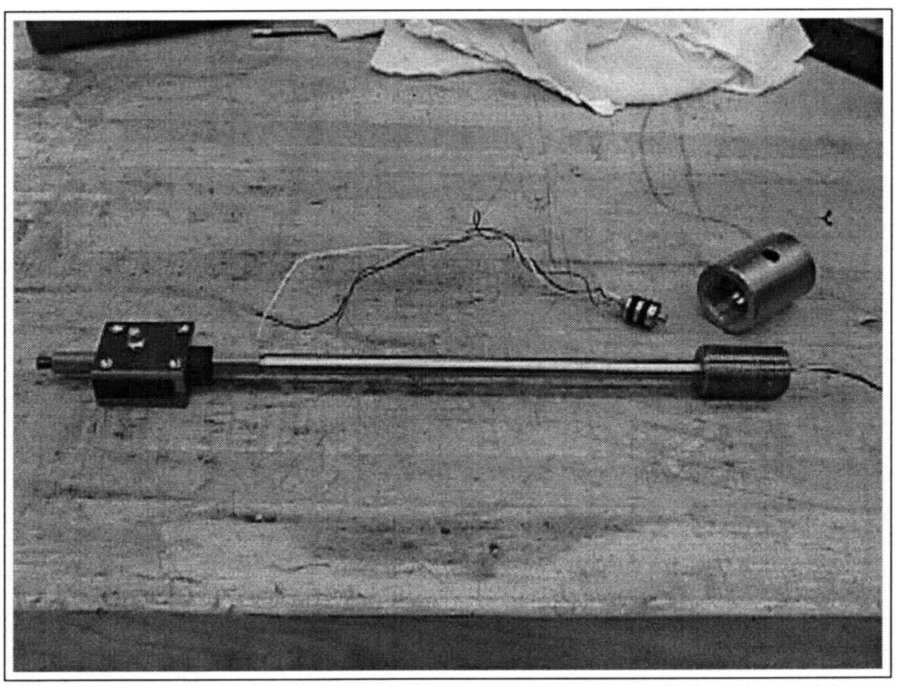

Figure 3-8: Picture of Load Cell Components

3.4 Housing Assembly

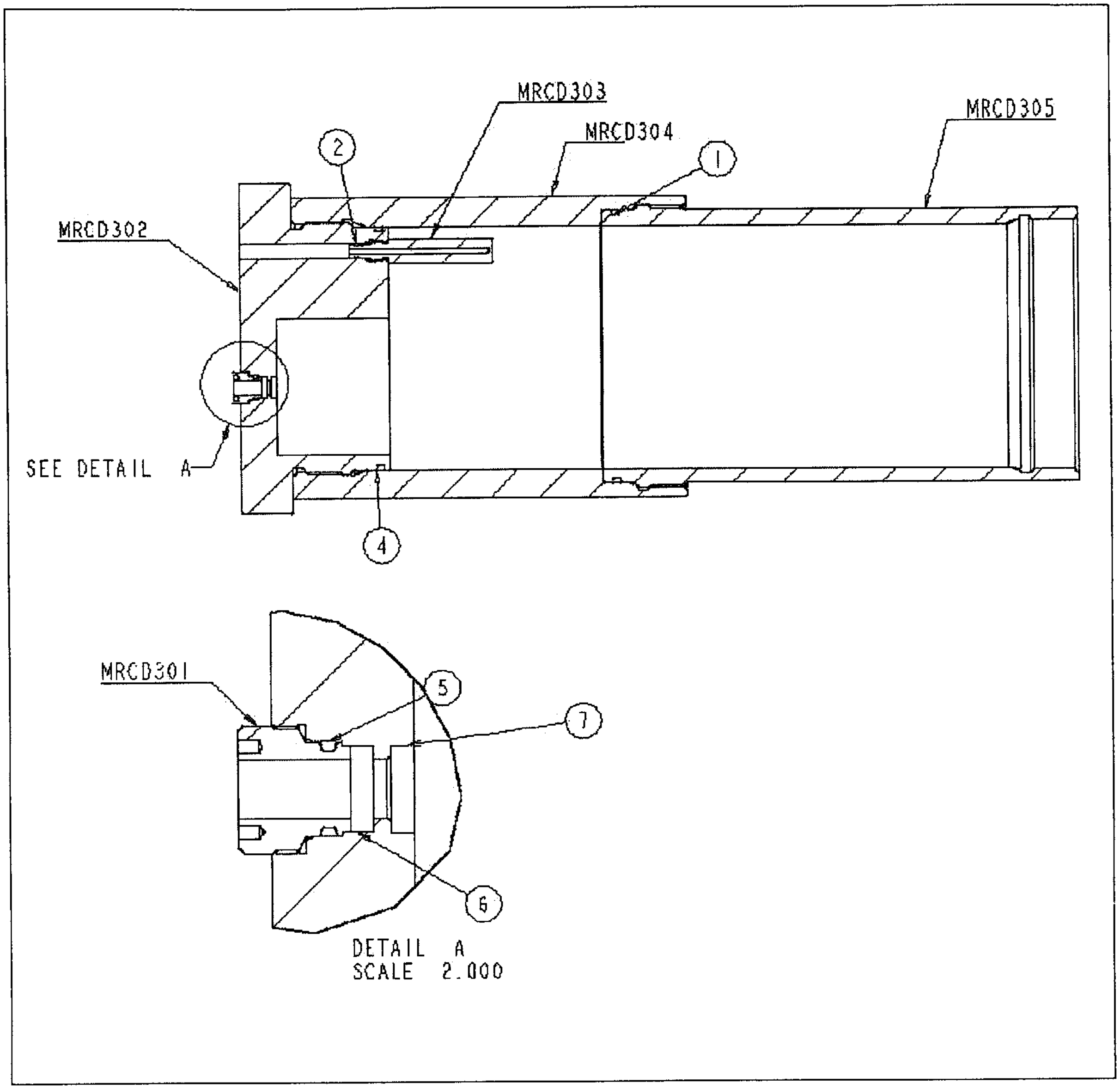

Figure 3-9: Cross-Section of the Housing Assembly

Figure 3-9 shows a cross sectional drawing of the housing assembly. The rod penetrates the pressurized vessel through the o-ring cap (mrcd301) and the top cap (mrcd302). It maintains a seal with a Green Tweed 2510 rod seal (6), which is the same low friction seal used in the prototype (see Appendix A.3 for specifications). During the assembly of the prototype, it was very difficult to place the o-ring inside the top cap because of its small size and required tight tolerances. Thus, in this design, an o-ring cap is machined leaving enough space in the top cap for the o-ring to slide in easily. The o-ring is then secured in place with the o-ring cap.

A Shamban Turcite Excluder(7) sits at the end of the top cap to scrape the mud off from the rod and give the rod more stability. This is the same excluder used in the prototype and it is held in place with a seal retainer (see Figure A-5 in Appendix A.2 for part drawing).

To measure the temperature inside the vessel, the thermocouple housing (mrcd303) is screwed to the bottom of the cap. This housing allows a thermocouple to slide from the top of the cap to the inside of the housing. The top cap also has a 1/4 inch diameter orifice with a 1/4-18NPT thread which is connected to the pressure line of the nitrogen tank. See Figure B-7 in Appendix B.1 for engineering drawing of the top cap to see this feature.

Standard o-rings used at Schlumberger (1), (2), (4) and (5) are placed in this assembly to maintain a full seal of the pressurized vessel.

3.5 Air Cylinder Actuator

A Bimba Stainless Steel Body Air Cylinder is used to displace the actuator rod (see Figure B-27 in Appendix B.2 for air cylinder specifications). It is connected to the rod (mrcd316) by screwing it to the shaft connector (mrcd317). Once the vessel has been pressurized, the rod will be pushed up by the pressure force [2]. Thus to maintain the rod stationary, the cylinder has to counter acts this force, acting as a stopper. To pull the test piece free, air is let out slowly from the air cylinder until the rod begins to move. The main function of the actuator, then, is to control the speed of the upward motion. If however, the sticking force is higher than the pressure force, the air cylinder needs to apply an additional upward force, acting as an actuator. The air cylinder can apply up to 500 lbs of force in either direction if given an air

[2]If pressurized at a 1000 psi, the rod will push upwards with 250 lbs. This is calculated by multiplying the pressure times the area the pressure is applying. This area corresponds to the diameter of the pressure bulk head.

pressure of 100 psi (this is the air pressure at the Schlumberger laboratory facility).

Note that the inside diameter of the actuator rod is at the same pressure as the vessel because it has not been sealed. Therefore, the load cell is pressure balanced and it does not measure any pressure force.

3.6 Full Assembly

The test stand is assembled by screwing three 1/2-20UNF-2A thread rods to the bottom plate (mrcd318). These rods are held in place by screw nuts and with a spacer between the nut and the plate to secure the rods. The middle plate (mrcd319) is placed 21.25 inches above the bottom plate resting on the nuts, which have been screwed into the rods at that height. Three additional nuts are screwed on top of the middle plate to secure it. See Figure 3-1 and Figure 3-10 for a schematic of the total assembly.

The housing assembly (Figure 3-9) and the load cell assembly (Figure 3-6) are fitted together and placed on the middle plate. The bottom filter assembly (Figure 3-3) is then screwed to the housing assembly. However, because the test piece and the filter assembly are non-concentric, the test piece could jam against the inside of the filter during the process. To prevent this from happening, the test piece and actuator rod must be pulled up as far as possible. When the assembly process is almost completed, the actuator rod is slid down until it hits the bottom cap and the bottom filter assembly is screwed in until the side of the test piece hits the inside of the filter. This final step can be easily done even though one cannot see the point of contact.

Next, the top plate (mrcd 320) is placed about 1/2 inch above the vessel and the air cylinder is assembled on top of it as shown in Figure 3-10. An aluminum plate, which is held above the plate with two rods, has a hole cut out for the air cylinder. The cylinder is placed face down on this plate and it is screwed to the shaft connector (mrcd 317). It should be noted that because the aluminum plate and rods were machined in the laboratory, precise engineering drawings do not exist. Finally

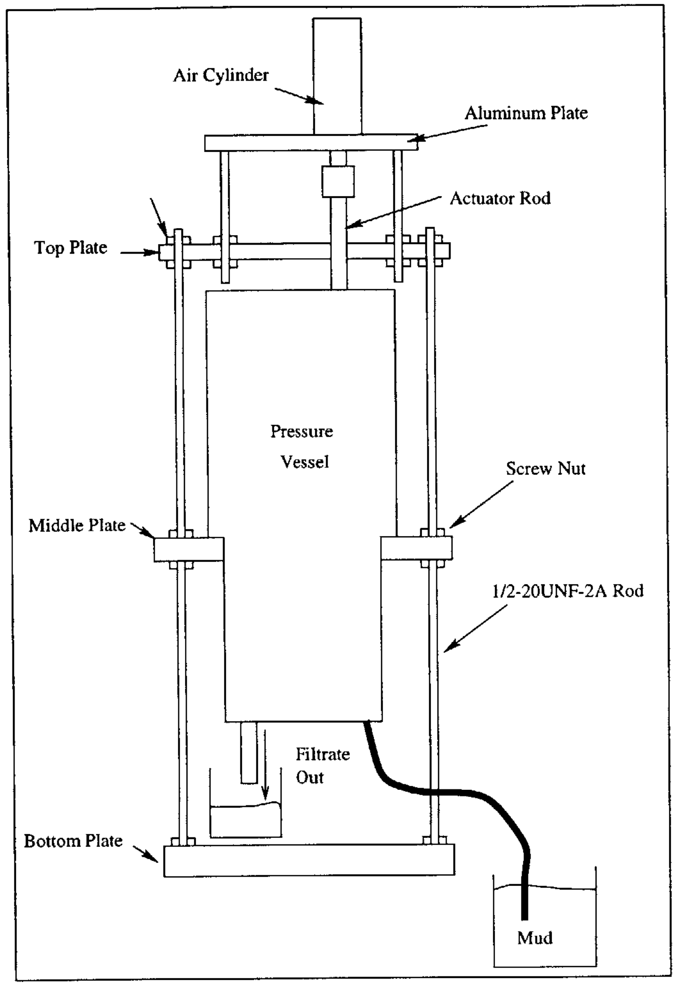

Figure 3-10: Schematic of Full Assembly

the nitrogen tank is hooked to the tester through a hose connected to the 1/4-18NPT opening in the top cap.

3.7 Testing Procedures

To perform a test, the following steps are necessary:

1. Fill the vessel with mud.

2. Pressurize the vessel to filter mud and build mudcake.

3. Move test piece down until it touches the bottom of the Pressure Line Screw. (This procedure will scrape the mudcake of the filter wall, breaking the seal).
4. Let the test piece stand stationary for a determined time interval.
5. Pull up the test piece slowly and measure the peak force.
6. Let the test piece remain stationary for a time interval and and repeat step (5).
7. Repeat step (5) and (6) until the test piece has moved up 2 inches from its original position (the point at which the test piece is no longer touching the whole face of the filter).
8. Plot the force against time.
9. Depressurize the vessel.
10. Drain the mud.
11. Unscrew the bottom piece to change filter or test piece.

To fill the vessel with mud, a vacuum pump is connected to the 1/4-18NPT opening on the top cap and the bottom cap is connected to a hose and a bucket of mud. To control the mud flow, an open/close valve is screwed to the bottom cap and connected to the hose. The vacuum pump sucks the mud into the vessel until the mud starts flowing out of the top cap. The valve is then closed and the vacuum pump is unhooked from the vessel. The nitrogen tank is hooked at that same point.

Place an open/close valve to the 1/4-NPT pressure line opening on the bottom cap. Open this valve as soon as the vessel is pressurized. This will produce a differential pressure across the filter and begin filtering the mud.

To perform force measurements, hook the load cell wires coming out of the shaft connector to a 10VDC power supply and a ohm meter. The microvolt measurements are converted to force. (see Figure B-30 in Appendix B.3 for calibration sheet).

To drain the mud, apply a few psi to the vessel and open the mud valve.

Chapter 4

Testing and Recommendations

4.1 Test Results

See Figure 4-1 for a picture of the assembled Stickance Tester during testing. The tester is connected to the nitrogen tank, and the mud is filtered and drained to a container at the bottom. To the left of the Tester is the vacuum pump, which has been used to fill the Tester with mud. The air cylinder is connected to an air pressure line.

A total of six tests were performed. For the first test, the Tester was filled with water and pressurized to 1000 psi in order to check for any leaks and for overall functionality. The low pressure line valve was opened, and the water flowed through the filter as expected.

The next five tests were performed with 9 lb/gal, 10 lb/gal and 11 lb/gal density water-based mud. Two different pore size ceramic filters were tested, 35 micro-inch and 60 micro-inch. However, when the Tester was filled with mud and pressurized, the filters were found to break at 400 psi. The manufacturer of the filters had not guaranteed a 1000 psi differential pressure but had believed that it would not be a problem. This was not the case.

Because the filters were found to break at 400 psi, the tests were completed only to 350 psi. The lower pressure caused the mudcake to form at a slower rate. After four hours of filtering, only 1/4 inch mudcake was built. See Figure 4-2 for a picture

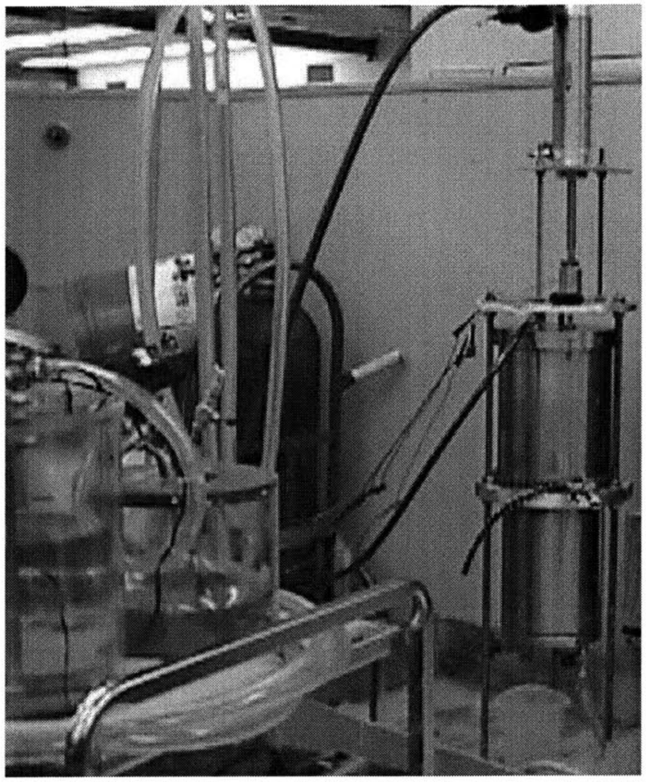

Figure 4-1: Picture of The Full Assembled Stickance Tester

of the mudcake formed inside the filter. In addition, the thin mudcake caused the sticking forces to be much smaller than predicted. Because the load cell was designed to measure forces up to 500 lbs, the accuracy was reduced when smaller forces were measured. Thus, the force measurements did not show a drastic change when plotted against time.

During assembly and disassembly, it became very hard to screw the filter assembly to the Stickance Tester. The large weight of the filter assembly and the necessity of screwing it in from below made the process extremely difficult. A lever arm was finally used to help with the weight.

Figure 4-2: Picture of Mudcake Inside the Filter

4.2 Conclusion and Recommendations

The Stickance Tester design worked well. The load cell inside the pressurized vessel maintained a simple design and eliminated any force measurement errors resulting from the pressure force or the seal. The air cylinder also worked well allowing easy control of the displacement of the rod. The filtering mechanism was effective and the filling, pressurizing and draining of mud was simple.

However, other types of filters need to be found. Even though the present ceramic filters are effective, they can not withstand the 1000 psi differential pressure that is required to build a thick mudcake in a short amount of time. Therefore, it is recommended to change the type of filter or design a filter retainer to prevent the filter from expanding and breaking.

Even though the filtering mechanism worked well, a solution to screwing and unscrewing the Filter Assembly needs to be designed. If this same design is maintained, then a lifting mechanism needs to be added to the tester. A hydraulic pump or a ball screw actuator could be used to lift the filter assembly and screw it to the bottom of the tester.

Finally, a sensor with higher accuracy for smaller forces needs to be used. It is predicted, that the sticking forces will be high when pressurized at 1000 psi. However, for a more flexible design, a load cell that is accurate for a whole range of forces would be optimal.

Appendix A

Prototype

A.1 Dynamic Fluid Loss Cell

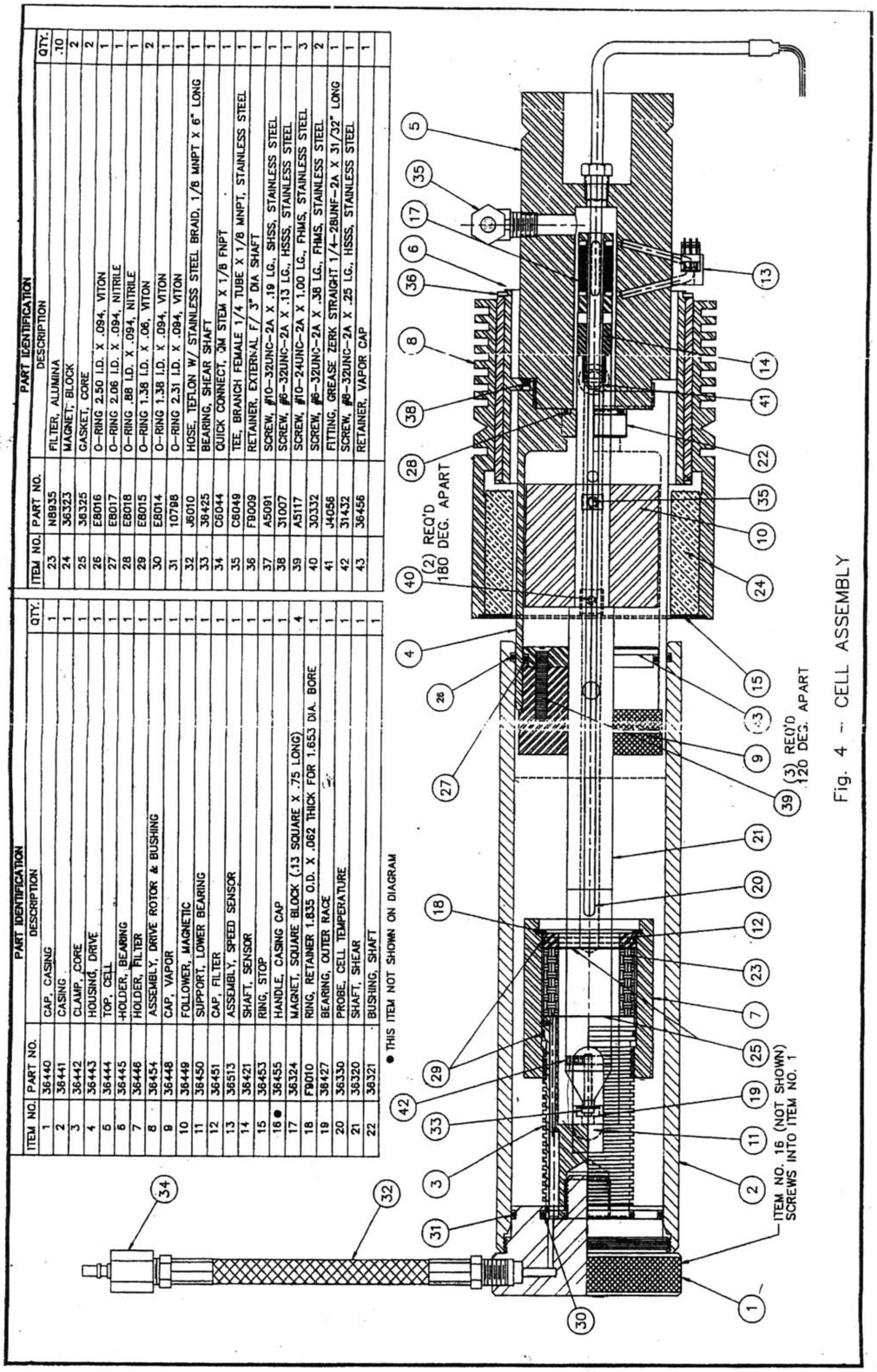

PART IDENTIFICATION

ITEM NO.	PART NO.	DESCRIPTION	QTY.
1	36440	CAP, CASING	1
2	36441	CASING	1
3	36442	CLAMP, CORE	1
4	36443	HOUSING, DRIVE	1
5	36444	TOP, CELL	1
6	36445	HOLDER, BEARING	1
7	36446	HOLDER, FILTER	1
8	36454	ASSEMBLY, DRIVE ROTOR & BUSHING	1
9	36448	CAP, VAPOR	1
10	36449	FOLLOWER, MAGNETIC	1
11	36450	SUPPORT, LOWER BEARING	1
12	36451	CAP, FILTER	1
13	36513	ASSEMBLY, SPEED SENSOR	1
14	36421	SHAFT, SENSOR	1
15	36453	RING, STOP	1
16●	36455	HANDLE, CASING CAP	1
17	36324	MAGNET, SQUARE BLOCK (.13 SQUARE X .75 LONG)	4
18	F9010	RING, RETAINER 1.835 O.D. X .062 THICK FOR 1.653 DIA. BORE	1
19	36427	BEARING, OUTER RACE	1
20	36330	PROBE, CELL TEMPERATURE	1
21	36320	SHAFT, SHEAR	1
22	36321	BUSHING, SHAFT	1

● THIS ITEM NOT SHOWN ON DIAGRAM

PART IDENTIFICATION

ITEM NO.	PART NO.	DESCRIPTION	QTY.
23	N8935	FILTER, ALUMINA	.10
24	36323	MAGNET, BLOCK	2
25	36325	GASKET, CORE	2
26	E8016	O-RING 2.50 I.D. X .094, VITON	1
27	E8017	O-RING 2.06 I.D. X .094, NITRILE	1
28	E8018	O-RING .88 I.D. X .094, NITRILE	1
29	E8015	O-RING 1.38 I.D. X .06, VITON	2
30	E8014	O-RING 1.38 I.D. X .094, VITON	1
31	10788	O-RING 2.31 I.D. X .094, VITON	1
32	J6010	HOSE, TEFLON W/ STAINLESS STEEL BRAID, 1/8 MNPT X 6" LONG	1
33	36425	BEARING, SHEAR SHAFT	1
34	C6044	QUICK CONNECT, OM STEM X 1/8 FNPT	1
35	C6049	TEE, BRANCH FEMALE 1/4 TUBE X 1/8 MNPT, STAINLESS STEEL	1
36	F9009	RETAINER, EXTERNAL F/ 3" DIA SHAFT	1
37	A5091	SCREW, #10-32UNC-2A X .19 LG., SHSS, STAINLESS STEEL	1
38	31007	SCREW, #6-32UNC-2A X .13 LG., HSSS, STAINLESS STEEL	1
39	A5117	SCREW, #10-24UNC-2A X 1.00 LG., FHMS, STAINLESS STEEL	3
40	30332	SCREW, #6-32UNC-2A X .38 LG., FHMS, STAINLESS STEEL	2
41	J4056	FITTING, GREASE ZERK STRAIGHT 1/4-28UNF-2A X 31/32" LONG	1
42	31432	SCREW, #8-32UNC-2A X .25 LG., HSSS, STAINLESS STEEL	1
43	36456	RETAINER, VAPOR CAP	1

Figure A-1: Engineering Drawing of the Dynamic Fluid Loss Cell

A.2 Machined Parts

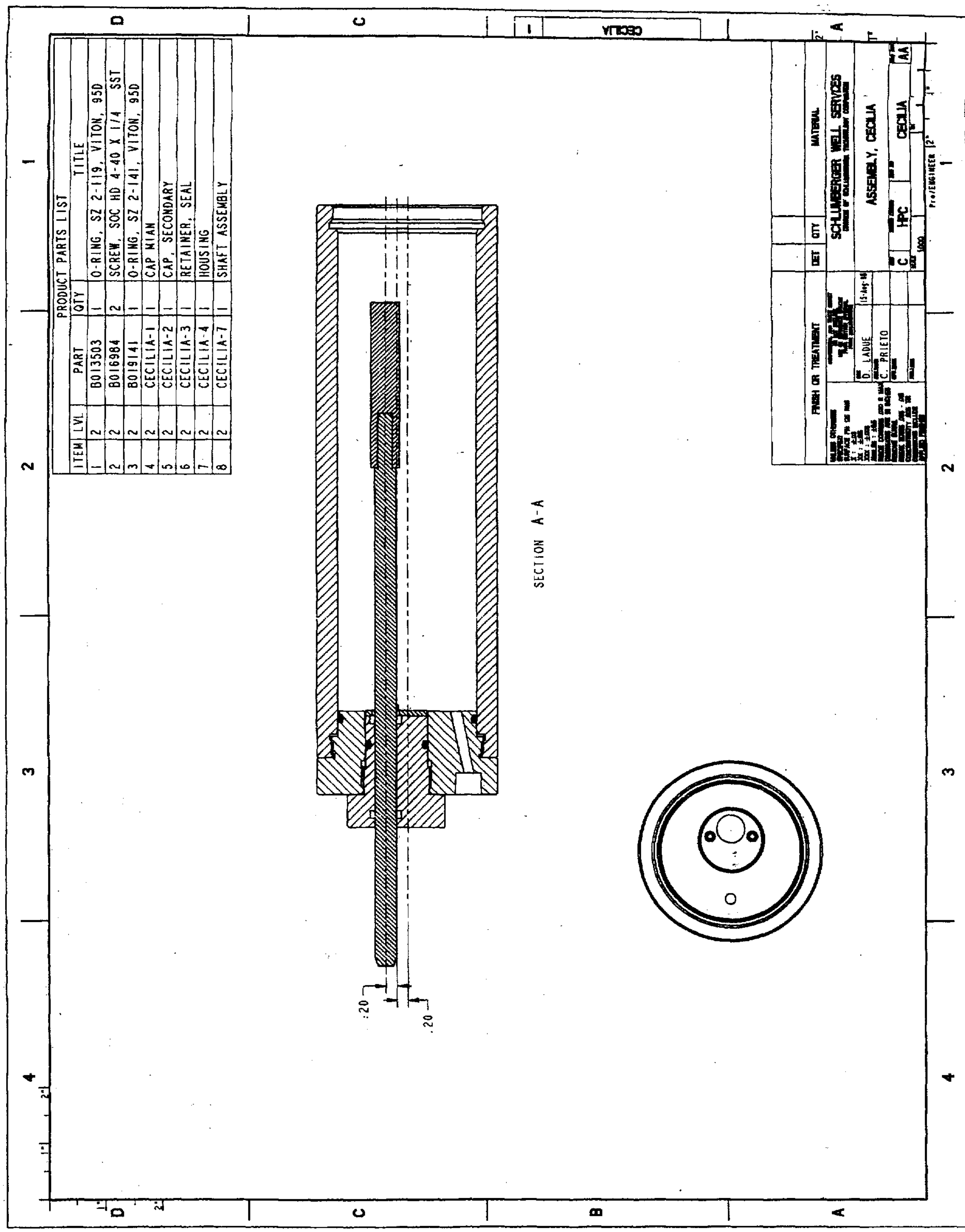

Figure A-2: Assembly of Prototypē

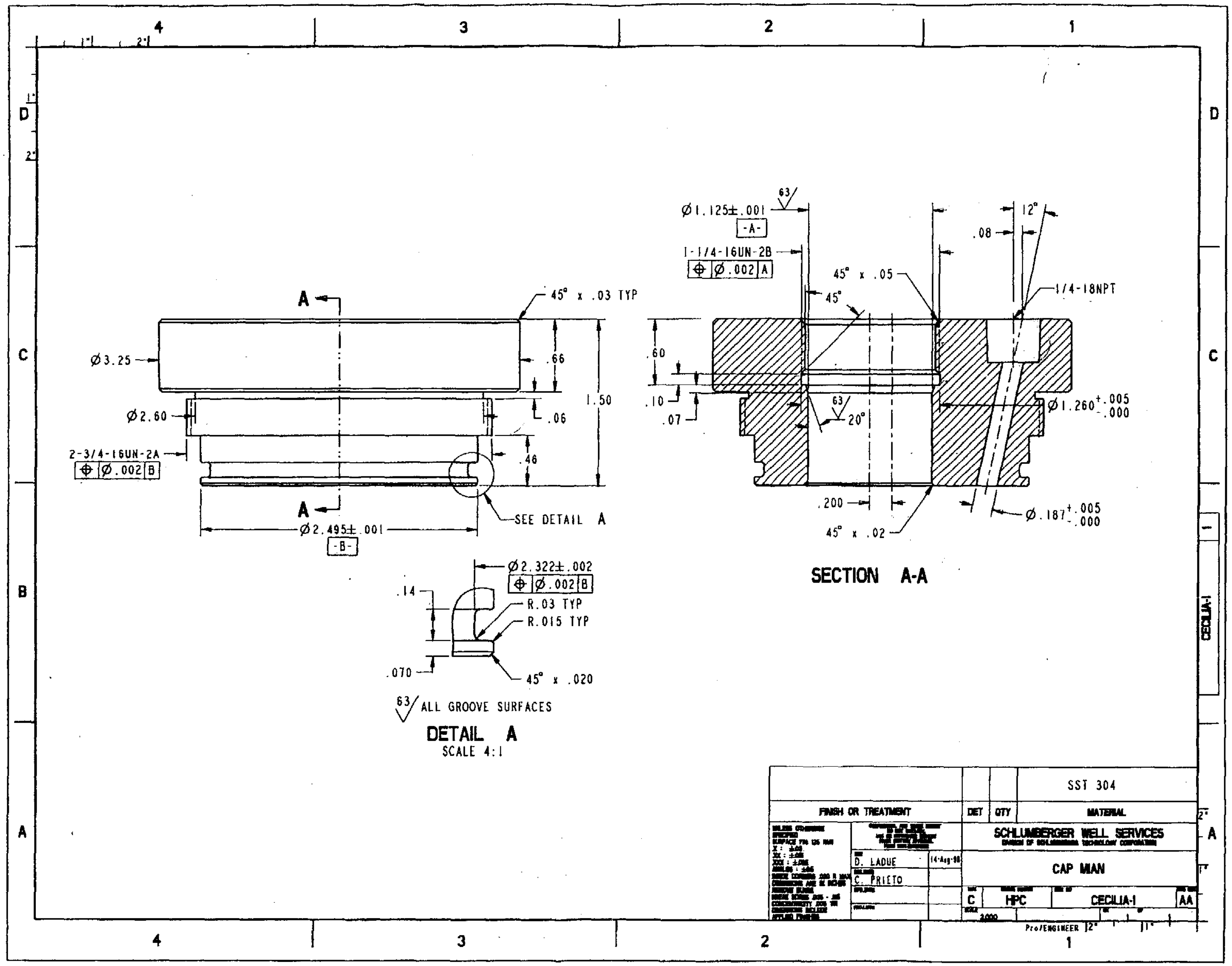

Figure A-3: Top Cap

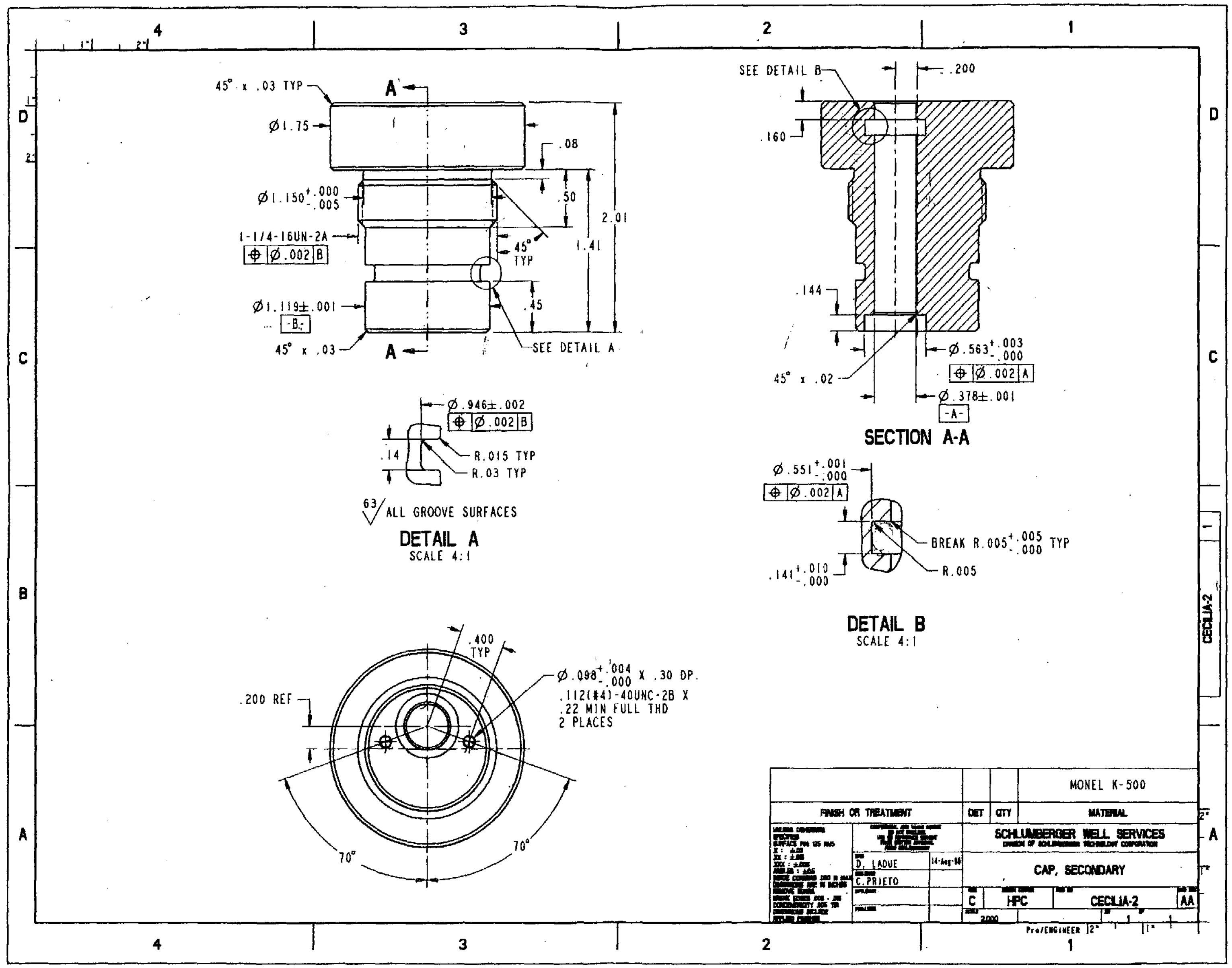

Figure A-4: Middle Cap

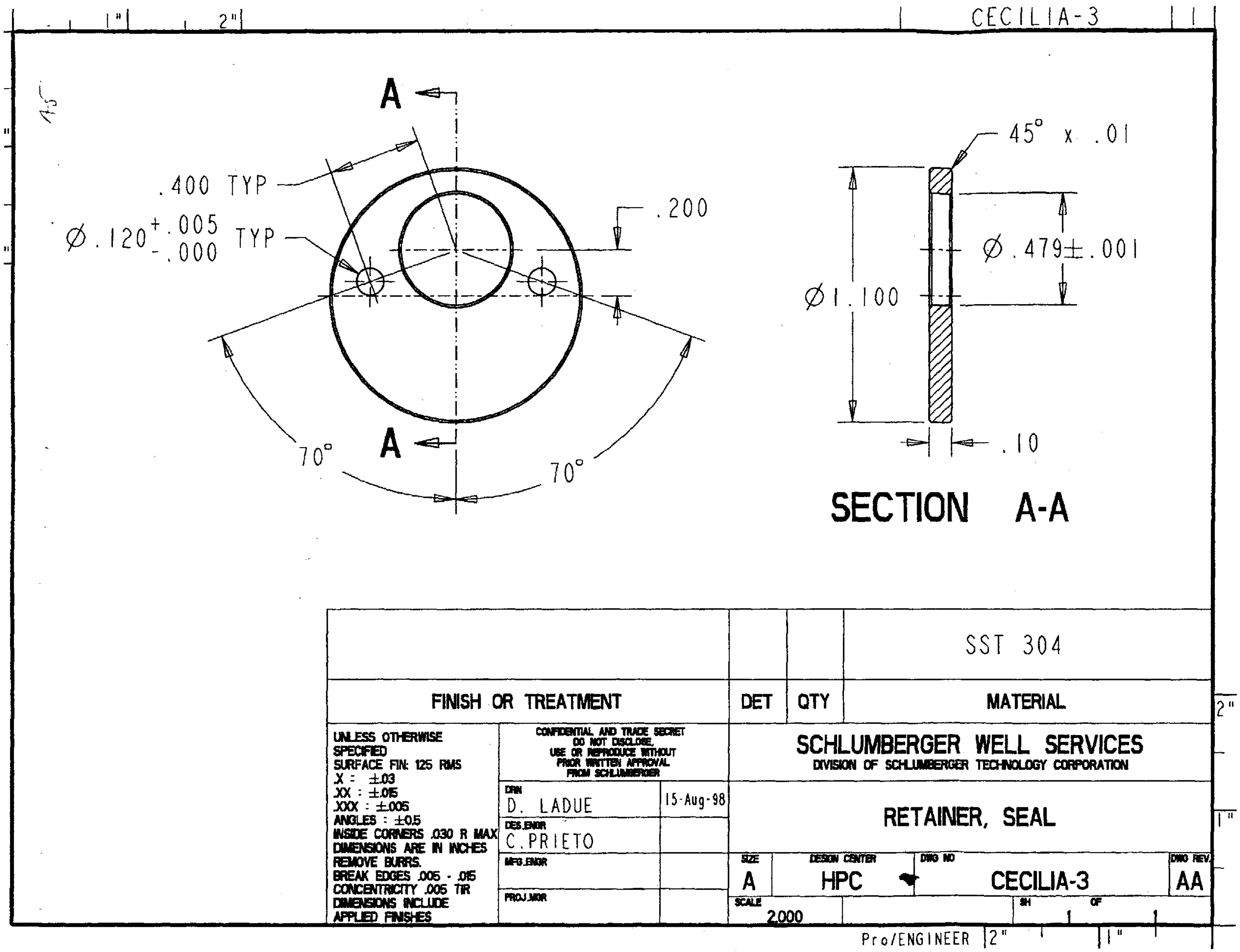

Figure A-5: Seal Retainer

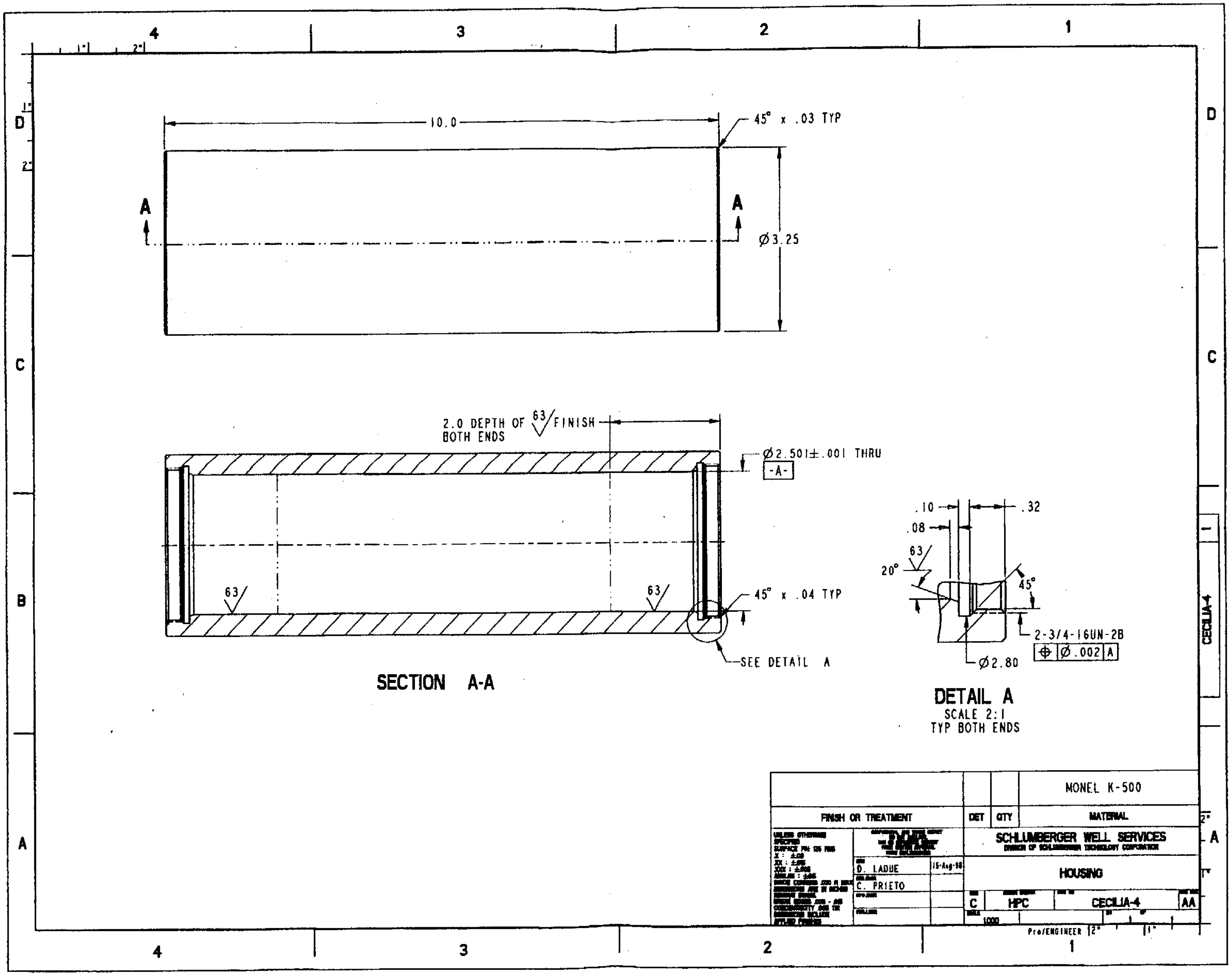

Figure A-6: Housing

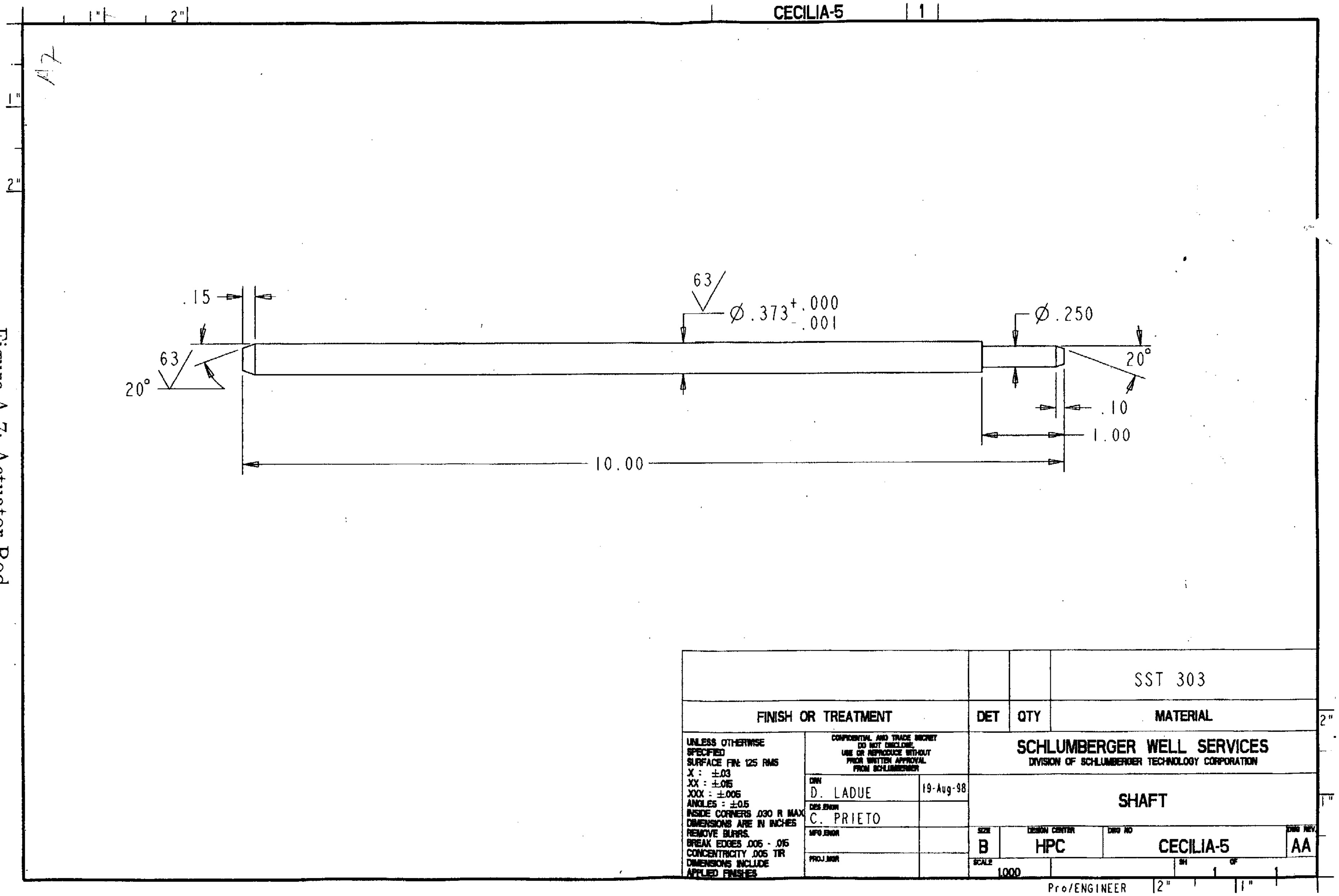

Figure A-7: Actuator Rod

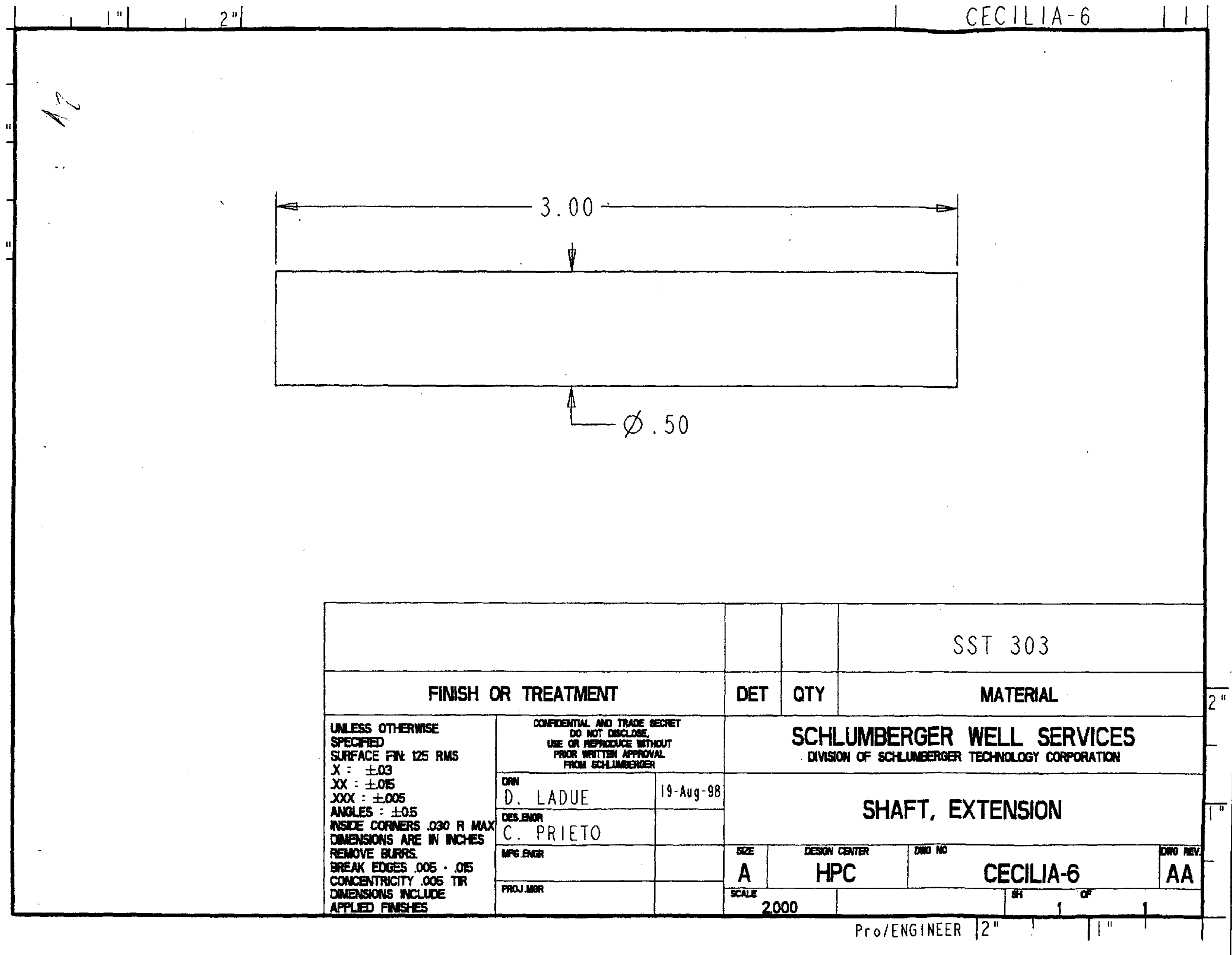

Figure A-8: Test Piece

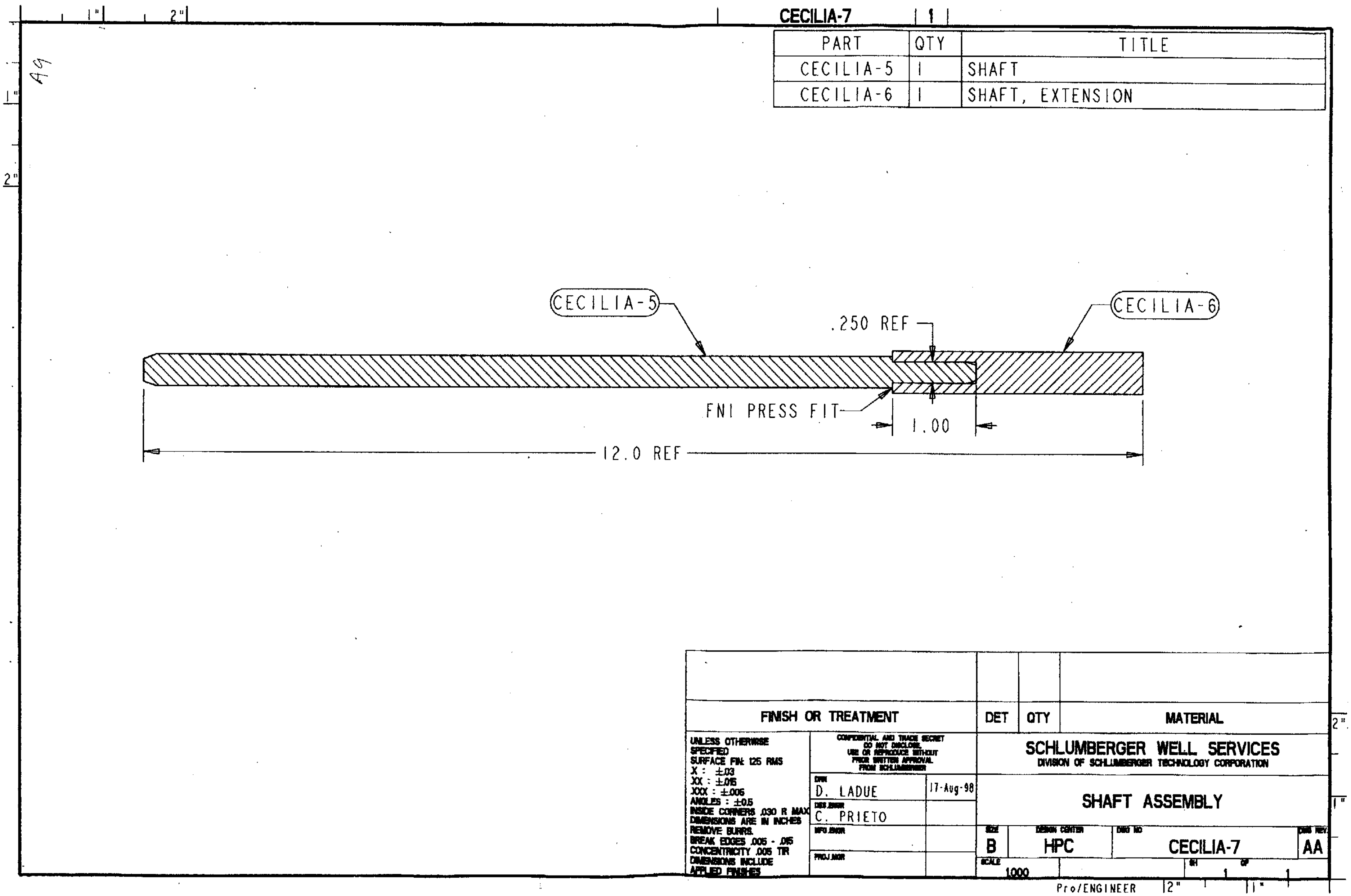

Figure A-9: Actuator Rod and Test Piece Assembly

A.3 Seal and Excruder Specifications

GREENE, TWEED ADVANCAP™ 2510 ROD SEALS

FOR *NO*-BACKUP RING GLAND PER MIL-G-5514F

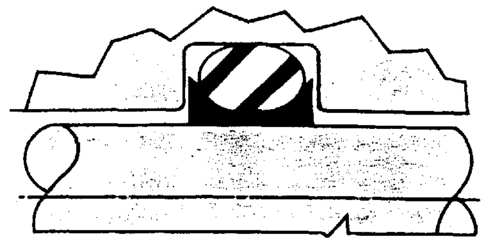

- OPERATE WITH LOW FRICTION
- ELIMINATE "O" RING SPIRAL FAILURE
- PREVENT EXTRUSION
- USE STANDARD "O" RINGS

HOW TO SPECIFY

2510 | ___ | _____ | ___ - _____ - ___

2510	_	___	__	___	__
Series Number	N = notched caps U = caps without notches	Dash size no. (Table 3)	Non-standard size indicator to be assigned by Advantec Engineering	GTC material code (Table 1)	O-ring elastomer type code (Table 2)

TABLE 1
CAP MATERIAL SELECTION

MATERIAL CODE	DESCRIPTION	USE
019	(P4) Graphite Filled PTFE	Low friction material with good wear properties. Recommended for static and dynamic applications at low and high pressure.
022	(P5) Glass & MoS_2 Filled PTFE	Good extrusion resistance & wear properties. Recommended for high pressure & loads. (Not recommended with soft metals i.e., aluminum.)
041	(P1) ENERLON™ Pigmented PTFE	Similar to virgin PTFE, but with improved wear properties.
069	AVALON 50	High-temperature, wear resistant. For high-temperature, high surface speed applications. (May abrade soft metals)
096	ROTOLON 100 Glass, MoS_2, PTFE	High-pressure-, wear-, extrusion-resistant. For high-pressure, high-temperature, high loads, high surface speed applications. (Not recommended for sealing against soft metals)

TABLE 2
OPTIONAL "O" RING ENERGIZER SELECTION

DESIGNATOR	ELASTOMER MATERIAL	ELASTOMER SPECIFICATION	TEMPERATURE RANGE	SERVICE
11	Nitrile	MIL-P-25732	− 65 to 275F	MIL-H-5606 Fluid
12	Nitrile	MIL-P-83461	− 65 to 275F	MIL-H-83282 Fluid
13	Nitrile	MIL-P-5315	− 65 to 225F	Jet fuels
21	Ethylene Propylene	NAS 1613	− 65 to 300F	Skydrol, Aerosafe and similar phosphate-based fluids
31	Fluorocarbon	MIL-R-83248 Class 1	− 20 to 437F	High-temperature hydrocarbon and synthetic fluids. Di-ester lubricant, MIL-L-7808, Oronite 8515, MIL-L-6085, and silicone fluids and greases.
00	If "O" ring is to be ordered as separate component.			

NOTE: For pressures above 3000 psi, clearances above standard and alternative cap and energizer materials, contact Advantec, Division of Greene, Tweed Industries, (714) 893-0903.

Figure A-10: Green Tweed Rod Seals

2510 ROD SEALS

FOR *NO*-BACKUP RING GLAND PER MIL-G-5514F

ROD SEAL INSTALLATION

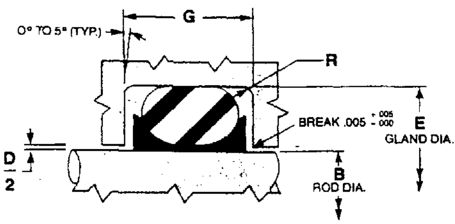

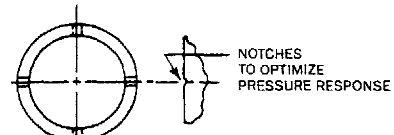

NOTCHES ARE RECOMMENDED ON ALL SEALS WITH ALTERNATE PRESSURE ON BOTH SIDES OF THE SEAL; I.E. PISTON APPLICATIONS.

TABLE 3
DIMENSIONAL INFORMATION

AS 568A UNIFORM DASH NO	E DIA.	B DIA.
	+.001 −.000	+.000 −.001
006	.235	.123
007	.266	.154
008	.297	.185
009	.329	.217
010	.360	.248
011	.422	.310
012	.485	.373
	+.002 −.000	+.000 −.002
013	.547	.435
014	.610	.498
015	.672	.560
016	.735	.623
017	.797	.685
018	860	.748
019	.922	.810
020	.985	.873
021	1.047	.935
022	1.110	.998
023	1.172	1.060
024	1.235	1.123
025	1.297	1.185
026	1.360	1.248
027	1.422	1.310
028	1.485	1.373
110	.551	.373
111	.613	.435
112	.676	.498
113	.738	.560
114	.801	.623
115	.863	.685
116	.926	.748
117	.988	.810
118	1.051	.873
119	1.113	.935
120	1.176	.998
121	1.238	1.060
122	1.301	1.123
123	1.363	1.185
124	1.426	1.248

AS 568A UNIFORM DASH NO.	E DIA.	B DIA.
	+.002 −.000	+.000 −.002
125	1.488	1.310
126	1.551	1.373
127	1.613	1.435
128	1.676	1.498
129	1.738	1.560
130	1.801	1.623
131	1.863	1.685
132	1.926	1.748
133	1.988	1.810
134	2.051	1.873
135	2.114	1.936
136	2.176	1.998
137	2.239	2.061
138	2.301	2.123
139	2.364	2.186
140	2.426	2.248
141	2.489	2.311
142	2.551	2.373
143	2.614	2.436
144	2.676	2.498
145	2.739	2.561
146	2.801	2.623
147	2.864	2.686
148	2.926	2.748
149	2.989	2.811
210	.991	.748
211	1.053	.810
212	1.116	.873
213	1.178	.935
214	1.241	.998
215	1.303	1.060
216	1.366	1.123
217	1.428	1.185
218	1.491	1.248
219	1.553	1.310
220	1.616	1.373
221	1.678	1.435
222	1.741	1.498
223	1.866	1.623
224	1.991	1.748
225	2.116	1.873
226	2.241	1.998
227	2.366	2.123

AS 568A UNIFORM DASH NO.	E DIA.	B DIA.
	+.002 −.000	+.000 −.002
228	2.491	2.248
229	2.616	2.373
230	2.741	2.498
231	2.866	2.623
232	2.991	2.748
233	3.116	2.873
234	3.240	2.997
235	3.365	3.122
236	3.490	3.247
237	3.615	3.372
238	3.740	3.497
239	3.865	3.622
240	3.990	3.747
241	4.115	3.872
242	4.240	3.997
243	4.365	4.122
244	4.490	4.247
245	4.615	4.372
246	4.740	4.497
247	4.865	4.622
325	1.870	1.498
326	1.995	1.623
327	2.120	1.748
328	2.245	1.873
329	2.370	1.998
330	2.495	2.123
331	2.620	2.248
332	2.745	2.373
333	2.870	2.498
334	2.995	2.623
335	3.120	2.748
336	3.245	2.873
337	3.369	2.997
338	3.494	3.122
339	3.619	3.247
340	3.744	3.372
341	3.869	3.497
342	3.994	3.622
343	4.119	3.747
344	4.244	3.872
345	4.369	3.997
346	4.494	4.122
347	4.619	4.247

AS 568A UNIFORM DASH NO.	E DIA.	B DIA.
	+.002 −.000	+.000 −.002
348	4.744	4.372
349	4.869	4.497
	+.003 −.000	+.000 −.003
425	4.974	4.497
426	5.099	4.622
427	5.224	4.747
428	5.349	4.872
429	5.474	4.997
430	5.599	5.122
431	5.724	5.247
432	5.849	5.372
433	5.974	5.497
434	6.099	5.622
435	6.224	5.747
436	6.349	5.872
437	6.474	5.997
438	6.724	6.247
439	6.974	6.497
440	7.224	6.747
441	7.474	6.997
442	7.724	7.247
443	7.974	7.497
444	8.224	7.747
445	8.474	7.997
446	8.974	8.497
	+.004 −.000	+.000 −.003
447	9.474	8.997
448	9.974	9.497
449	10.474	9.997
450	10.974	10.497
451	11.474	10.997
452	11.974	11.497
453	12.474	11.997
454	12.974	12.497
455	13.474	12.997
456	13.974	13.497
457	14.474	13.997
458	14.974	14.497
459	15.474	14.997
460	15.974	15.497

TABLE 4
GLAND DIMENSIONS

DASH NO.	G GROOVE WIDTH	R RADIUS	D DIAMETRAL CLEARANCE
	+.010 −.000		MAX.
006/012	.094	.005/.015	.004
013/028	.094	.005/.015	.005
110/126	.141	.005/.015	.005
127/132	.141	.005/.015	.006
133/149	.141	.005/.015	.007
210/222	.188	.010/.025	.005
223/224	.188	.010/.025	.006
225/245	.188	.010/.025	.007
246/247	.188	.010/.025	.008
325/327	.281	.020/.035	.006
328/349	.281	.020/.035	.007
425/438	.375	.020/.035	.00[illegible]
439/460	.375	.020/.035	.010

***O-RING SQUEEZE LEVEL**

The addition of any cap to an O-ring gland will increase O-ring squeeze and gland occupancy. This may result in excessive friction, unsatisfactory service life or installation difficulty.
By increasing the gland diameter, as shown in Table 5, these problems can be alleviated without reducing O-ring squeeze below the minimum of MIL-G-5514F.

TABLE 5
GLAND DIAMETER CHANGE

O-RING DASH NO.	006 thru 028	110 thru 149	210 thru 247	325 thru 349	425 thru 460
"E" DIA.	010"	010"	018"	018"	025"

GREENE, TWEED & CO., Inc. *At the Forefront of Sealing Technology*

P.O. Box 305 • Detwiler Road • Kulpsville, PA 19443-0305 • (215) 256-9521 • TLX: 6851164 GRN TWD • Fax. (215) 256-0189

Wholly-owned subsidiaries and divisions:

GREENE, TWEED & CO., LTD
Finch Close Nottingham NG7 2NN England
Tel: 0602-866555 TLX: 378248 GRN TWD-G
Fax. 0602-866235

GREENE, TWEED & CO. France S.A.
9 Chaussée Jules César
95520 Osny Cergy-Pontoise France
Tel: (1) 3073.54.44 TLX: GTCFRA 609099F
Fax. 130734575

GREENE, TWEED & CO. GmbH
Kirchstrasse 9
6240 Koenigstein/TS, W. Germany
Tel: 06174-3073/74 TLX: 410872 GTC D
Fax. 617422012

GREENE, TWEED & CO., Japan
Room 710, Furuinto-Mita Bldg. 14-5,
Mita 2-Chome, Minato-Ku, Tokyo 108 Japan
Tel: 03-454-1050 Fax. 03-454-1040

ENGINEERED PLASTICS
A division of Greene, Tweed & Co., Inc.
P.O. Box 578, 1880-B North Penn Road,
Hatfield, PA 19440 Tel: (215) 997-2555
TLX: 6851164 GRN TWD Fax. (215) 997-2490

PALMETTO, Inc.
Denton Industrial Park, 25 Engerman Ave.
Denton, MD 21629, Tel: (301) 479-2244
Fax. (301) 479-0836

ADVANTEC
A division of Greene, Tweed Industries, Inc.
7101 Patterson Drive, Box 5037
Garden Grove, CA 92645-5037
Tel: (714) 897-0515
Fax. (714) 373-1763
District Sales Offices
Atlanta, GA (404) 491-9434 Fax: (404) 593-3520
Boston, MA (508) 392-0696 Fax: (508) 392-0838
Chicago, IL (708) 851-9063 Fax: (708) 851-9083
Cleveland, OH (216) 292-6066 Fax: (216) 292-6076
Houston, TX (713) 537-5112 Fax: (713) 537-0197
Garden Grove, CA (714) 897-0515
Fax: (714) 373-1763

Figure A-11: Green Tweed Rod Seals

Shamban Turcite® Excluder®

● CONTAMINATION BARRIER ● SCRAPER RING ● SECONDARY SEAL

The Multi-Purpose PTFE® Wiper for Industrial Fluid Power Piston Rods and Valve Spools

- Seals out fine particle contamination
- Scrapes and cleans without damaging rod
- Offers low friction of filled PTFE®-Turcite®
- Protects primary rod seal and acts as secondary seal
- Prevents rod scoring and improves service life
- Installs quickly and easily • Rugged and dependable

Excluder Assembly is made up of an Excluder ring and an o-ring.

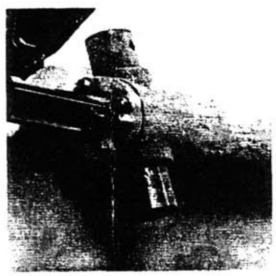

Hydraulic Actuator after cycling tests under exposure to a turbulent environment containing Arizona road dust.

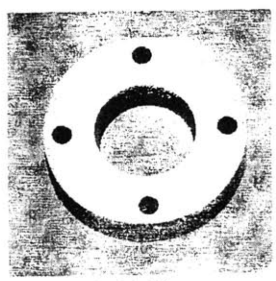

Inside View

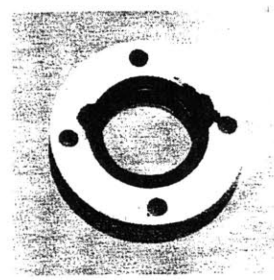

Outside View

Gland as removed after test of the hydraulic actuator shown above

Shamban has proven the effectiveness of the Excluder in actual field tests. Dust and other abrasive contaminating materials such as would be encountered on skip loaders, power steering units, machine tools and hydraulic or pneumatic presses, are prevented by the Excluder from migrating into rod end bearings and seals, or on into the entire fluid power system.

In critical applications when damage or wear of a primary rod seal can cause loss of hydraulic fluid and system pressure, the Excluder as a *secondary seal* will provide an additional margin of safety by preventing excessive leakage until repairs can be made.

The total effect of the Excluder means that hydraulic and pneumatic actuators and valves can be completely protected from external contamination and when unexpected rod seal replacement becomes necessary, it can be accomplished at a convenient time due to the interim fluid sealing capability of the Excluder, even at high pressure. Thus maintenance costs and unscheduled over-haul are significantly reduced.

Shamban Turcite Excluders are available in standard sizes ranging from a nominal 1/4" to 13" dia. rod. See reverse side for complete listing of standard sizes and hardware design details.

SHAMBAN SEALS DIVISION

INDUSTRIAL PRODUCTS GROUP

2531 BREMER DRIVE
P.O. BOX 176
FORT WAYNE, INDIANA 46801
219-749-9631 TELEX: 22-8480
TELEFAX: 219-749-0066

Figure A-12: Shamban Turcite Excluder

STANDARD SIZES AND HARDWARE DESIGN DETAILS

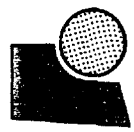

ROD SIZE NO.	USA STD. ROD DIA. B93.3 1968	SERIES 23E* REGULAR DUTY EXCLUDERS GROOVE DIA. A	SERIES 23E* ARP O-RING SIZE	SERIES 25E** LIGHT DUTY EXCLUDERS GROOVE DIA. A	SERIES 25E** ARP O-RING SIZE
	+.000 -.003	+.003 -.000		+.003 -.000	
00312	5/16	.500	012		
00375	3/8	.563	013		
00500	1/2	.768	113	.688	015
00625	5/8	.893	115	.813	017
00687	11/16	.955	116	.875	018
	+.000 -.004	+.004 -.000		+.004 -.000	
00750	3/4	1.018	117	.938	019
00875	7/8	1.143	119	1.063	021
01000	1	1.268	121	1.188	023
01125	1-1/8	1.393	123	1.313	025
01250	1-1/4	1.518	125	1.438	027
01375	1-3/8	1.643	127	1.563	028
	+.000 -.005	+.005 -.000		+.005 -.000	
01500	1-1/2	1.768	129	1.688	029
01750	1-3/4	2.018	133	1.938	031
02000	2	2.268	137	2.188	033
02250	2-1/4	2.518	141	2.438	035
02500	2-1/2	2.768	145	2.688	037
02750	2-3/4	3.098	233		
03000	3	3.348	235		
03500	3-1/2	3.848	239		
04000	4	4.348	243		
	+.000 -.006	+.006 -.000			
04500	4-1/2	4.848	247		
05000	5	5.348	251		
05500	5-1/2	5.848	255		
06000	6	6.348	258		
07000	7	7.348	262		
08000	8	8.348	266		
08500	8-1/2	8.848	268		
09000	9	9.348	270		
10000	10	10.348	274		

*Best for general purpose applications. Use in severe environments when maximum possible protection is necessary, when regular maintenance is limited or conditions of use are unpredictable. Best when Excluder must act as a secondary hydraulic seal.

**Adequate for most pneumatics.

GLAND DESIGN TABLE

ROD DIA.	GROOVE WIDTH G +.005 -.000	F MAX
SERIES NO. 23E		
5/16—3/8	.144	.053
1/2—2-1/2	.195	.068
2-3/4—10	.240	.078
SERIES NO. 25E		
1/2—2-1/2	.144	.053

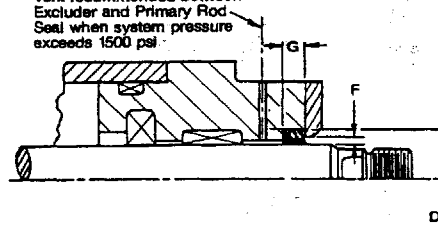

HOW TO ORDER
Use descriptive part number as follows

EXAMPLE 23E 00750 A 42
SERIES NO.
ROD SIZE NO.
O-RING CODE LETTER (See Table I)
EXCLUDER TURCITE CODE NO. (See Table II)

TABLE I

SEAL MATERIAL SELECTION O-Ring compound code letters for Shamban sealing system			
ENVIRONMENT		COMPOUND CODE LETTERS	
TYPE OF FLUID	TEMPERATURE	PREFERRED	ALTERNATE
AIR	Up to 250°F	A	H
Water and water based fluids		A	H
STEAM	Up to 300°F	H	C
Petroleum Oils including MIL-0-5606	-40° to 250°F	A	G, E
	-65° to 250°F	G	
SYNTHETIC OILS e.g. phosphate esters, skydrol, pydraul, etc.	-65° to 300°F	H	C E (Pydraul only)
A=BUNA-N, G=BUNA-N, C=BUTYL, H=ETHYLENE PROPYLENE E=VITON			

TABLE II

SEAL MATERIAL SELECTION Turcite® Code Numbers for Shamban Sealing Systems								
COMPONENT		ENVIRONMENT						
		PNEUMATIC				HYDRAULIC		
CODE LETTER	DESCRIPTION	Nitrogen, Air, Bottled Gas				Water and water based fluids	Petroleum and synthetic oils	
		DRY		LUBRICATED			2000 PSI	2000 PSI
		Up to 160°F	Up to 250°F	Up to 160°F	Up to 250°F	3000 PSI°F	Up to 180°F	Up to 250°F
E	EXCLUDERS™	46	46	42	42	46	42	42

Note: To specify excluder ring only substitute X for O-Ring compound Code Letter.

SD 002-A2

Figure A-13: Shamban Turcite Excluder

A.4 Test Results

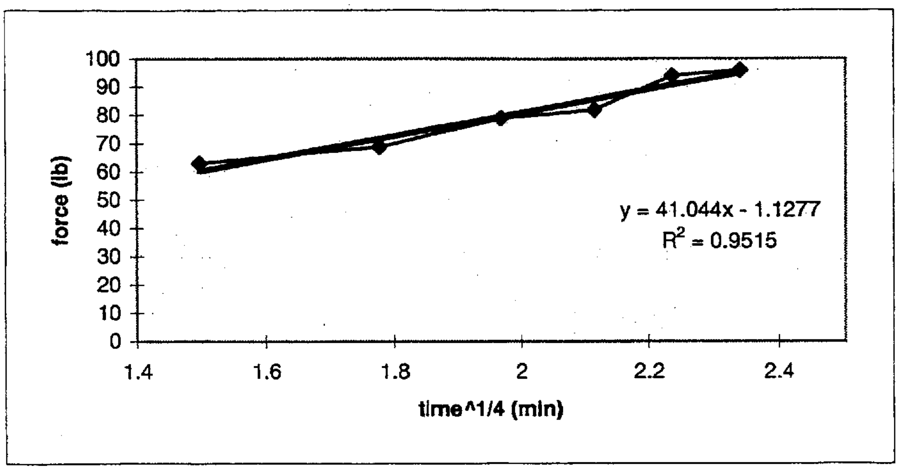

Figure A-14: Sticking Force versus Time, Test 1

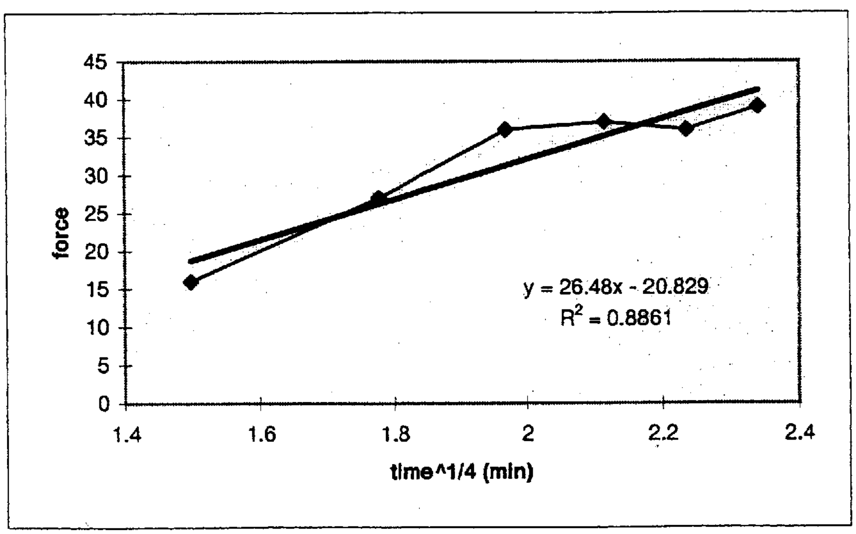

Figure A-15: Sticking Force versus Time, Test 2

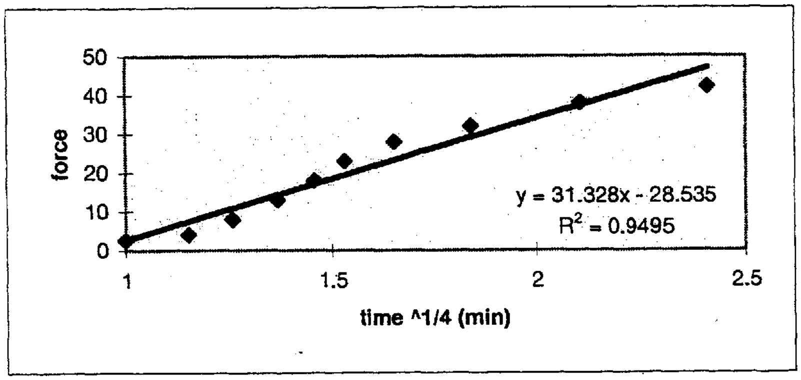

Figure A-16: Sticking Force versus Time, Test 3

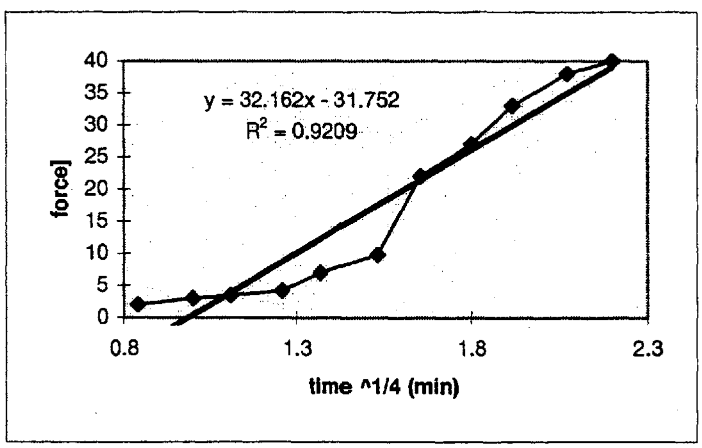

Figure A-17: Sticking Force versus Time, Test 4

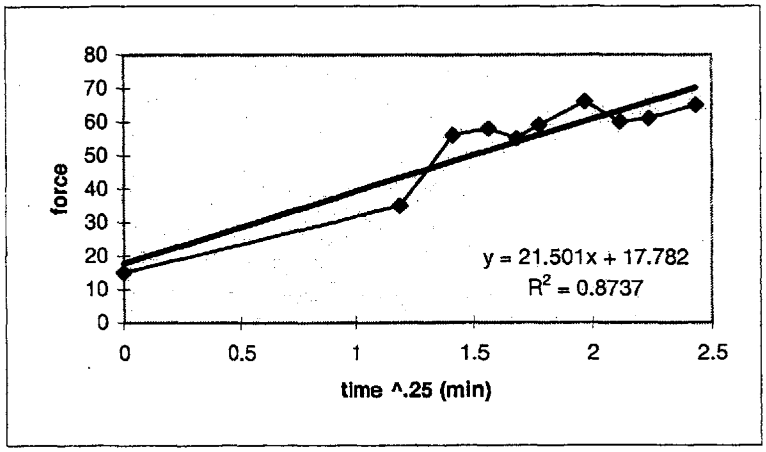

Figure A-18: Sticking Force versus Time, Test 5

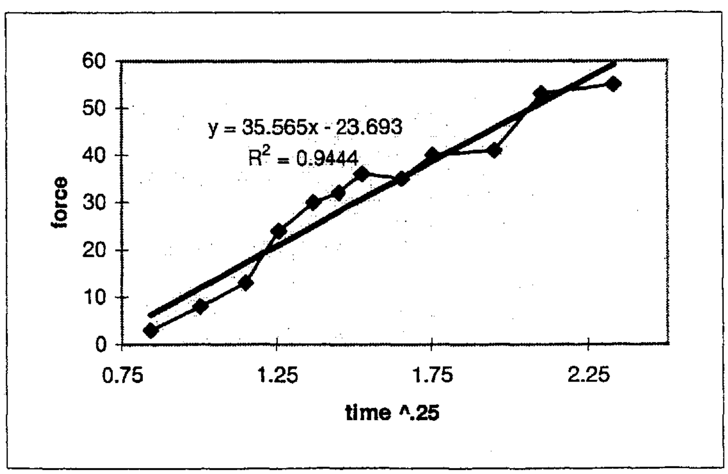

Figure A-19: Sticking Force versus Time, Test 6

Appendix B

Wireline Stickance Tester

B.1 Enginering Drawings of Machined Parts

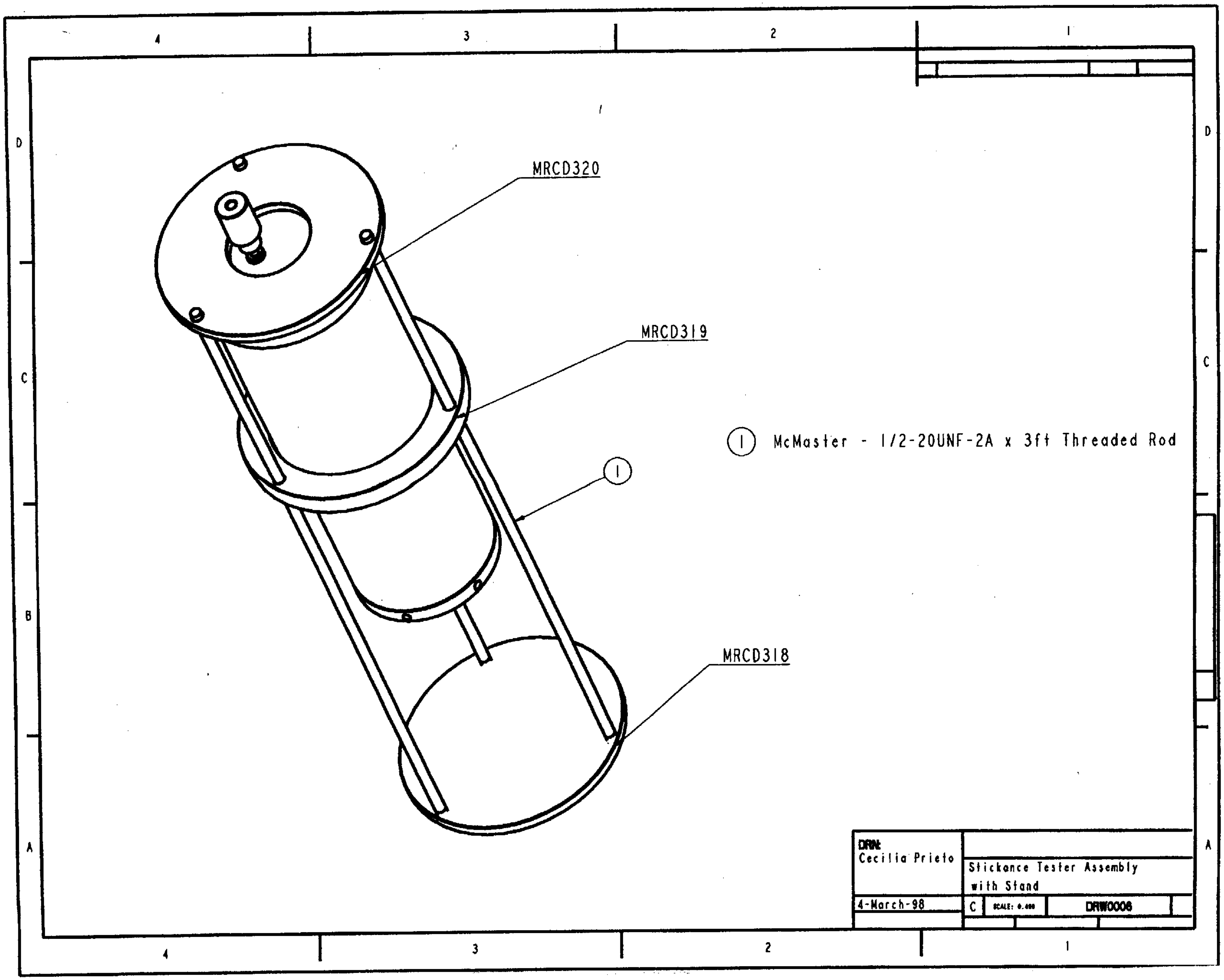

Figure B-1: Full Assembly, DRW0006

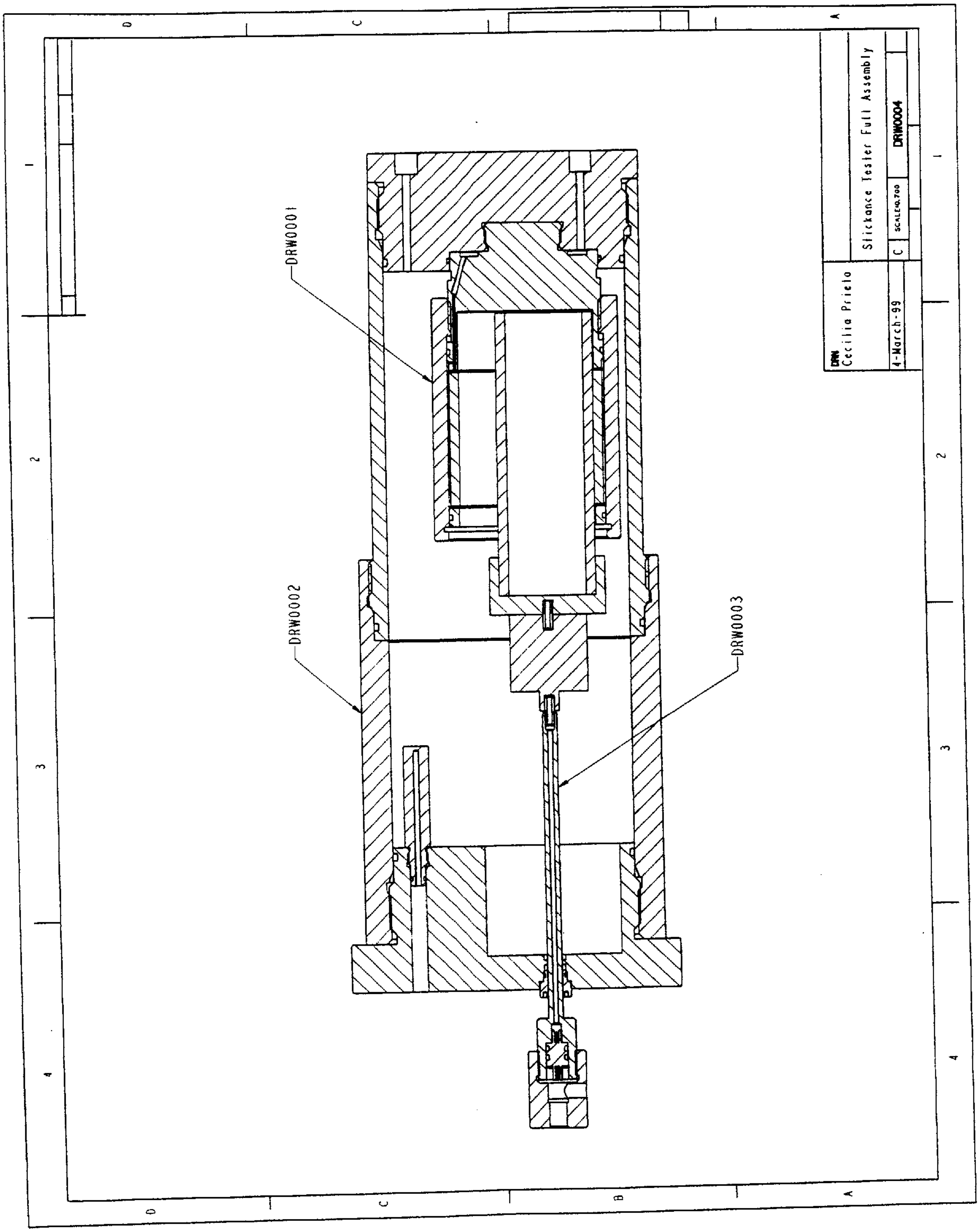

Figure B-2: Pressre Vessel, DRW0004

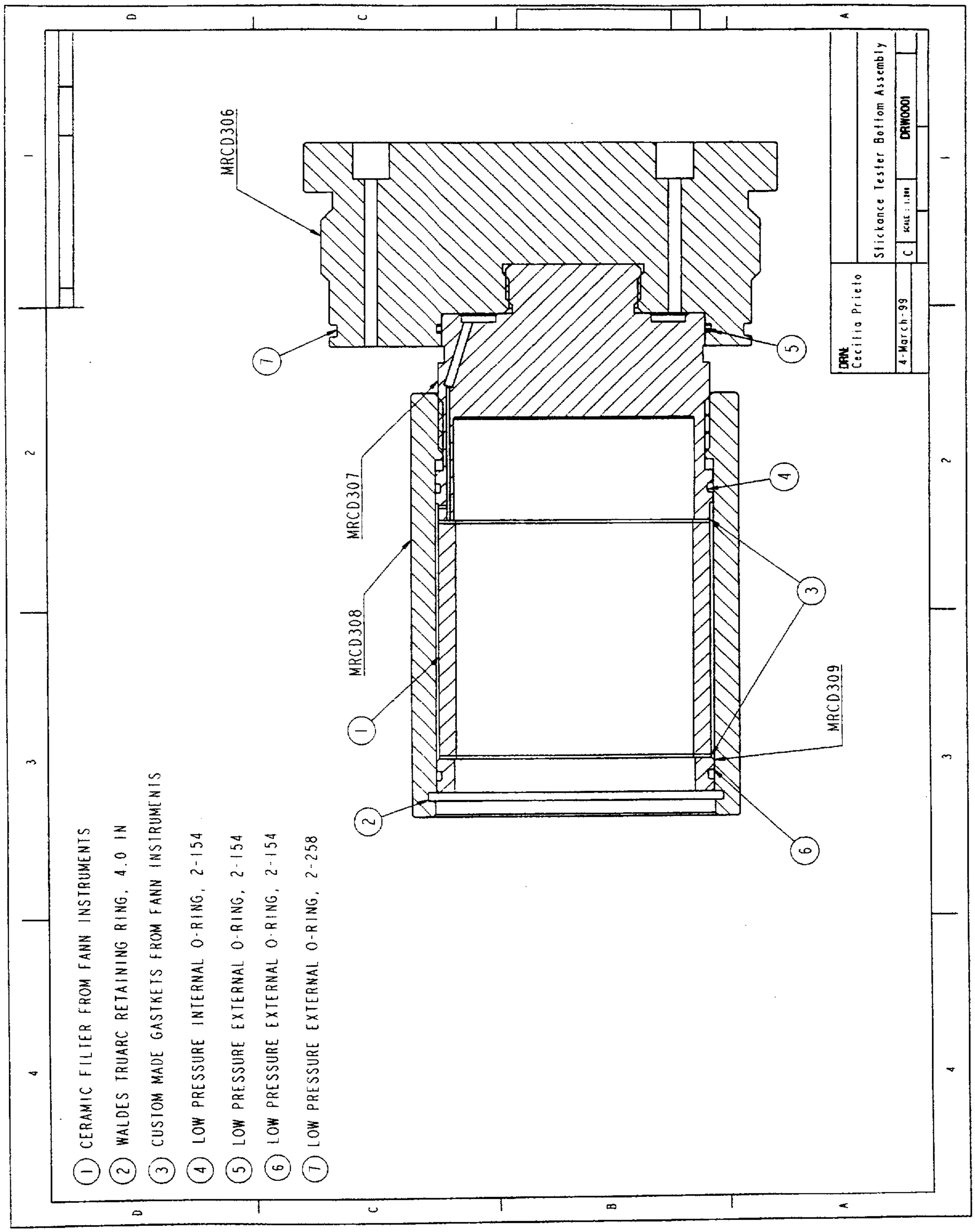

Figure B-3: Filter Assembly, DRW0001

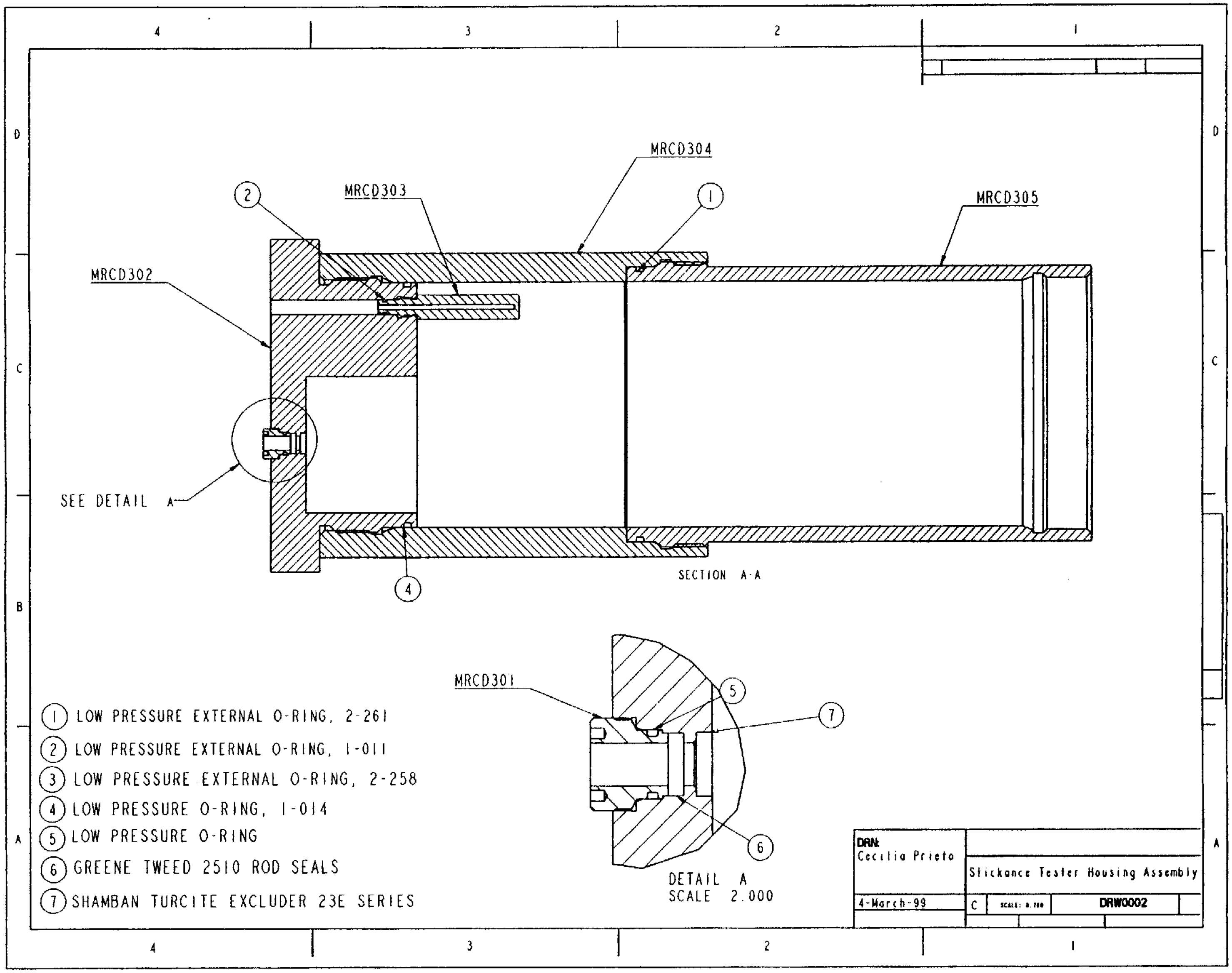

Figure B-4: Housing Assembly, DRW0002

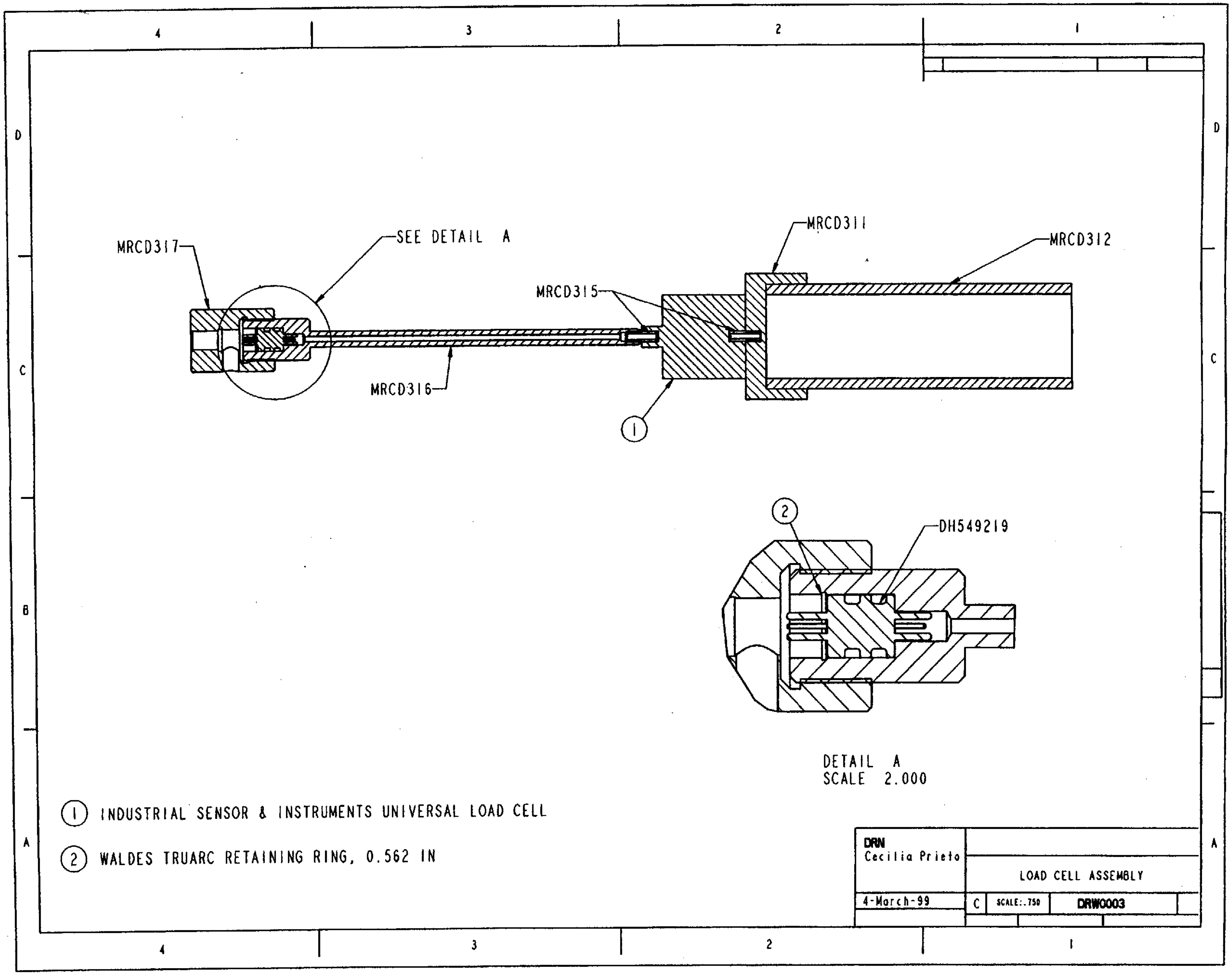

Figure B-5: Load Cell Assembly, DRW0003

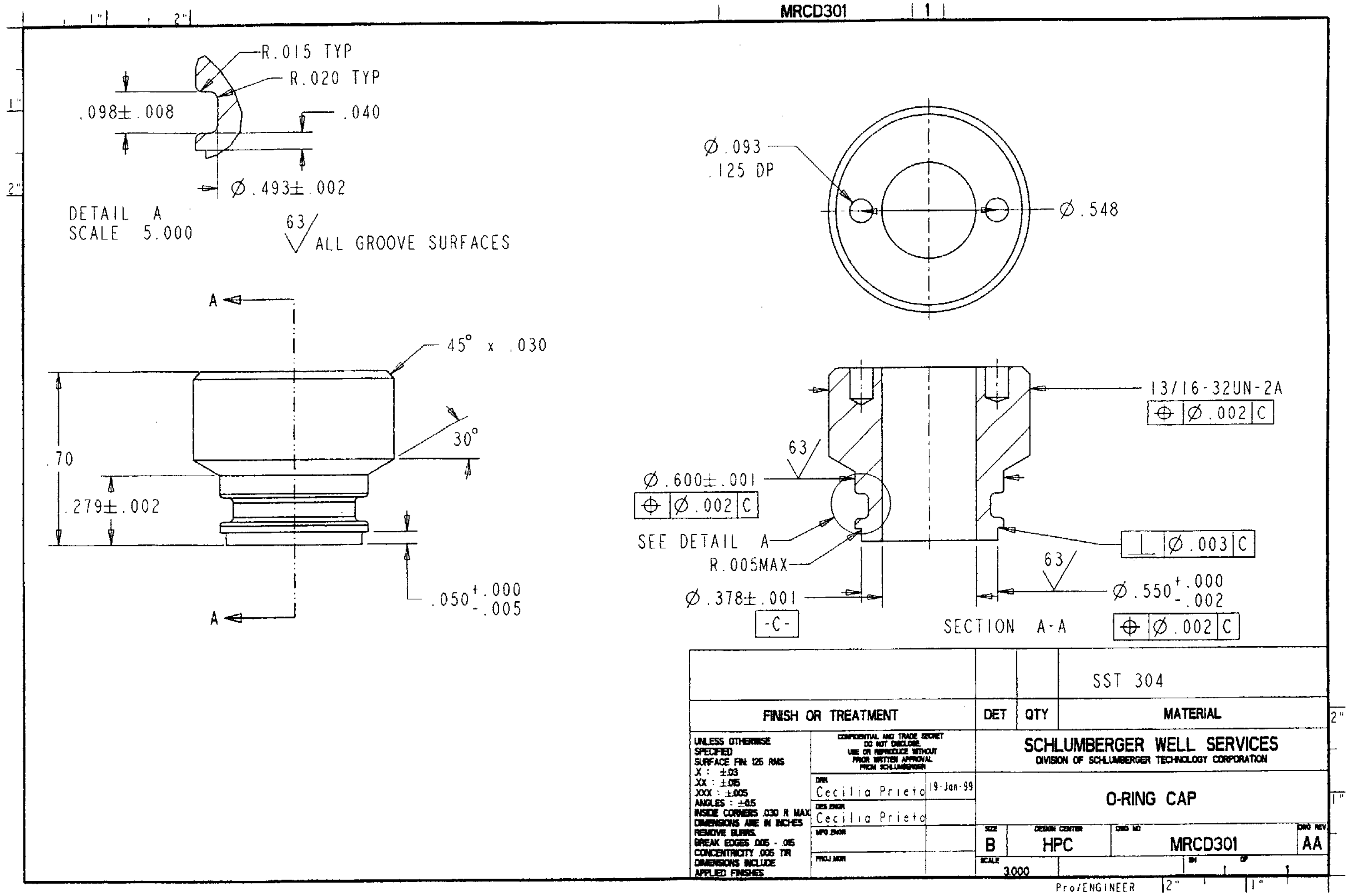

Figure B-6: O-ring Cap, MRCD301

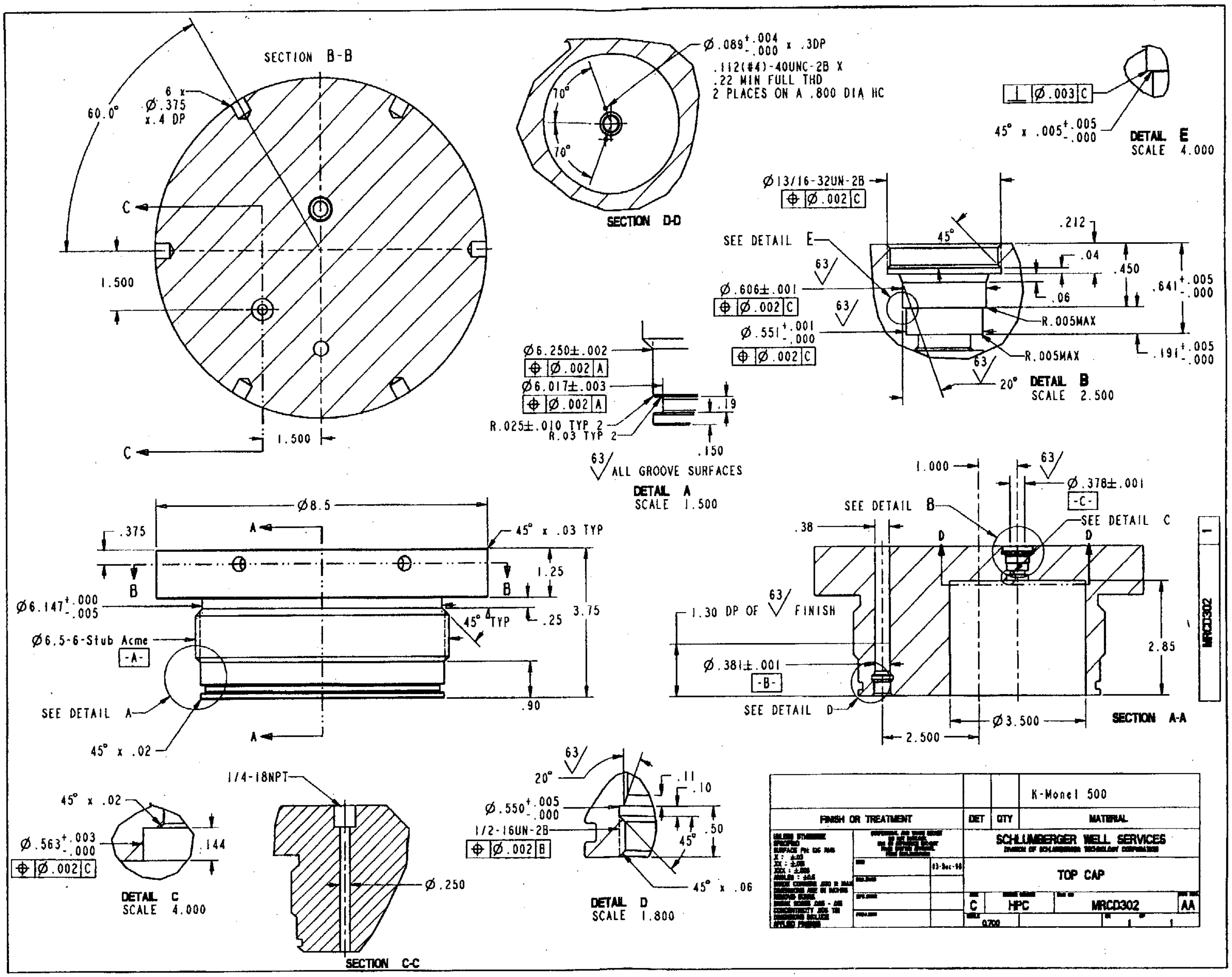

Figure B-7: Top Cap, MRCD302

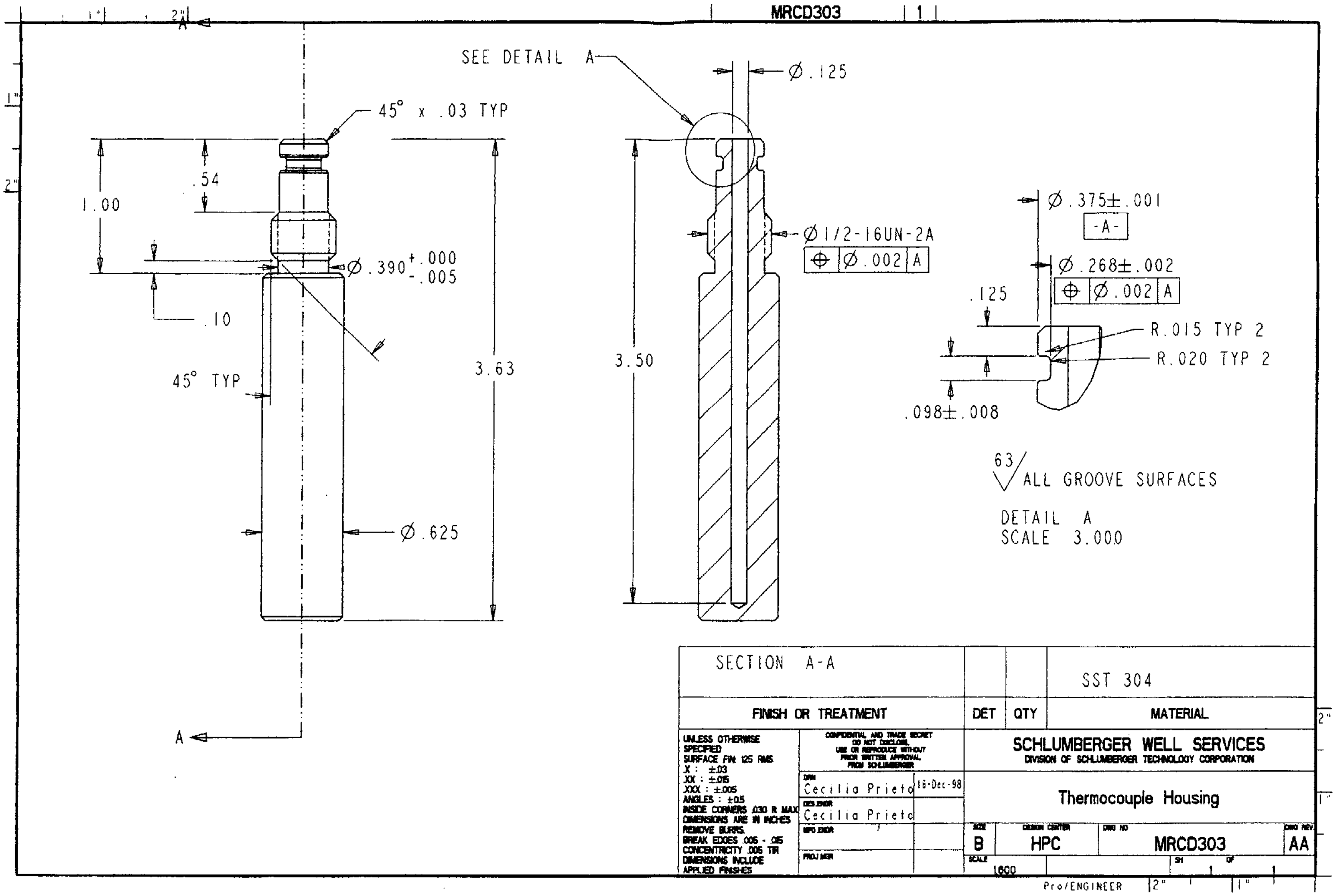

Figure B-8: Thermocouple Housing, MRCD303

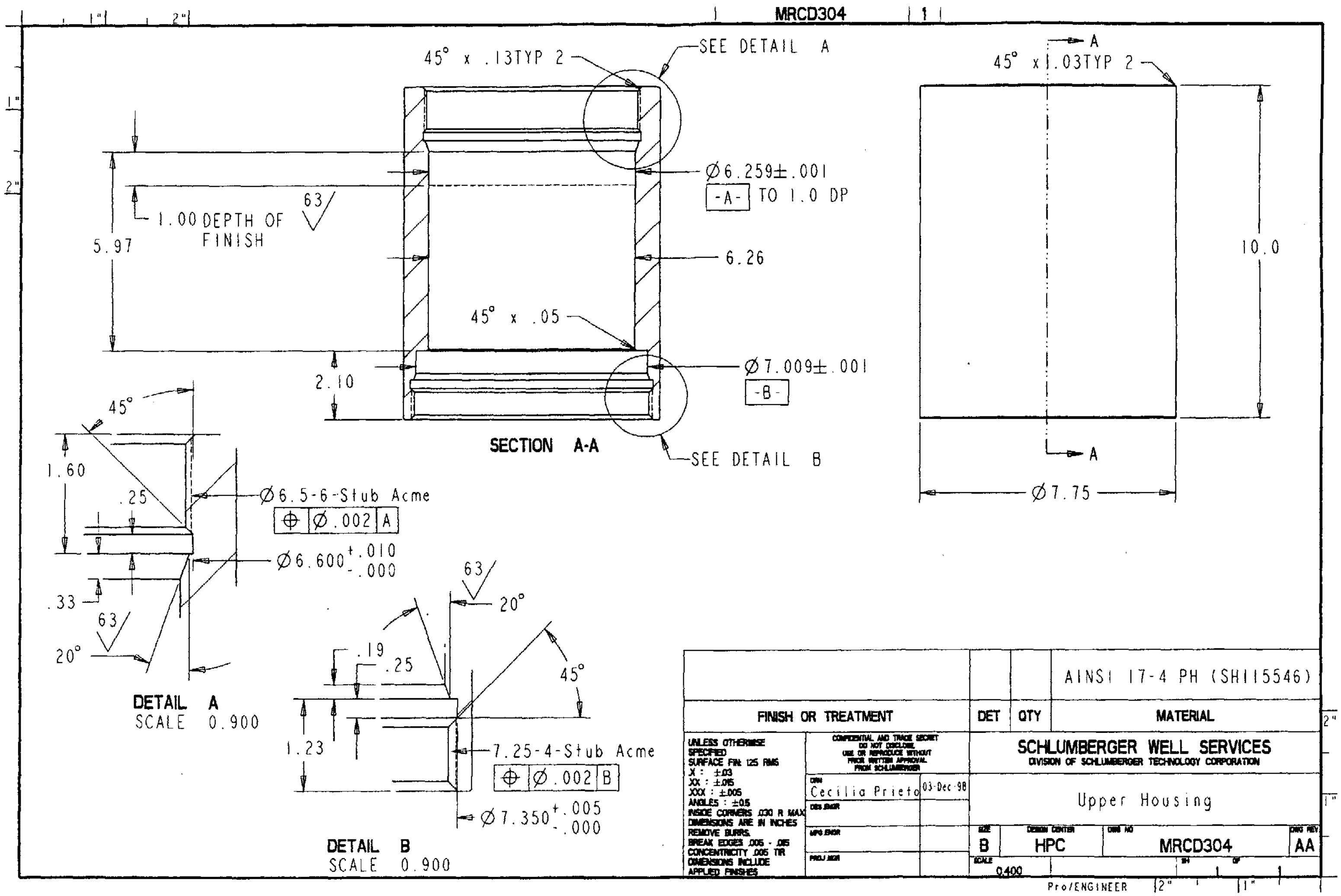

Figure B-9: Upper Housing, MRCD304

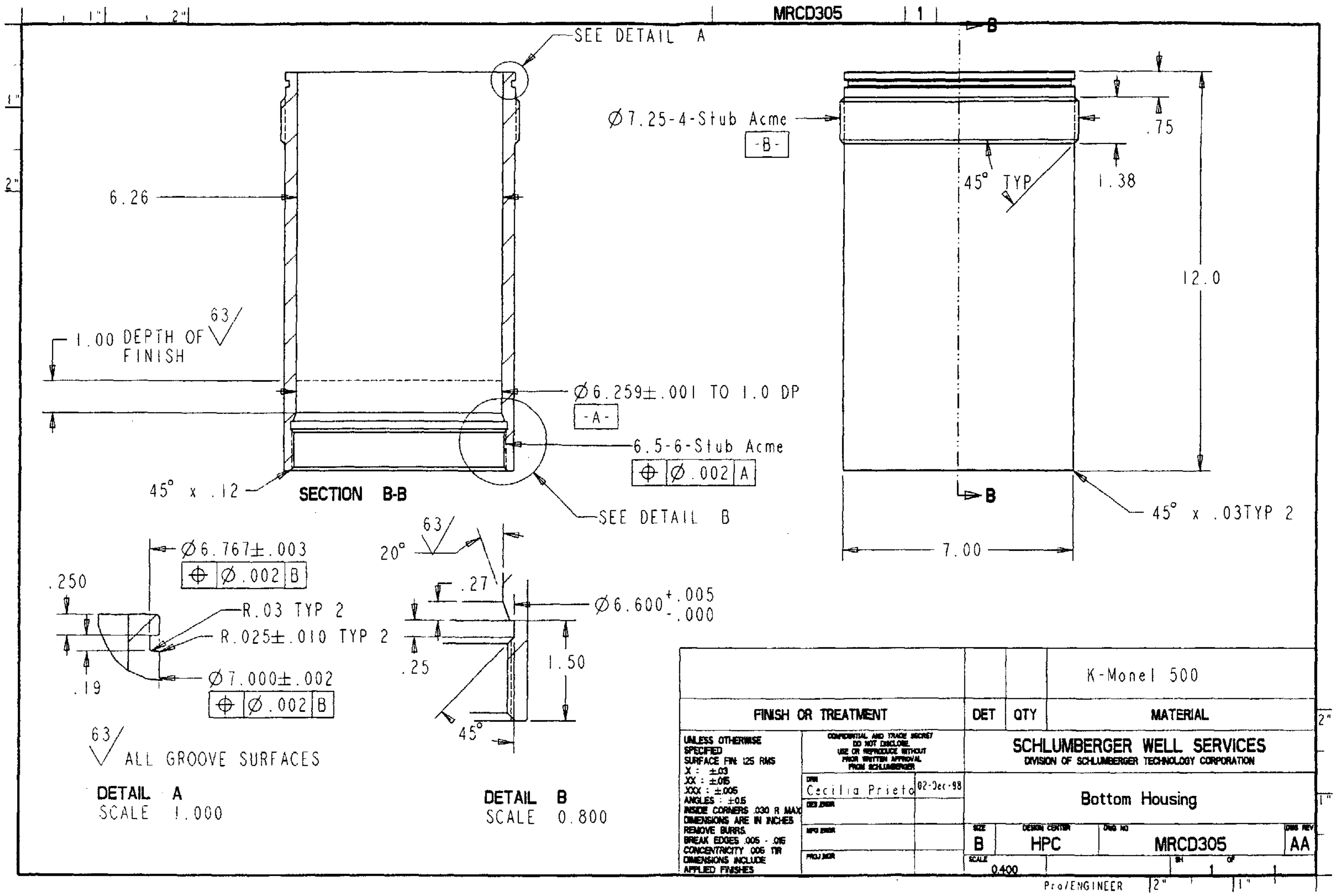

Figure B-10: Bottom Housing, MRCD305

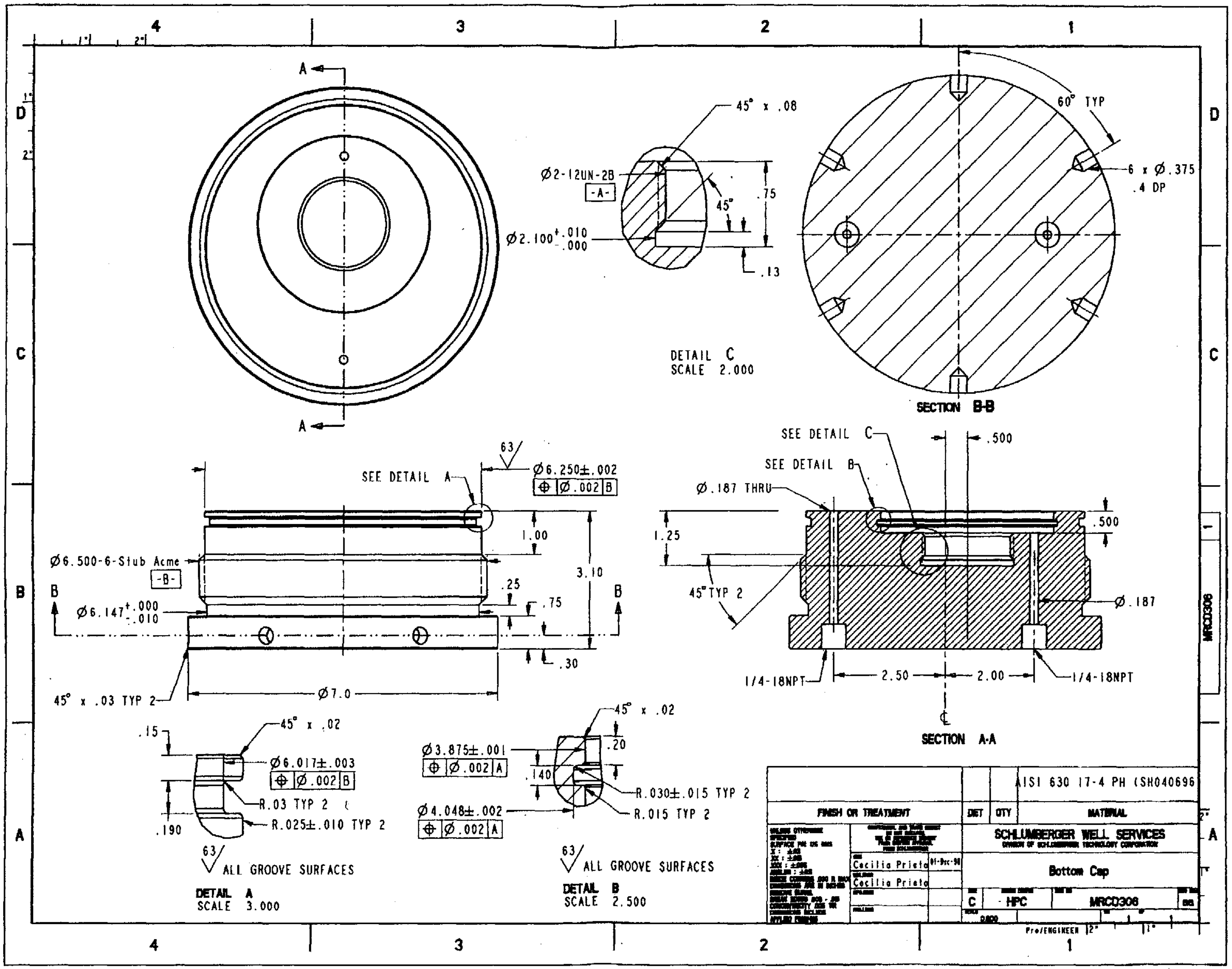

Figure B-11: Bottom Cap, MRCD306

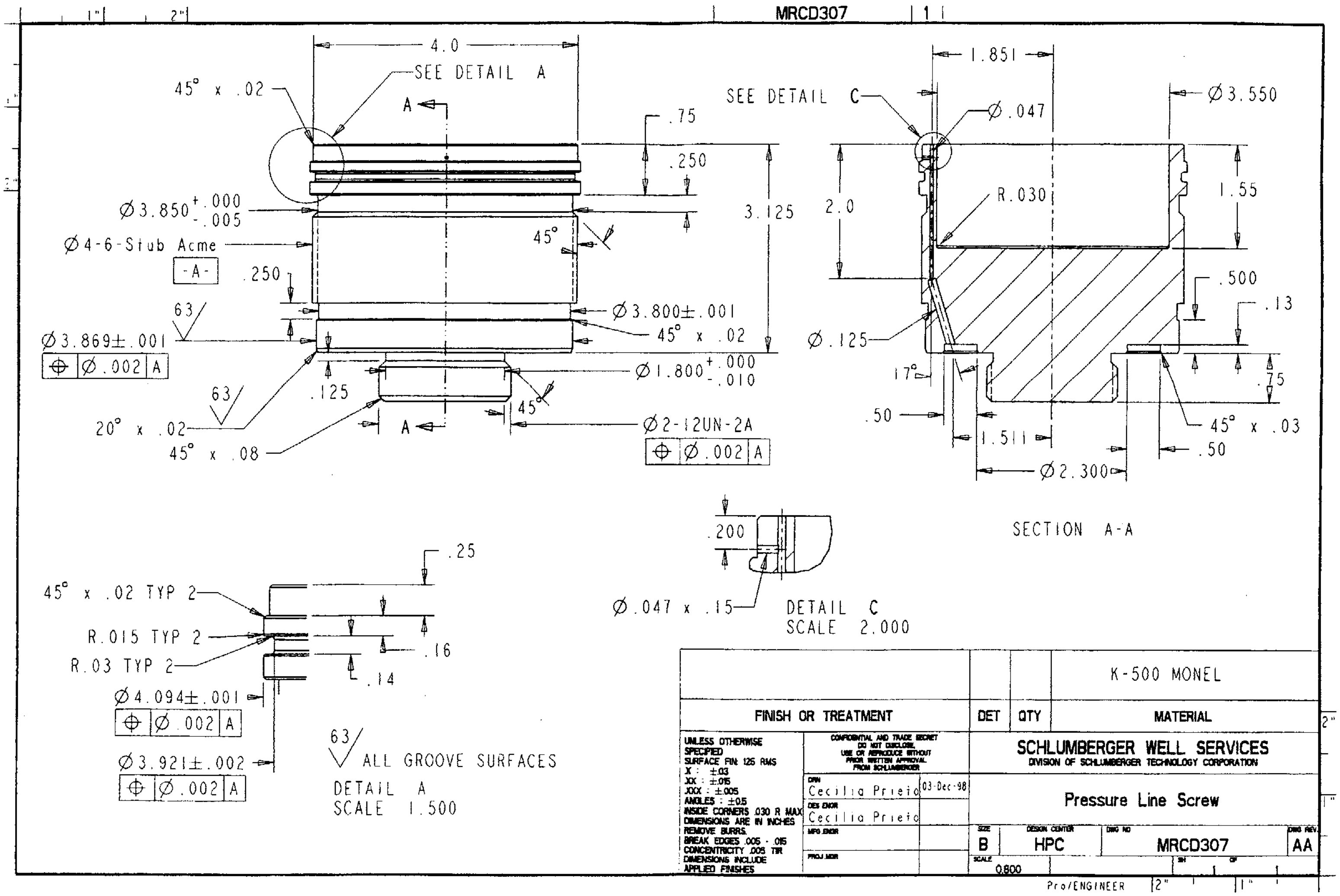

Figure B-12: Pressure Line Screw, MRCD307

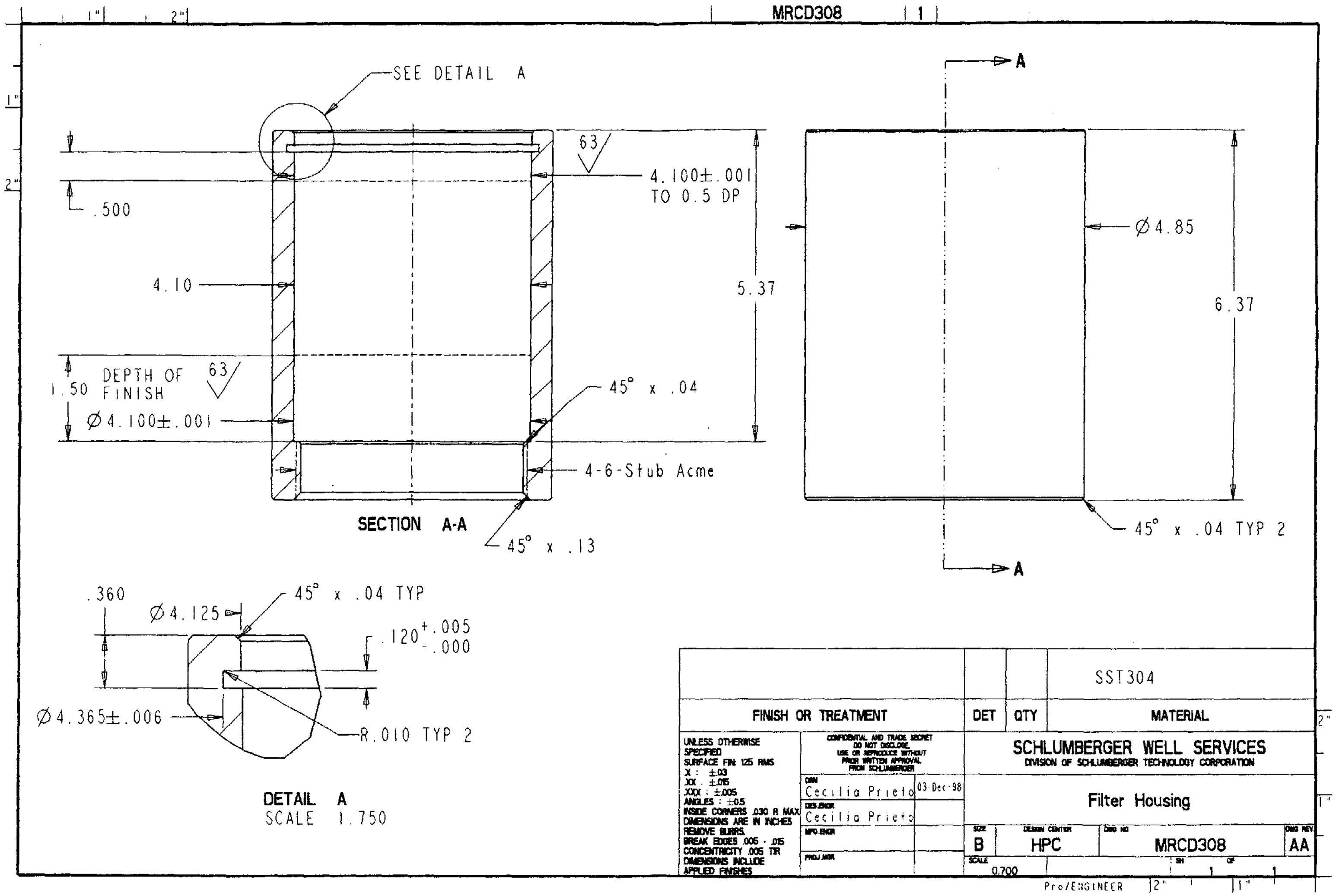

Figure B-13: Filter Housing, MRCD308

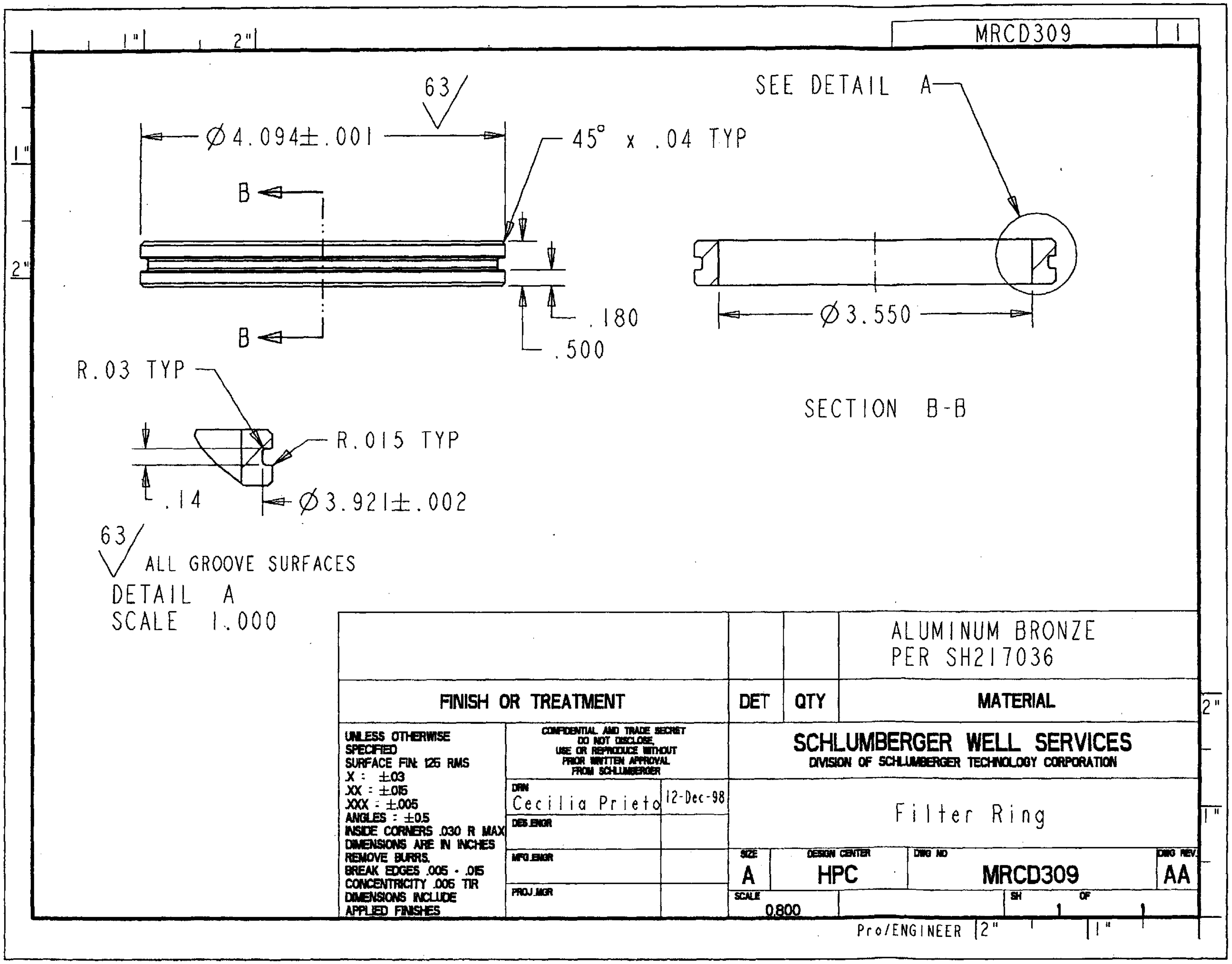

Figure B-14: Filter Ring, MRCD309

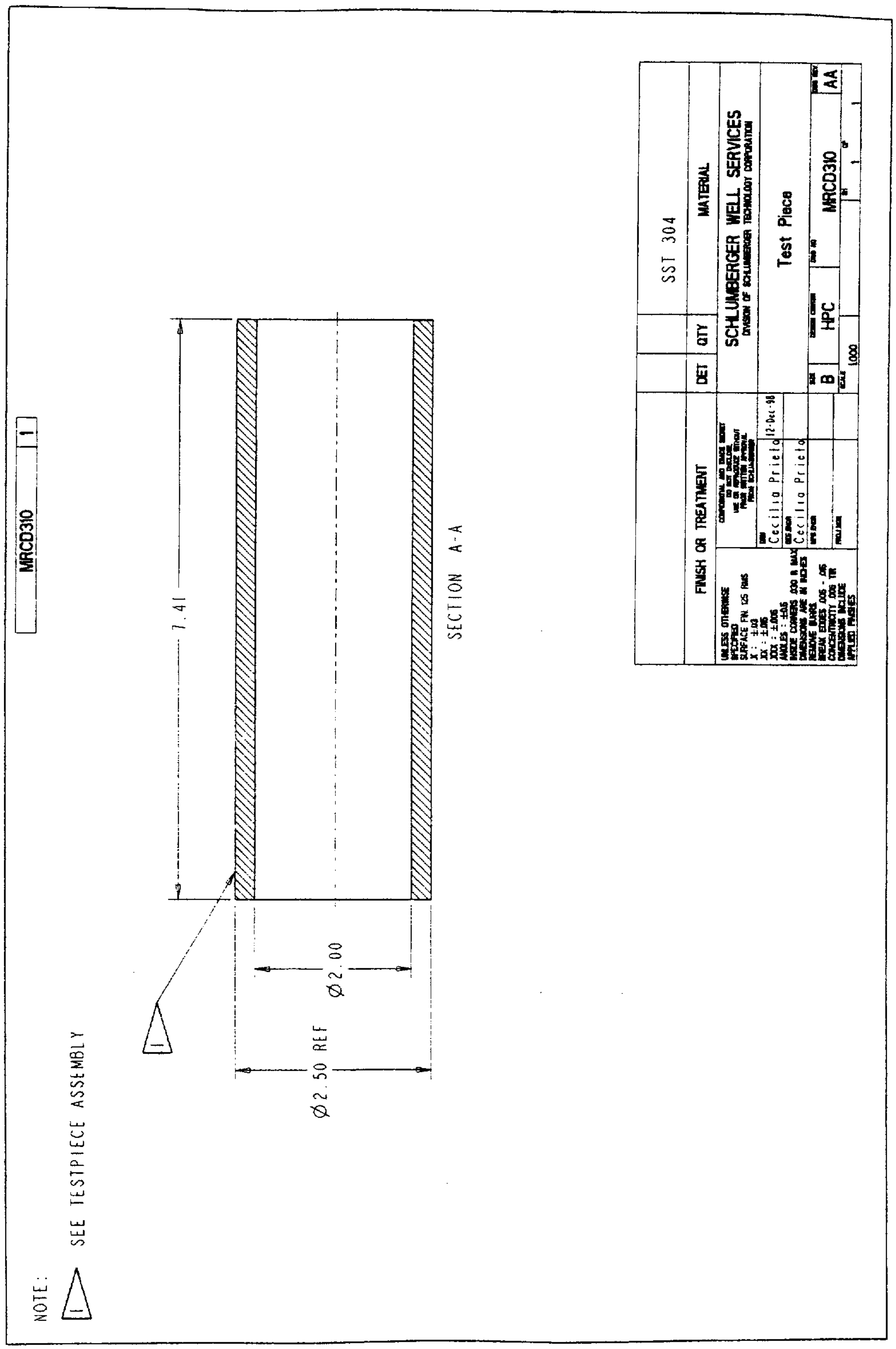

Figure B-15: Test Piece, MRCD310

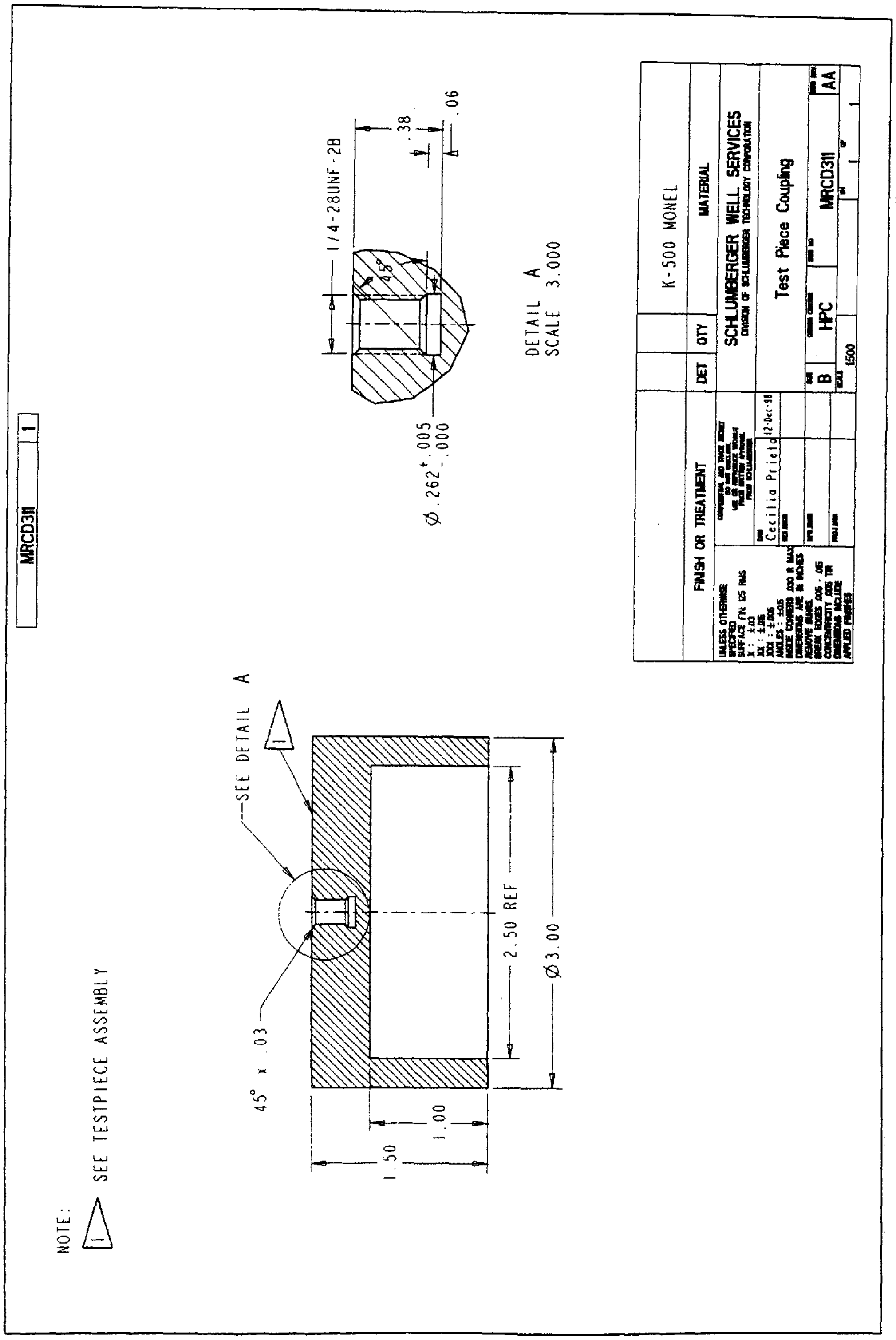

Figure B-16: Test Piece Coupling, MRCD311

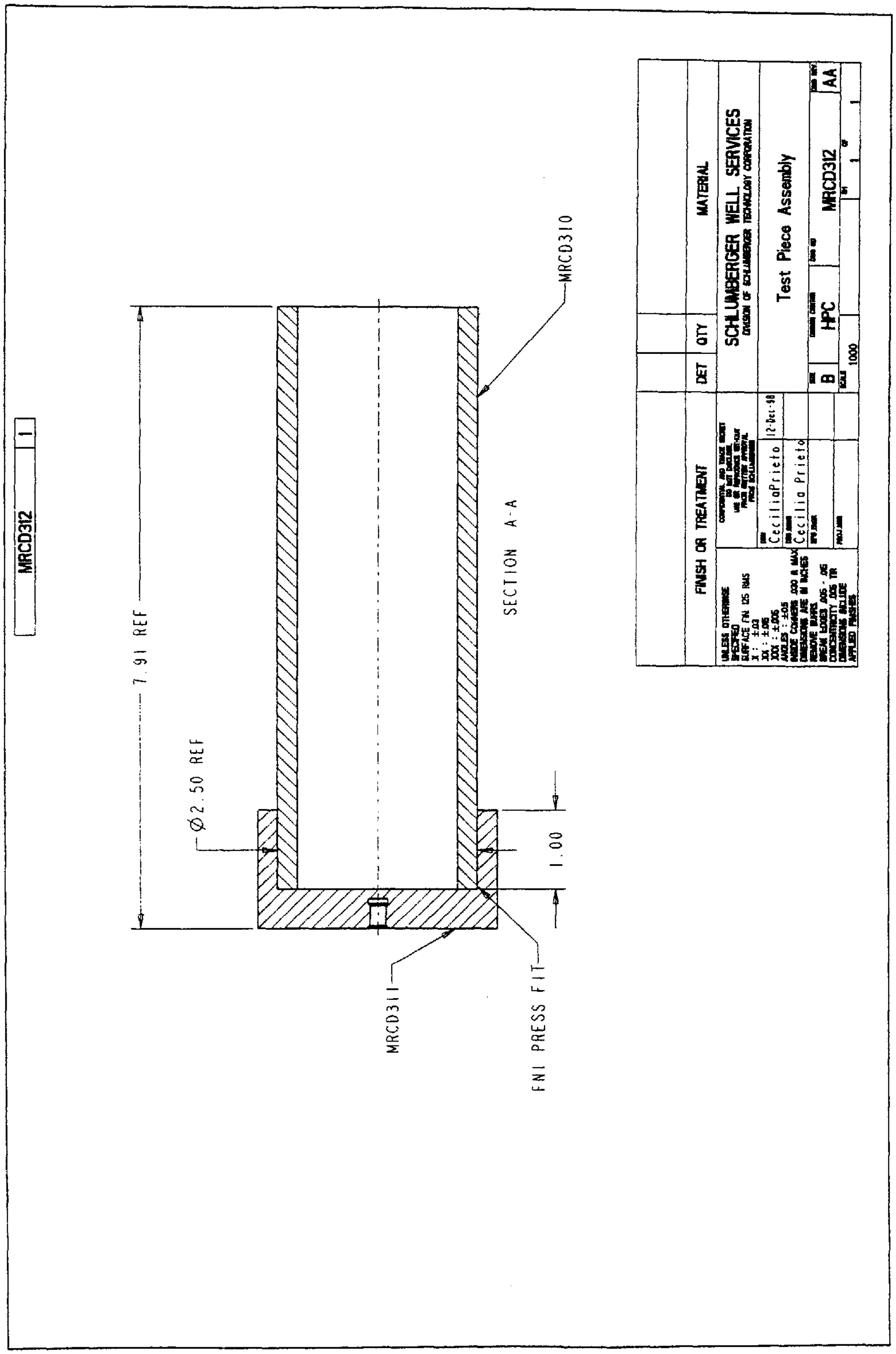

Figure B-17: Test Piece Assembly, MRCD312

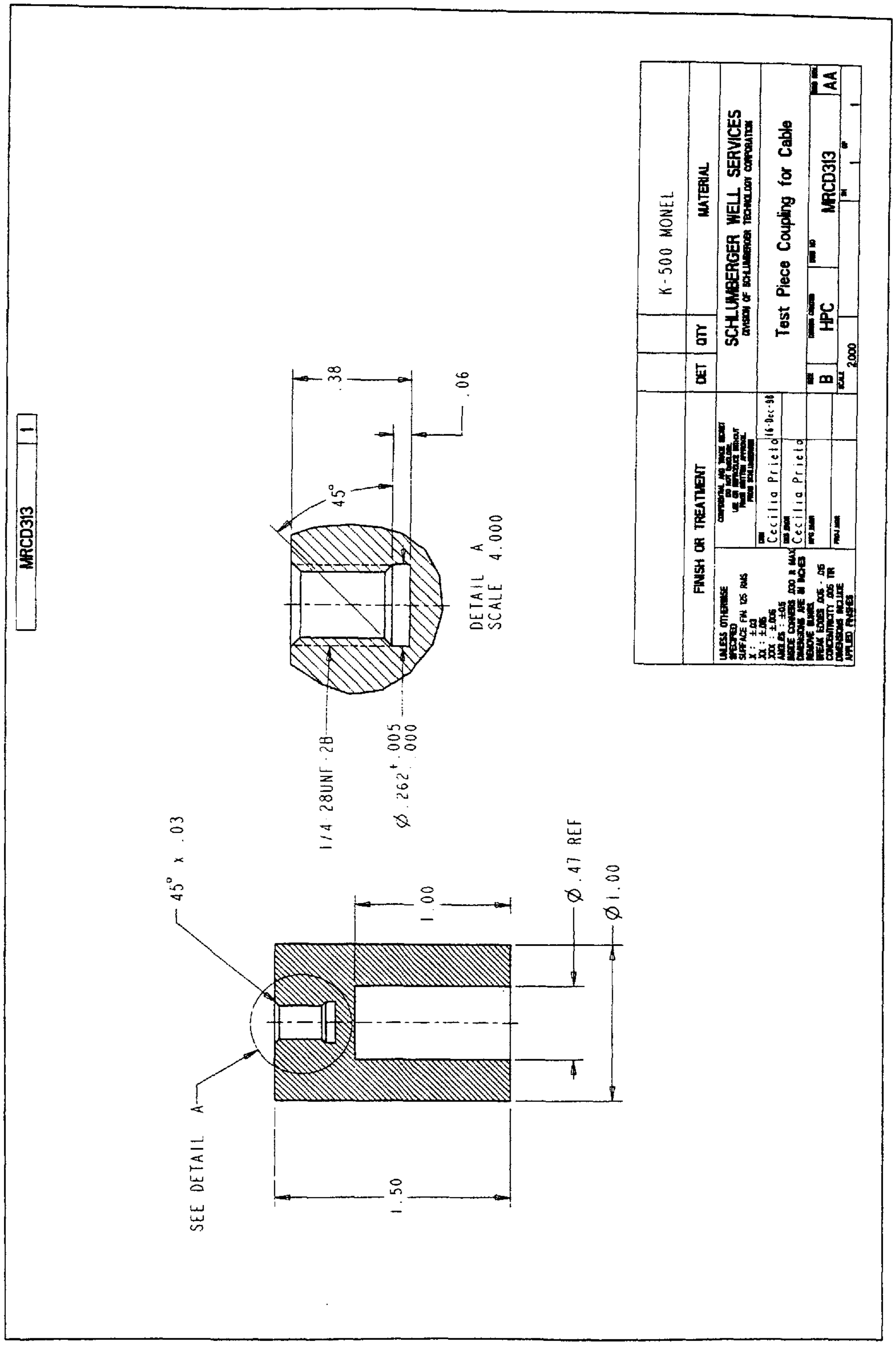

Figure B-18: Test Piece Coupling for Cable, MRCD313

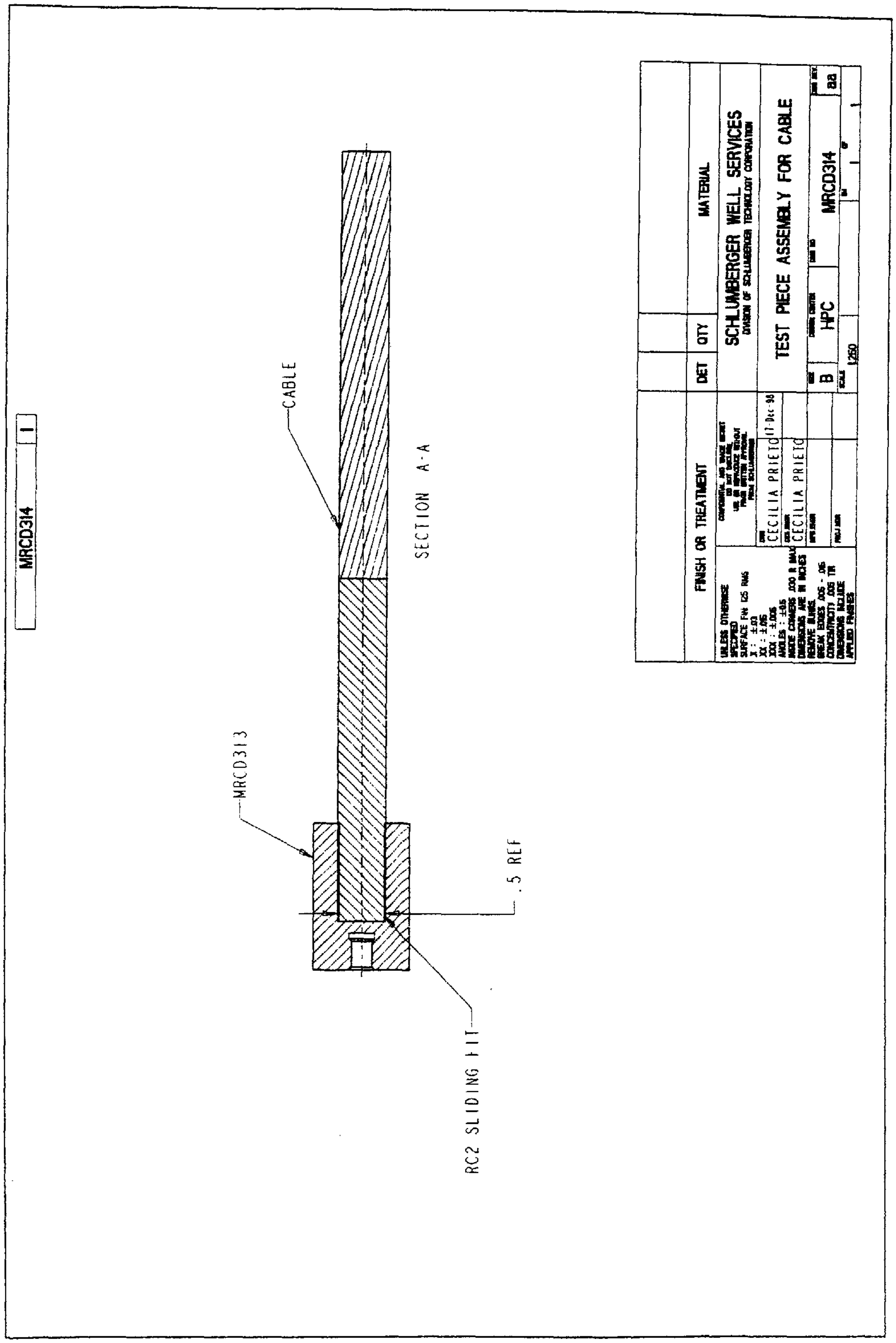

Figure B-19: Test Piece Assembly for Cable, MRCD314

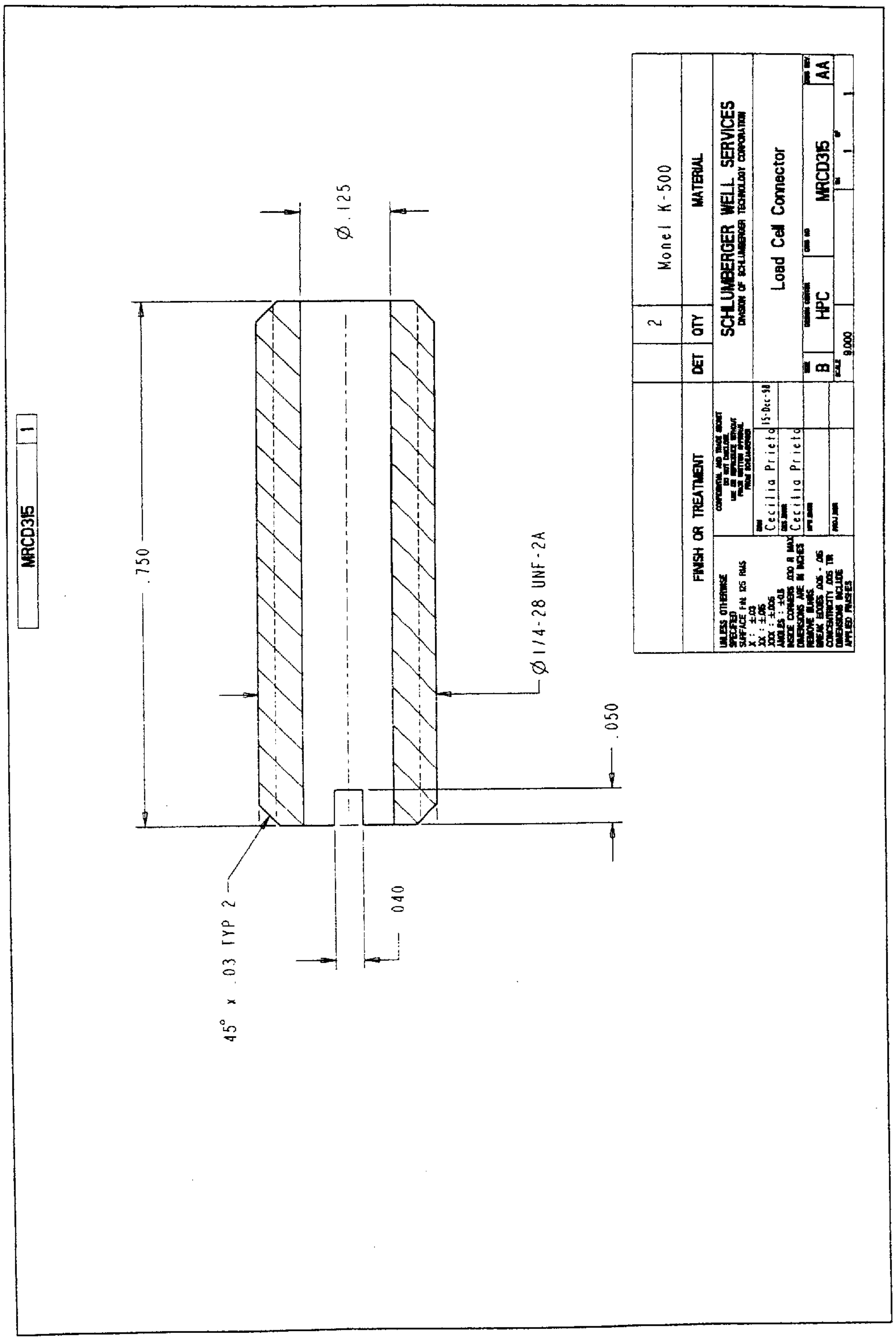

Figure B-20: Load Cell Connector, MRCD315

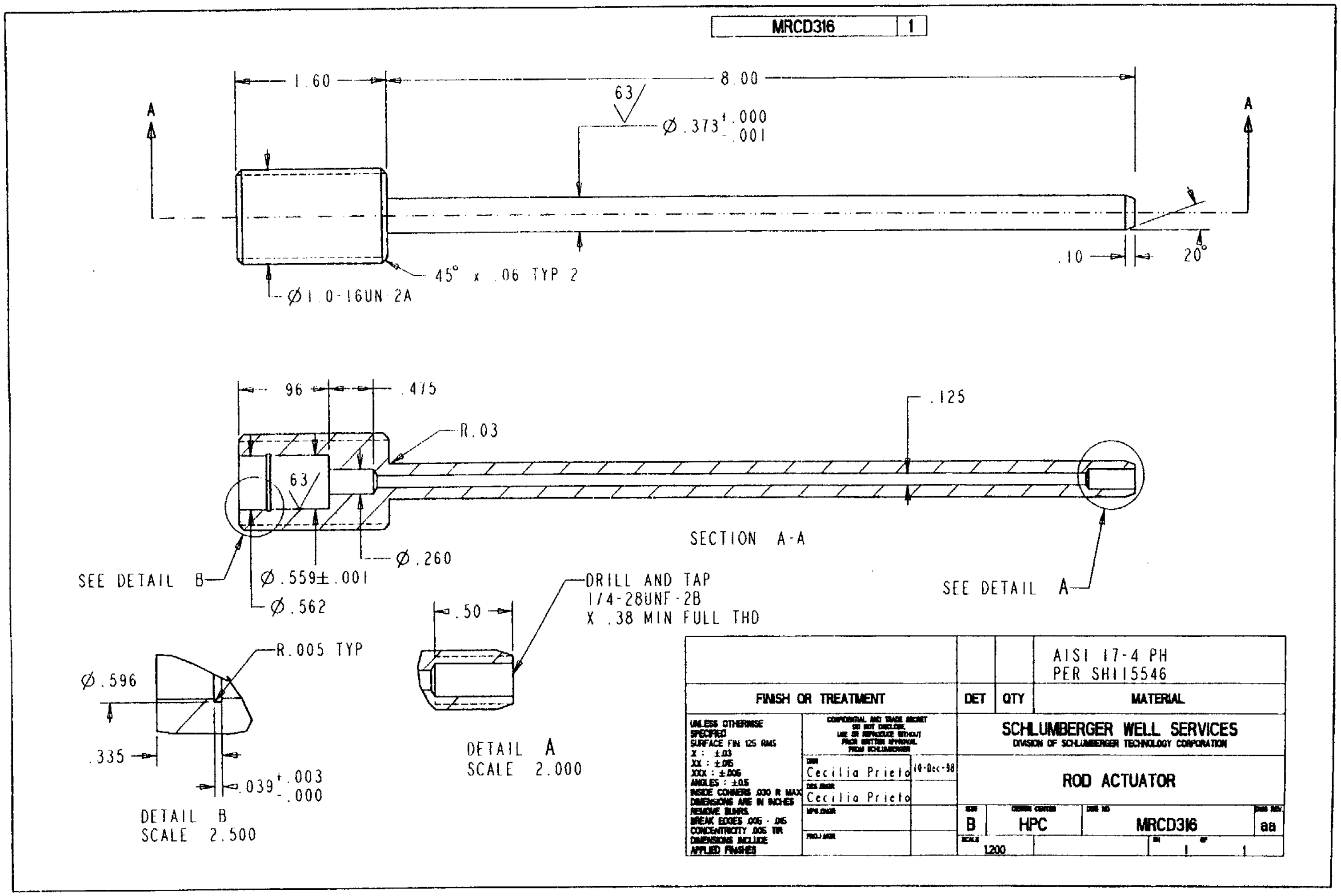

Figure B-21: Actuator Rod, MRCD316

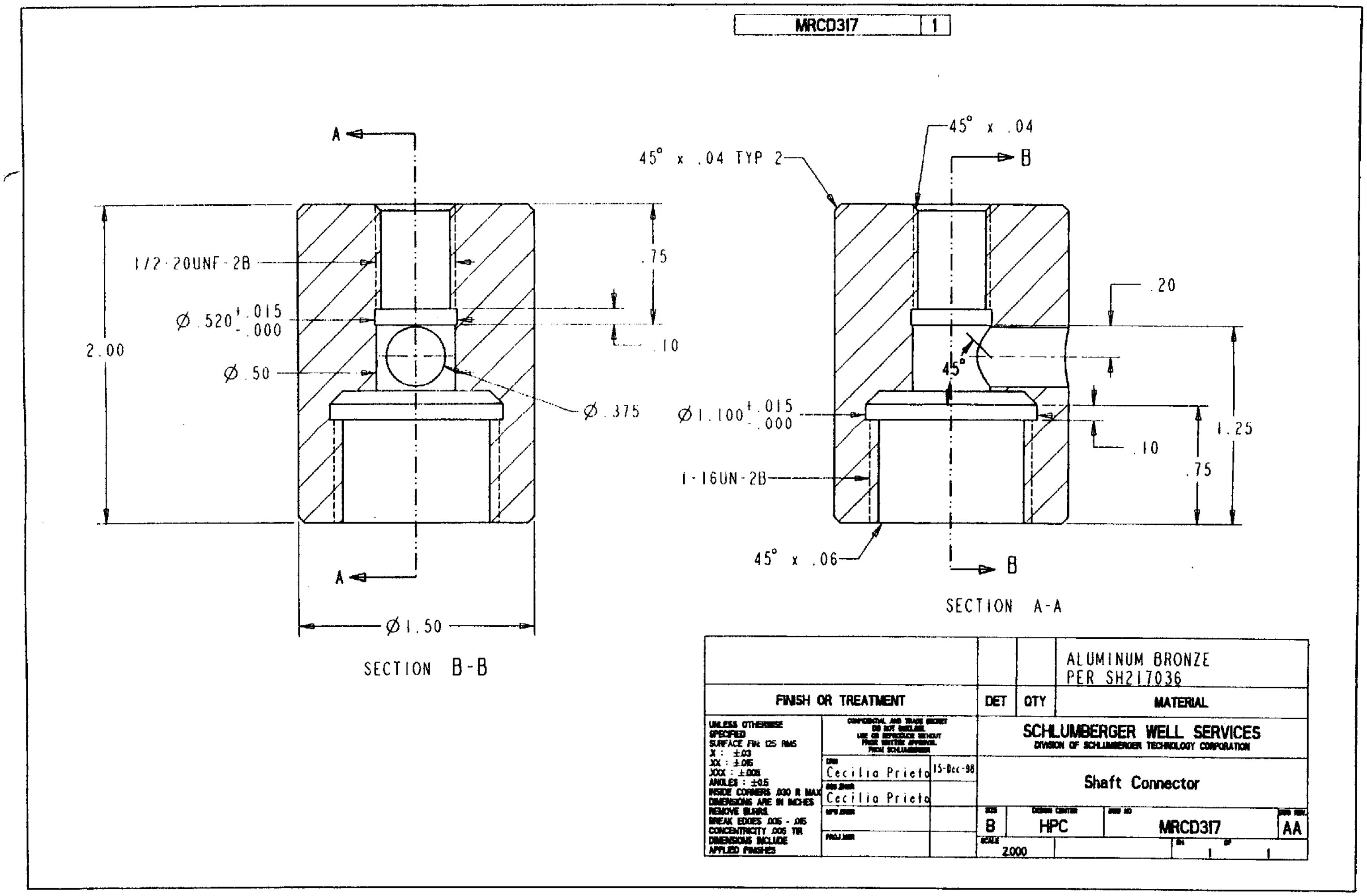

Figure B-22: Shaft Connector, MRCD317

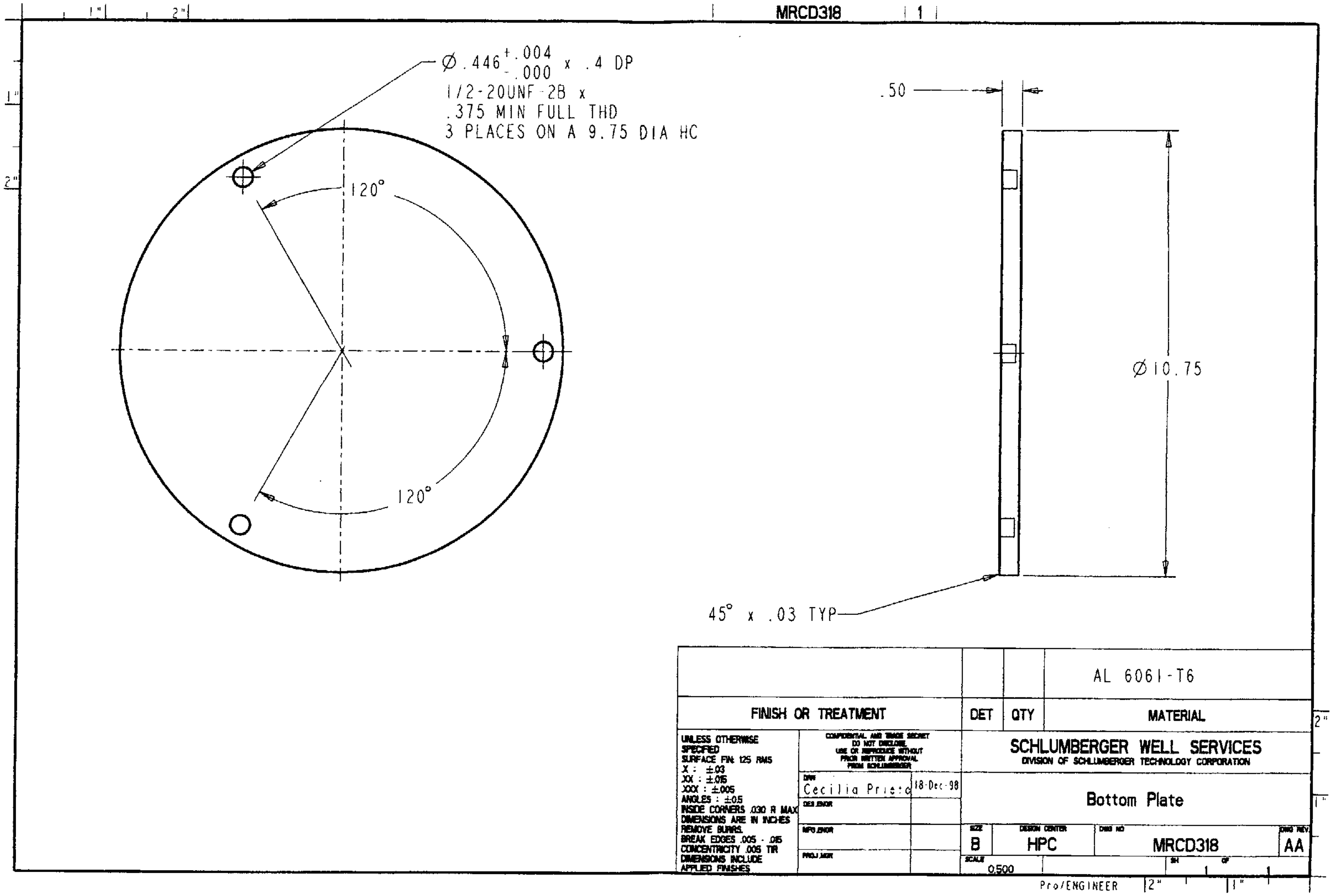

Figure B-23: Bottom Plate, MRCD318

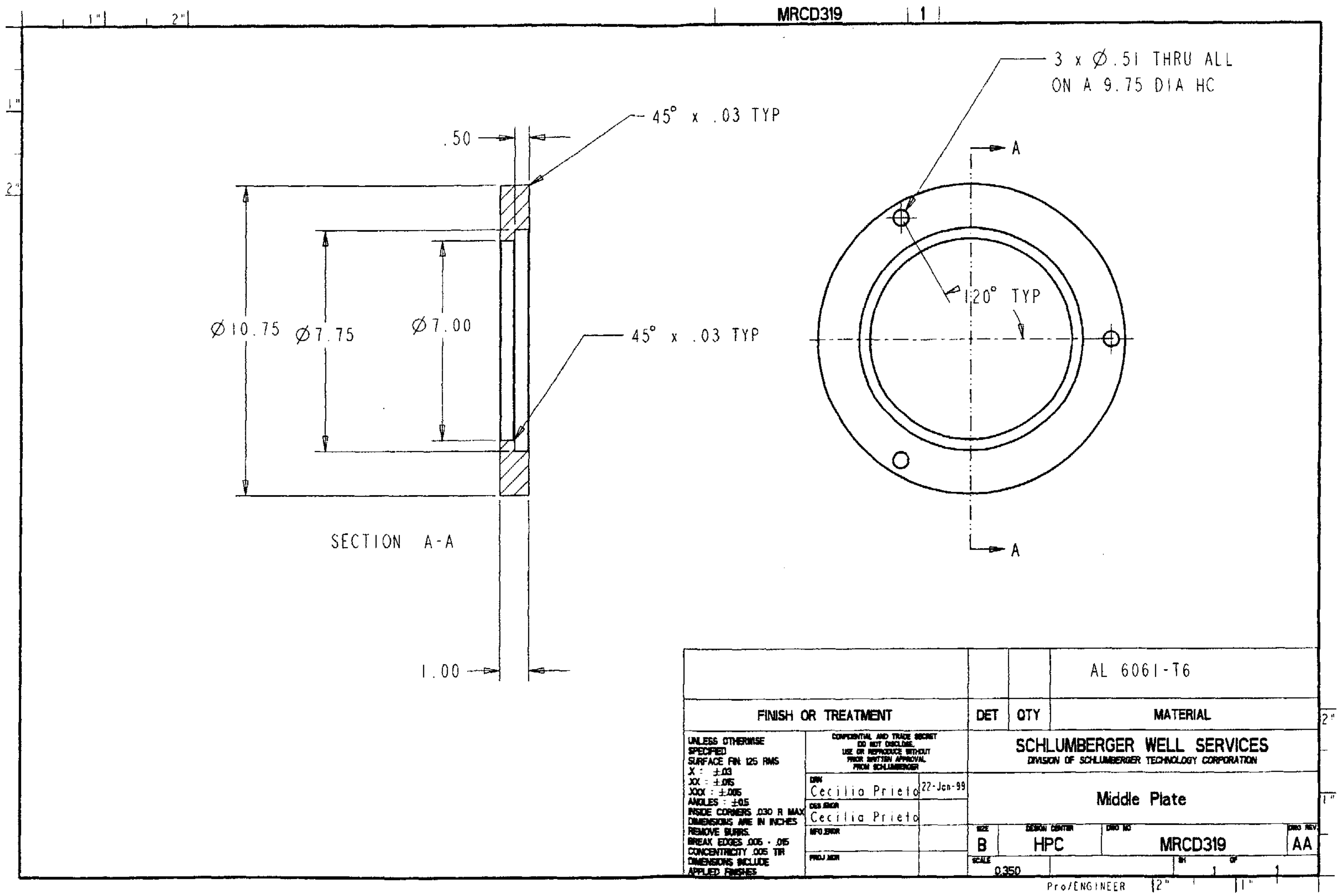

Figure B-24: Middle Plate, MRCD319

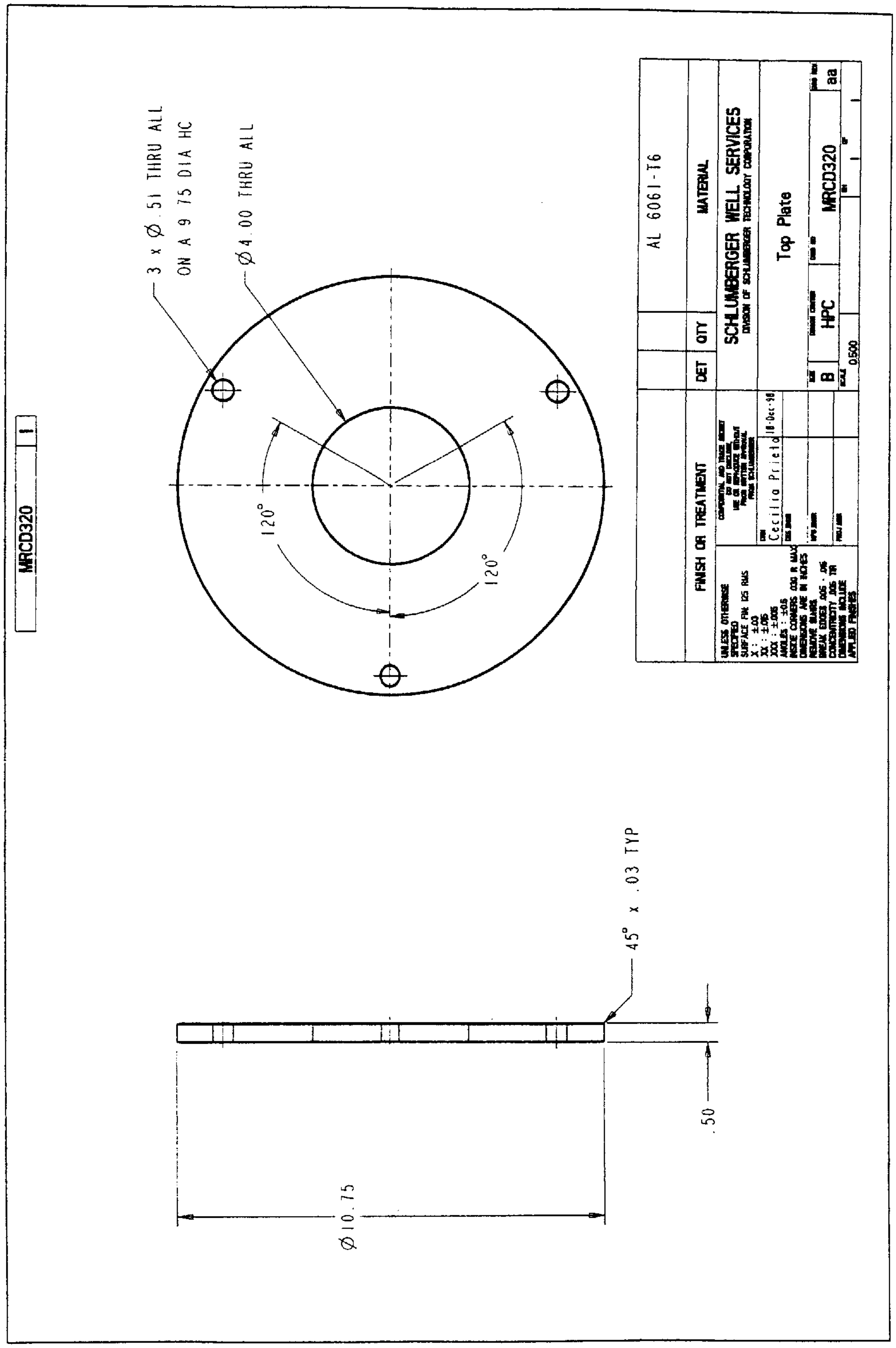

Figure B-25: Top Plate, MRCD320

B.2 Outsourced Parts

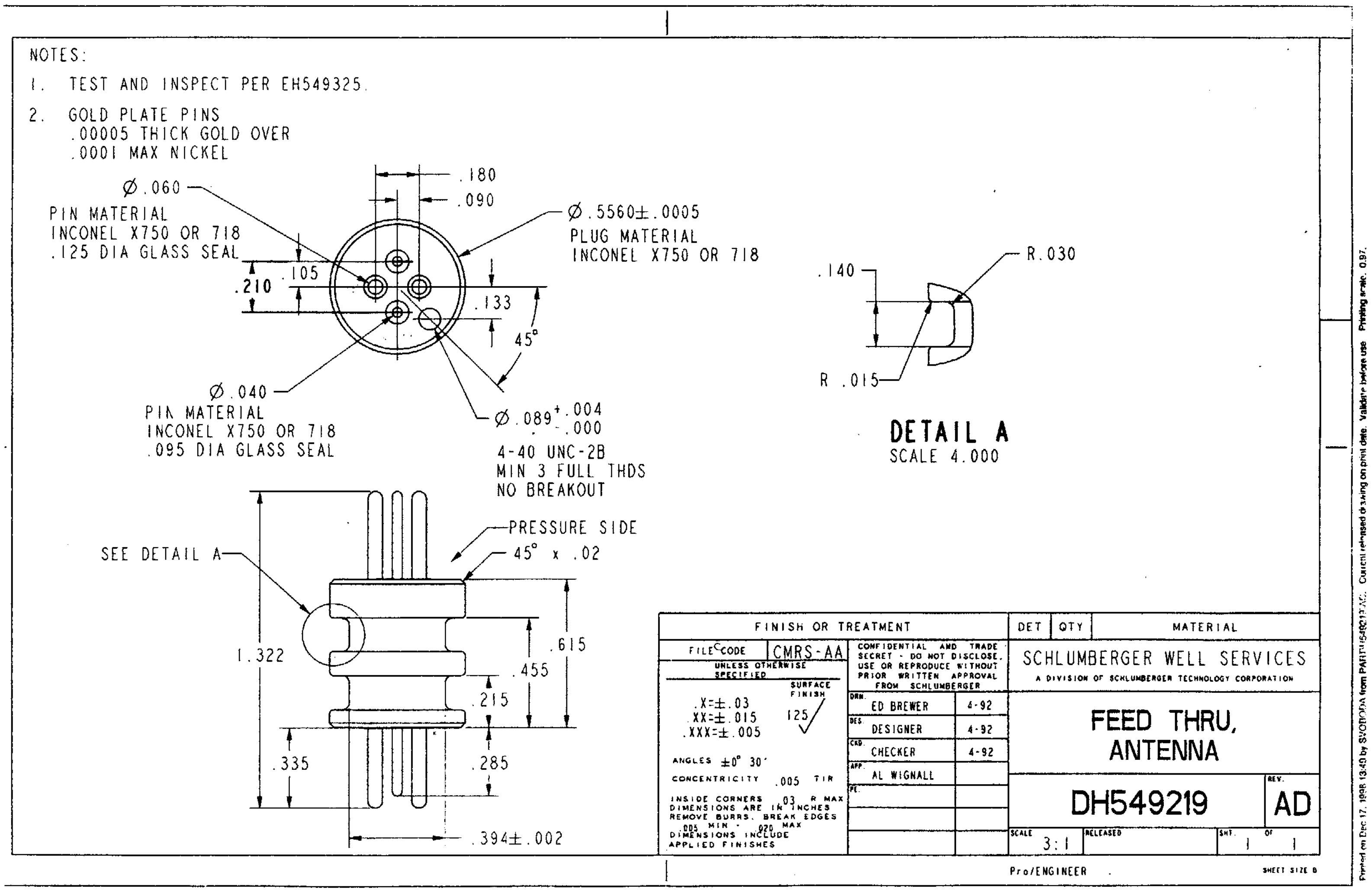

Figure B-26: Pressure Bulk Head, DH549219

2-1/2" Bore Air Cylinders

- Ground and Polished, High Strength Carbon Steel Piston Rod Standard – 303 Stainless Steel Rod Available as an Option – Bronze Rod Guide Bushing Standard
- Force Exerted Approximately 5.0 of Air Line Pressure
- Double Acting Only
- Mounting Nuts Not Included

OPTIONS:

NO CHARGE:
- *MAGNALUBE G (G)*
- *PORTS ROTATED (K)*
- *NO THREAD (NT)*
- *SIDE PORTED REAR HEAD (Q)*
  Add .38" to nose mount overall length.

OPTIONS continued...

DOUBLE ACTING BUMPERS (B)
- *$5.40 additional*
- *Add .250 to overall length*

EXTRA EXTENSION (EE)
- *Double acting, add $1.20 per inch of extension*
- *DXDE, add $2.00 per inch of extension; extension added to each end*

MAGNET (prefix M) – Add $14.00
- *Stainless steel rod becomes standard with this option*

LOW TEMPERATURE (N)
Temperature Range: -40° to 200°F
- *Double acting add $3.00*
- *DXDE add $4.00*

VITON "U" CUPS (V)
Temperature Range: 0° to 400°F (-18° to 205°C)
- *Double acting add $15.40*
- *DXDE add $20.35*

☐ Enter Stroke Length as 3rd Digit

MODEL/PRICE	DESCRIPTION/WEIGHT (lbs.)	DIMENSIONS
50☐-D  **$61.90** *BASE PRICE* *Add $2.40 per inch of stroke*	***Double Acting** – Air Return – Front Nose Mounting* *Standard Stroke Lengths:* ½", 1", 1½", 2", 2½", 3", 4", 5", 6" Maximum Stroke – 12" Stainless Steel Rod Add $3.30 *Optional Accessories:* D-615-1 Mounting Bracket D-2540 Mounting Nut *Base Weight: 1.98* *Adder Per Inch of Stroke: .17*	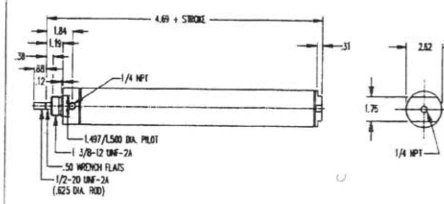
50☐-DXP  **$72.70** *BASE PRICE* *Add $2.50 per inch of stroke*	***Double Acting** – Universal Mounting Type – Pivot or Double End – Air Return – Bronze Rod Bushing and Bronze Pivot Bushing* *Standard Stroke Lengths:* ½", 1", 1½", 2", 2½", 3", 4", 5", 6", 7", 8", 9", 10", 11", 12", 13", 14", 15", 16", 17", 18", 19", 20", 21", 22", 23", 24" Maximum Stroke – 32" Stainless Steel Rod Standard *Optional Accessories:* D-231-3 Piston Rod Clevis D-615-1 Mounting Bracket D-620 Pivot Brackets D-2540 Mounting Nut *Base Weight: 2.27* *Adder Per Inch of Stroke: .17*	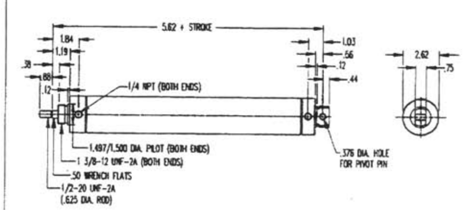

65

Figure B-27: Bimba Stainless Steel Body Air Cylinders

BASIC
internal series
N5000

WALDES TRUARC RETAINING RINGS

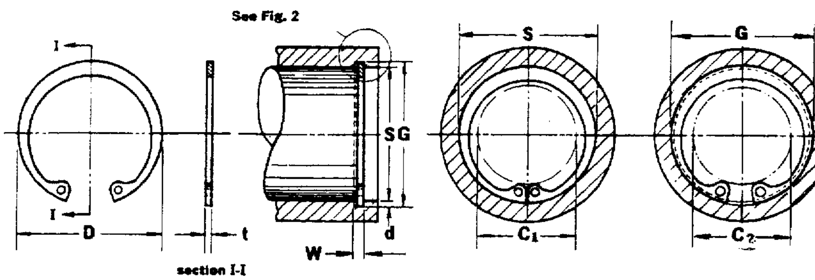

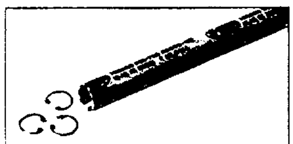

Sizes -25 thru -250 are available in tape-wrapped **Rol-Pak®** cartridges for an extra charge.

HOUSING DIA.			MIL-R-21248 MS 16625 INTERNAL SERIES N5000	TRUARC RING DIMENSIONS (Thickness t applies only to unplated rings. For plated and stainless steel (Type H) rings, add .002" to the listed maximum thickness. Maximum ring thickness will be at least .0002" less than the listed minimum groove width (W).)				Approx. weight per 1000 pieces	GROOVE DIMENSIONS (T.I.R. (total indicator reading) is the maximum allowable deviation of concentricity between groove and housing.)					APPLICATION DATA			
Dec. equiv. inch	Approx. fract. equiv. inch	Approx. mm.		FREE DIA.		THICKNESS			DIAMETER		WIDTH		Nominal groove depth	CLEARANCE DIAMETER When sprung into housing S	CLEARANCE DIAMETER When sprung into groove G	ALLOW. THRUST LOAD (lbs.) Sharp corner abutment — RINGS (Standard material) Safety factor = 4	GROOVES (Cold rolled steel bores and housings) Safety factor = 2 (Important See Page 27)
S	S	S	size—no.	D	tol.	t	tol.	lbs.	G	tol.	W	tol.	d	C_1	C_2	P_r	P_g
.250	1/4	6.4	N5000-25	.280		.015		.08	.268	±.001 .0015 T.I.R.	.020	+.002 −.000	.009	.115	.133	420	190
.312	5/16	7.9	N5000-31	.346		.015		.11	.330		.020		.009	.173	.191	530	240
.375	3/8	9.5	N5000-37	.415		.025		.25	.397	±.002 .002 T.I.R.	.029		.011	.204	.226	1050	350
.438	7/16	11.1	N5000-43	.482		.025		.37	.461		.029		.012	.23	.254	1220	440
.453	29/64	11.5	N5000-45	.498		.025		.43	.477		.029		.012	.25	.274	1280	460
.500	1/2	12.7	N5000-50	.548	+.010 −.005	.035		.70	.530		.039		.015	.26	.29	1980	510
.512	—	13.0	N5000-51	.560		.035		.77	.542	±.002 .004 T.I.R.	.039		.015	.27	.30	2030	520
.562	9/16	14.3	N5000-56	.620		.035		.86	.596		.039		.017	.275	.305	2220	710
.625	5/8	15.9	N5000-62	.694		.035		1.0	.665		.039		.020	.34	.38	2470	1050
.688	11/16	17.5	N5000-68	.763		.035		1.2	.732		.039	+.003 −.000	.022	.40	.44	2700	1280
.750	3/4	19.0	N5000-75	.831		.035		1.3	.796		.039		.023	.45	.49	3000	1460
.777	—	19.7	N5000-77	.859		.042		1.7	.825		.046		.024	.475	.52	4550	1580
.812	13/16	20.6	N5000-81	.901		.042		1.9	.862		.046		.025	.49	.54	4800	1710
.866	—	22.0	N5000-86	.961		.042		2.0	.920		.046		.027	.54	.59	5100	1980
.875	7/8	22.2	N5000-87	.971	+.015 −.010	.042		2.1	.931	±.003 .004 T.I.R.	.046		.028	.545	.60	5150	2080
.901	—	22.9	N5000-90	1.000		.042	±.002	2.2	.959		.046		.029	.565	.62	5350	2200
.938	15/16	23.8	N5000-93	1.041		.042		2.4	1.000		.046		.031	.61	.67	5600	2450
1.000	1	25.4	N5000-100	1.111		.042		2.7	1.066		.046		.033	.665	.73	5950	2800
1.023	—	26.0	N5000-102	1.136		.042		2.8	1.091		.046		.034	.69	.755	6050	3000
1.062	1 1/16	27.0	N5000-106	1.180		.050		3.7	1.130		.056		.034	.685	.75	7450	3050
1.125	1 1/8	28.6	N5000-112	1.249		.050		4.0	1.197		.056		.036	.745	.815	7900	3400
1.181	—	30.0	N5000-118	1.319		.050		4.3	1.255		.056		.037	.79	.86	8400	3700
1.188	1 3/16	30.2	N5000-118	1.319		.050		4.3	1.262		.056		.037	.80	.87	8400	3700
1.250	1 1/4	31.7	N5000-125	1.388		.050		4.8	1.330		.056		.040	.875	.955	8800	4250
1.259	—	32.0	N5000-125	1.388	+.025 −.020	.050		4.8	1.339		.056		.040	.885	.965	8800	4250
1.312	1 5/16	33.3	N5000-131	1.456		.050		5.0	1.396		.056		.042	.93	1.01	9300	4700
1.375	1 3/8	34.9	N5000-137	1.526		.050		5.1	1.461	±.004 .005 T.I.R.	.056		.043	.99	1.07	9700	5050
1.378	—	35.0	N5000-137	1.526		.050		5.1	1.464		.056	+.004 −.000	.043	.99	1.07	9700	5050
1.438	1 7/16	36.5	N5000-143	1.596		.050		5.8	1.528		.056		.045	1.06	1.15	10200	5500
1.456	—	37.0	N5000-145	1.616		.050		6.4	1.548		.056		.046	1.08	1.17	10300	5700
1.500	1 1/2	38.1	N5000-150	1.660		.050		6.5	1.594		.056		.047	1.12	1.21	10550	6000
1.562	1 9/16	39.7	N5000-156	1.734		.062		8.9	1.658		.068		.048	1.14	1.23	13700	6350
1.575	—	40.0	N5000-156	1.734	+.035 −.025	.062		8.9	1.671	±.005 .005 T.I.R.	.068		.048	1.15	1.24	13700	6350
1.625	1 5/8	41.3	N5000-162	1.804		.062	±.003	10.0	1.725		.068		.050	1.15	1.25	14200	6900
1.653	—	42.0	N5000-165	1.835		.062		10.4	1.755		.068		.051	1.17	1.27	14500	7200
1.688	1 11/16	42.9	N5000-168	1.874		.062		10.8	1.792		.068		.052	1.21	1.31	14800	7450

Figure B-28: Waldes Truarc 0.562 in Retainer Ring

BASIC
internal series
N5000
(continued)

WALDES TRUARC® RETAINING RINGS

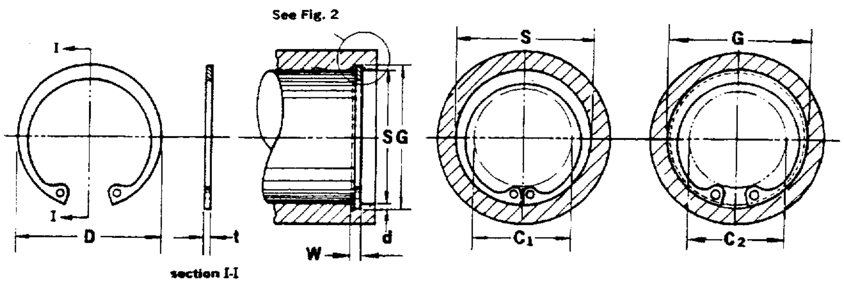

HOUSING DIA.			MIL-R-21248 MS 16625 INTERNAL SERIES N5000	TRUARC RING DIMENSIONS (Thickness t applies only to unplated rings. For plated and stainless steel (Type H) rings, add .002" to the listed maximum thickness. Maximum ring thickness will be at least .0002" less than the listed minimum groove width (W).)					GROOVE DIMENSIONS (T.I.R. (total indicator reading) is the maximum allowable deviation of concentricity between groove and housing.)					APPLICATION DATA			
Dec. equiv. inch	Approx. fract. equiv. inch	Approx. mm.		FREE DIA.		THICKNESS		Approx. weight per 1000 pieces	DIAMETER		WIDTH		Nominal groove depth	CLEARANCE DIAMETER: When sprung into housing S	CLEARANCE DIAMETER: When sprung into groove G	ALLOW. THRUST LOAD (lbs.) Sharp corner abutment: RINGS (Standard material) Safety factor = 4	ALLOW. THRUST LOAD (lbs.) Sharp corner abutment: GROOVES (Cold rolled steel bores and housings) Safety factor = 2
																Important! See Page 27	
S	S	S	size—no.	D	tol.	t	tol.	lbs.	G	tol.	W	tol.	d	C_1	C_2	P_r	P_g
3.625	3 5/8	92.1	N5000-362	4.024	±.055	.109		73.0	3.841		.120		.108	2.91	3.12	55900	33200
3.740	—	95.0	N5000-375	4.157		.109		78.0	3.964		.120		.112	3.02	3.24	57700	35600
3.750	3 3/4	95.2	N5000-375	4.157		.109		78.0	3.974		.120		.112	3.03	3.25	57700	35600
3.875	3 7/8	98.4	N5000-387	4.291		.109		87.0	4.107		.120		.116	3.11	3.34	59600	38000
3.938	3 15/16	100.0	N5000-393	4.358		.109		88.0	4.174		.120		.118	3.17	3.40	60700	39300
4.000	4	101.6	N5000-400	4.424		.109		93.0	4.240	±.006	.120		.120	3.23	3.47	61700	40700
4.125	4 1/8	104.8	N5000-412	4.558		.109	±.003	97.0	4.365	.006	.120	+.005	.120	3.36	3.60	63600	42000
4.250	4 1/4	108.0	N5000-425	4.691		.109		101.0	4.490	T.I.R.	.120	−.000	.120	3.48	3.72	65500	43200
4.331	—	110.0	N5000-433	4.756		.109		105.0	4.571		.120		.120	3.50	3.74	66600	44500
4.500	4 1/2	114.3	N5000-450	4.940		.109		111.0	4.740		.120		.120	3.66	3.90	69300	45800
4.625	4 5/8	117.5	N5000-462	5.076	±.065	.109		117.0	4.865		.120		.120	3.79	4.03	71300	47000
4.724	—	120.0	N5000-475	5.213		.109		124.0	4.969		.120		.122	3.88	4.12	73200	49000
4.750	4 3/4	120.6	N5000-475	5.213		.109		124.0	4.995		.120		.122	3.90	4.14	73200	49000
5.000	5	127.0	N5000-500	5.485		.109		136.0	5.260		.120		.130	4.08	4.34	77000	.55000
5.250	5 1/4	133.3	N5000-525	5.770		.125		174.0	5.520		.139		.135	4.31	4.58	92700	60000
5.375	5 3/8	136.5	N5000-537	5.910		.125	±.004	179.0	5.650	±.007	.139	+.006	.135	4.41	4.68	94900	61500
5.500	5 1/2	139.7	N5000-550	6.066		.125		183.0	5.770	.006	.139	−.000	.135	4.53	4.80	97200	63300
5.750	5 3/4	146.0	N5000-575	6.336		.125		192.0	6.020	T.I.R.	.139		.135	4.78	5.05	101600	65900
6.000	6	152.4	N5000-600	6.620		.125		201.0	6.270		.139		.135	5.03	5.30	105900	68600
6.250	6 1/4	158.7	N5000-625	6.895		.156		266.0	6.530		.174		.140	5.24	5.52	137700	74100
6.500	6 1/2	165.1	N5000-650	7.170		.156		281.0	6.790		.174		.145	5.49	5.78	143300	79900
6.625	6 5/8	168.3	N5000-662	7.308	±.080	.156		305.0	6.925		.174		.150	5.60	5.90	146000	84200
6.750	6 3/4	171.4	N5000-675	7.445		.156		325.0	7.055		.174		.152	5.65	5.95	148800	87000
7.000	7	177.8	N5000-700	7.720		.156		344.0	7.315		.174		.157	5.88	6.19	154300	93100
7.250	7 1/4	184.1	N5000-725	7.995		.187		428.0	7.575		.209		.162	6.08	6.40	191500	99600
7.500	7 1/2	190.5	N5000-750	8.270		.187		485.0	7.840		.209		.170	6.33	6.67	198200	108100
7.750	7 3/4	196.8	N5000-775	8.545		.187		520.0	8.100	±.008	.209	+.008	.175	6.58	6.93	204800	115000
8.000	8	203.2	N5000-800	8.820		.187	±.005	555.0	8.360	.006	.209	−.000	.180	6.75	7.11	211400	122000
8.250	8 1/4	209.5	N5000-825	9.095		.187		603.0	8.620	T.I.R.	.209		.185	7.00	7.37	218000	129300
8.500	8 1/2	215.9	N5000-850	9.285	±.090	.187		634.0	8.880		.209		.190	7.13	7.51	224600	136900
8.750	8 3/4	222.2	N5000-875	9.558		.187		653.0	9.145		.209		.197	7.38	7.77	230400	145500
9.000	9	228.6	N5000-900	9.830		.187		732.0	9.405		.209		.202	7.63	8.03	237800	154100
9.250	9 1/4	235.0	N5000-925	10.102		.187		767.0	9.668		.209		.209	7.88	8.30	244400	163600
9.500	9 1/2	241.3	N5000-950	10.375		.187		803.0	9.930		.209		.215	7.98	8.41	251000	173100
9.750	9 3/4	247.7	N5000-975	10.648		.187		833.0	10.190		.209		.220	8.23	8.67	257600	181900
10.000	10	254.0	N5000-1000	10.920		.187		863.0	10.450		.209		.225	8.48	8.93	264200	190700

Figure B-29: Waldes Truarc 4.0 in Retainer Ring

B.3 Load Cell Calibration Data

DATE: 1/14/99

ISI

INDUSTRIAL SENSORS & INSTRUMENTS, INC.
308 TEXAS AVENUE, SUITE 104
ROUND ROCK, TEXAS 78664
FAX (512) 255-8855
(512) 255-3790

CALIBRATION DATA

ISI P/N: DUG-0.5
CUST. P/N: Engr. Proto.
CAPACITY: ±500 lbs
EXCITATION: 10.0031 V dc
SOURCE: Satec 60HVL

S/N: 3655
CUSTOMER: Schlumberger
P.O. NO.: 3GP08542-2
SENSITIVITY: See Below

LOAD (lb)	OUTPUT (μV)
500	15680
400	12524
300	9378
200	6227
100	3080
0	-56
-100	-3199
-200	-6339
-300	-9489
-400	-12639
-500	-15791

Tension Sensitivity: 1.5731 mV/V at +500 lbs.
Compression Sensitivity: -1.5730 mV/V at -500 lbs.

CONNECTIONS:

RED	+ EXCITATION
BLACK	- EXCITATION
GREEN	+ SIGNAL
WHITE	- SIGNAL

Figure B-30: Calibration Data

Bibliography

[1] J. L. Lummus A. Park. New surfactant mixture eases differential sticking. *Oil and Gas Journal*, pages 62–56, November 1962.

[2] G.R. Welch E.L. Haden. How to prevent differential pressure sticking of drill pipe. *Oil and Gas Journal*, pages 214–219, April 1961.

[3] P. Way G.H. Meeten. Force exerted by a growing mudcake on a sphere and a cylinder. *Schlumberger Cambridge Research Center*, May 1992.

[4] C. Zurdo J. M. Courteille. A new approach to differential sticking. In *SPE 14244, 60th Annual Technical Conference*, Las Vegas, June 1985.

[5] D. A. Krol. Laboratory evaluation of stuck pipe spotting fluid. In *SPE 10096, 56th Annual Fall Technical Conference*, San Antonio, October 1981.

[6] D. A. Krol. Additives cut differential pressure sticking in drillpipe. *Oil and Gas Journal*, pages 55–59, June 1984.

[7] P. H. Monaghan M. R. Annis. Differential pressure sticking - laboratory studies of friction between steel and mud filter cake. *Journal of Petroleum Technology*, pages 537–543, May 1962.

[8] Davies Meeten. Sticking by differential pressure. *Schlumberger*, 1993.

[9] H. D Outmans. Mechanics of differential pressure sticking of drill collars. *Petroleum Transactions AIME*, 213:265–274, 1958.

[10] P.W. Way P.I. Reid, G.H. Meeten. Mechanisms of differential sticking and a simple well-site test for monitoring and optimizing drilling mud properties. *SPE 35100.*

[11] S.G. Almquist R.K. Clark. Evaluation of spotting fluids in a full-scale differential pressures sticking apparatus. *SPE 22550*, pages 121–129, June 1992.

[12] Schlumberger. Drillsure marketing plan. *SRPC*, 1998.

[13] W.B. Underhill. Model-based sticking risk assessment for wireline formation testing tools in the u.s. gulf coast. In *SPE 48963, SPE Annual Technical Conference*, New Orleans, 1998.